

Molecular role of Kon-tiki during myotube migration and attachment

Dissertation zur Erlangung des Doktorgrades der
Naturwissenschaften (Dr. rer. nat.) der Fakultät für Biologie der
Ludwig-Maximilians-Universität München



vorgelegt von

Irene Rebelo da Silva Ferreira

angefertigt am

Max-Planck-Institut für Biochemie, in Martinsried (München)

München, den 16.06.2016

Erstgutachter:	Prof. Dr. Barbara Conradt
Zweitgutachter:	Prof. Dr. Charles David
Tag der Abgabe:	16.06.2016
Tag der mündlichen Prüfung:	25.11.2016

Eidesstattliche Erklärung

Ich versichere hiermit an Eides statt, dass die von mir vorgelegte Dissertation von mir selbstständig und ohne unerlaubte Hilfe angefertigt ist.

München, den 16.06. 2016

.....
Irene Rebelo da Silva Ferreira

Erklärung

Hiermit erkläre ich, dass die Dissertation nicht ganz oder in wesentlichen Teilen einer anderen Prüfungskommission vorgelegt worden ist, und dass ich mich anderweitig einer Doktorprüfung ohne Erfolg nicht unterzogen habe.

München, den 16.06. 2016

.....
Irene Rebelo da Silva Ferreira

To Marc

Table of Contents

List of Figures	v
List of Tables.....	vi
List of abbreviations	vii
ABSTRACT	VIII
1 INTRODUCTION	9
1.1 DEVELOPMENT OF THE LARVAL SOMATIC MUSCULATURE	9
1.1.1 Mesoderm formation.....	10
1.1.2 Formation of the larval musculature in the embryo	11
1.1.2.1 Founder Cells provide instructions for muscle development.....	14
1.1.2.2 Fusion and elongation of the larval muscles.....	15
1.1.2.3 Specification of tendon cells	16
1.1.2.4 Muscle attachment: formation of myotendinous junctions.....	17
1.2 DEVELOPMENT OF THE SOMATIC ADULT MUSCULATURE	20
1.2.1 Formation of the adult abdominal muscles	20
1.2.2 Formation of the indirect flight muscles.....	24
1.2.2.1 The developmental program of the DVMs	24
1.2.2.2 The developmental program of the DLMs	25
1.3 KON IS ESSENTIAL FOR THE TWO PHASES OF <i>DROSOPHILA</i> MYOGENESIS 27	
1.3.1 The role of Kon in the larval myogenesis, in the embryo.....	27
1.3.2 The role of Kon in the adult myogenesis, in the pupa	30
1.3.3 Kon homologues and protein structure	31
1.3.4 <i>Drosophila</i> myogenesis: a system to study challenges in ligand sensing	35
1.4 THE GENOMIC FOSMID LIBRARY PROVIDES TOOLS FOR STUDYING KON....	36
1.5 AIM AND OBJECTIVES OF THIS WORK	37
2 RESULTS	38
2.1 TENDON CELL SPECIFICATION AND ECM ASSEMBLY IN <i>KON</i> MUTANT EMBRYOS	38
2.1.1 Tendon cells precursors were specified in <i>kon</i> mutant embryos	39
2.1.2 Tendon matrix components were present in <i>kon</i> mutant embryos ...	40
2.2 DEVELOPMENT AND VALIDATION OF MOLECULAR TOOLS TO STUDY THE FUNCTIONAL DOMAIN TYPES OF KON.....	44
2.2.1 Validation of the <i>kon</i> fosmid.....	45

2.2.2	Generation of tools to detect the localization of Kon during myogenesis.....	47
2.3	THE ROLE OF KON DOMAINS DURING MYOGENESIS OF THE LARVAL SOMATIC MUSCLES IN THE EMBRYO.....	49
2.3.1	Expression levels of the Kon fosmid derived constructs	49
2.3.2	The LamG domains and the PDZ-BD of Kon are essential for the formation of the VL muscles.....	51
2.3.3	The 15 CSPG domains have a minor role in attachment formation..	54
2.3.4	Kon requires the LamG domains to localize at the muscle attachment site	56
2.3.5	The CSPG domains synergize with the LamG domains	58
2.4	AN ESSENTIAL ROLE OF THE CSPG DOMAINS IN ADULT MYOGENESIS	60
2.4.1	The 15 CSPGs are essential for guidance of the dorsal abdominal muscles.....	61
2.4.2	The 15 CSPGs are essential for guidance of the DVMs	65
2.4.3	The CSPG domains have a minor role in DLM attachment (template-based)	67
2.5	STRATEGIES TO IDENTIFY KON INTERACTIONS PARTNERS	70
2.5.1	Kon interactions partners during larval myogenesis.....	71
2.5.2	Kon interaction partners during adult myogenesis	76
3	<u>DISCUSSION</u>	80
3.1	UNVEILING THE FUNCTION OF THE THREE KON PROTEIN DOMAIN TYPES ..	81
3.2	CHALLENGES TO FIND INTERACTION PARTNERS AND NEW STRATEGIES ...	85
3.3	POSSIBLE MECHANISMS UNDERLYING THE DUAL FUNCTION OF KON DURING MYOGENESIS	88
3.3.1	Myotube guidance via a secreted ligand.....	88
3.3.2	Myotube attachment via a tendon cell-bound ligand	89
3.3.3	Myotube attachment via integrin modulation.....	90
3.3.4	Myotube attachment with Kon homologues	90
3.3.5	Cytoskeleton remodelling necessary for myotube elongation and attachment	90
3.4	A COMPACT AND A FULL VERSION OF KON: ADJUSTMENTS TO TWO MYOGENIC PHASES	92
4	<u>CONCLUSION</u>	97
5	<u>MATERIAL AND METHODS</u>	98
5.1	MATERIALS.....	98
5.1.1	General reagents.....	98
5.1.2	Molecular biology reagents and equipments.....	98

5.1.2.1 General reagents	98
5.1.2.2 Kits	98
5.1.2.3 Equipments	98
5.1.2.4 Recombineering using <i>kan</i> resistance for selection	99
5.1.2.4.1 Bacteriological reagents.....	99
5.1.2.4.2 Solutions and media	99
5.1.2.4.3 Bacterial strains, plasmids and oligonucleotides	99
5.1.2.5 Recombineering using <i>galk</i> selection	100
5.1.2.5.1 Bacteriological reagents.....	100
5.1.2.5.2 Solutions and media	100
5.1.2.5.3 Bacterial strains, plasmids and oligonucleotides	102
5.1.3 Fly reagents.....	102
5.1.3.1 List of fly lines	102
5.1.4 Food for maintenance of fly stocks and collection of embryos	103
5.1.4.1 Dissection tools and materials	103
5.1.5 Immunofluorescence reagents.....	103
5.1.5.1 General solutions	103
5.1.5.2 Antibodies	103
5.1.5.3 Mounting materials and solutions	104
5.1.6 Biochemical reagents	104
5.1.6.1 Western blot analysis.....	104
5.1.6.1.1 Solutions	104
5.1.6.1.2 Antibodies	105
5.1.6.1.3 Materials and equipments.....	105
5.1.6.2 Immunoprecipitation.....	105
5.1.6.2.1 Buffers.....	105
5.1.6.2.2 Antibodies, peptides and immunoprecipitation beads	106
5.1.7 Software packages	106
5.2 METHODS	106
5.2.1 Generating <i>kon</i> constructs and transgenic flies	106
5.2.1.1 Engineering tagged versions of <i>kon</i>	106
5.2.1.1.1 Amplifying a GFP tag and a V5 tag for homologous recombination.....	108
5.2.1.1.2 Transforming the bacteria containing the fosmid FlyFos021621 with pRed/Flp4.....	109
5.2.1.1.3 Tagging by inducing the expression of the Red operon from pRed/Flp4 with L-rhamnose	110
5.2.1.1.4 Excising the <i>kan</i> resistance cassette.....	111
5.2.1.1.5 Eliminating the pRed/Flp4.....	111

5.2.1.1.6 Preparing fosmid DNA to generate transgenic flies.....	111
5.2.1.2 Seamlessly deleting or mutating the three main protein domain types of <i>kon</i>	112
5.2.1.2.1 Preparing the galk cassettes	116
5.2.1.2.2 Transforming the SW102 bacteria with <i>kon-V5</i> fosmid and <i>pRed/Flp4</i>	116
5.2.1.2.3 Inserting the galk cassette by inducing the expression of the <i>Red</i> operon from <i>pRed/Flp4</i> with <i>L-rhamnose</i>	117
5.2.1.2.4 Exchanging the galk cassette	119
5.2.1.2.5 Preparing fosmid DNA to generate transgenic flies.....	120
5.2.1.3 Generating transgenic flies	120
5.2.1.3.1 Injecting the constructs into <i>Drosophila</i> embryos	120
5.2.1.3.2 Crossing and screening for the genomic integration of the constructs.....	121
5.2.2 Analysing the muscular phenotype from the transgenic flies.....	121
5.2.2.1 Analysing the development of the larval somatic musculature	121
5.2.2.1.1 Collecting, fixing and staining embryos	121
5.2.2.1.2 Imaging L3 larvae	123
5.2.2.1.3 Measuring the VL length and attachment site size	124
5.2.2.1.4 Measuring the protein enrichment at the muscle attachment site	124
5.2.2.2 Development of the adult somatic musculature.....	125
5.2.2.2.1 Dissecting, fixing and staining 90h APF pupae	125
5.2.2.2.2 Dissecting, fixing and staining pupal abdomen (whole mount)	126
5.2.2.2.3 Live imaging pupal abdomen.....	126
5.2.2.2.4 Live imaging DLMs and DVMs	127
5.2.3 Biochemistry and mass spectrometry	127
5.2.3.1 Assessing the expression levels of the <i>kon-V5</i> derived constructs	127
5.2.3.1.1 Biological Samples.....	127
5.2.3.1.2 Workflow	127
5.2.3.1.3 Western blot analysis.....	128
5.2.3.2 Experimental approach to identify Kon interaction partners	129
5.2.3.2.1 Formation of the larval somatic musculature in the embryo: <i>Kon-V5</i> and <i>Kon-HA</i> pull-downs	129
5.2.3.2.2 Formation of the larval somatic musculature in the embryo: <i>Kon PDZ-BD</i> peptide pull-downs	129
5.2.3.2.3 Development of the adult somatic musculature in the pupa: <i>Kon-GFP</i> and <i>Kon-YFP</i> pull-downs	130
6 REFERENCES	131
Acknowledgements	145
Curriculum Vitae.....	146

List of Figures

Figure 1.1. Development of the larval somatic muscles in the embryo	13
Figure 1.2. Elongation and attachment of the larval muscles in the embryo	19
Figure 1.3. The larval and adult <i>Drosophila</i> musculatures	21
Figure 1.4. Development of the dorsal adult abdominal muscles in the pupa	23
Figure 1.5. Development of the indirect flight muscles, DVMs and DLMs, in the pupa	26
Figure 1.6. Kon is essential for the formation of the VL muscles	28
Figure 1.7. Kon protein structure	34
Figure 2.1. Tendon precursors are specified in <i>kon</i> mutant embryos.....	40
Figure 2.2. Attachment components are present in <i>kon</i> mutant embryos	43
Figure 2.3. <i>kon</i> from FlyFos021621 clone is completely functional	46
Figure 2.4. Tagging the intracellular part of Kon preserves its biological activity	49
Figure 2.5. Kon-V5 derived toolkit	50
Figure 2.6. A compact version of Kon is sufficient for the formation of VL muscles in the embryo	53
Figure 2.7. The 15 CSPG domains have a minor role in generating stable VL attachments	55
Figure 2.8. Kon requires the LamG domains to localize at the attachment site	57
Figure 2.9. The CSPG domains synergize with the LamG domains	59
Figure 2.10. The CSPGs have a pivotal role during adult dorsal muscles formation	62
Figure 2.11. The CSPGs are essential for guidance of the adult dorsal muscles.....	64
Figure 2.12. The CSPG domains are essential for the guidance of the DVMs	66
Figure 2.13. The 15 CSPG domains have a minor role the DLM formation .	68
Figure 2.14. The CSPG domains have a minor role in DLM development ...	69
Figure 2.15. Kon interaction partners in the embryo	73
Figure 2.16. PDZ-BD peptide as bait to identify PDZ containing interaction partners.....	75
Figure 2.17. Kon interaction partners in pupae	77

Figure 3.1. Model for the activity of Kon during *Drosophila* myogenesis..... 96

Figure 5.1. Workflow for generating a tagged version of *kon* (FlyFos021621)
..... 107

Figure 5.2. Tagging *kon* (FlyFos021621) either with a *GFP* or a *V5* tag 108

Figure 5.3. Deleting or mutating the protein domain types of *kon*..... 113

Figure 5.4. Workflow for *galk* recombineering: GFP tagging 115

List of Tables

Table 5.1. List of oligonucleotides for recombineering using *kan* resistance
..... 100

Table 5.2. List of oligonucleotides for recombineering using *galk* selection 102

Table 5.3. PDZ-BD peptides used for pull-down experiments..... 106

List of abbreviations

A	Anterior
AMP	Adult muscle precursor
A-P	Anterior-Posterior Axis
APF	After puparium formation
CSPG	Chondroitin sulphate proteoglycan
DGrip	<i>Drosophila</i> Glutamate receptor binding protein
DLM	Dorsolateral muscle
DVM	Dorsoventral muscles
ECM	Extracellular matrix
EGF	Epidermal growth factor
FC	Founder cell
FCM	Fusion competent myoblast
FGF	Fibroblast growth factor
GBM	Glioblastoma
IFM	Indirect flight muscle
LamG	LamininG domains
LOM	Larval oblique muscle
MTJ	Myotendinous junction
P	Posterior
PDGF	Platelet-derived growth factor
PDZ	Post-synaptic protein
PDZ-BD	PDZ-binding domain
OPC	Oligodendrocyte precursor cell
Tps	Thrombospondin

Abstract

The first homolog of Kon-tiki (Kon) was identified in human melanoma cells over 30 ago. However, numerous aspects of the function of Kon and its homologues are poorly understood, including how their three protein domain types, the lamininG domains, the chondroitin sulphate proteoglycan (CSPGs) repeats, and the PDZ-binding domain, interplay to mediate a multitude of biological processes. This study shed light on this question, using *Drosophila* myogenesis as a model system. Here, a *kon* genomic fosmid clone derived toolkit, which recapitulates the expression profile of endogenous *kon*, was applied to investigate how Kon adapts its activity in two distinct developmental scenarios: one in the embryo, in which the small larval muscles form, and a second one in the pupae, in which the larger adult muscles form. This study showed that a compact version of Kon, missing the long CSPG domains is sufficient for building the smaller larval muscles. However, during formation of larger muscles, this compact version is not sufficient, requiring thus to be synergized by the CSPG domains. Furthermore, this study identified the extracellular domain type, which renders Kon able to mediate myotube guidance, the CSPG domains. This is the first *in vivo* study, which establishes a link between guidance and Kon, thus providing insights to how Kon homologues, NG2/CSPG4, may increase the metastatic potential of melanomas or of soft tissue sarcoma.

1 Introduction

Muscles enable animals to develop an escape response, thus increasing their chances to survive and to generate offspring in hostile habitats. The sophistication of the escape response varies throughout the kingdom *Animalia*, and it is partially dependent on the complexity of each type of musculature.

The myogenesis of the somatic muscles is a stereotyped sequence of cellular processes, including cell specification, cell proliferation, fusion, migration and cell–cell interactions.

Evolutionary conservation both at levels of DNA sequence and of cellular morphogenesis makes model organisms, such as the fruit fly *Drosophila melanogaster*, a versatile experimental framework to investigate the general principles of muscle biology and disease. *Drosophila* myogenesis shares key aspects with vertebrate somatic myogenesis, including expression of myogenic genes, such as *MEF2* and *TWIST*; formation of syncytial myotubes; and the establishment of a contractile apparatus based on a conserved sarcomeric organization. Therefore, studying *Drosophila* myogenesis is of high relevance to understand general principles underlying human muscle formation, regeneration, aging, as well as myopathies, including Duchenne dystrophy, as the most common and severe example.

1.1 Development of the larval somatic musculature

Drosophila melanogaster has two phases of myogenesis. In the first phase, occurring during embryogenesis, the larval muscles are formed. While in the second phase, taking place during pupal metamorphosis, the adult muscles of the fly are built. The larval musculature consist of single-fiber muscles, while the adult musculature is composed of multi-

fiber arrays, rendering the *Drosophila* adult muscles more similar to vertebrate muscles (Baylies et al., 1998).

1.1.1 Mesoderm formation

The larval somatic muscles arise from the germ layer mesoderm. The formation of the mesoderm is triggered during *Drosophila* oogenesis by the mechanism that establishes the dorsal-ventral (D-V) axis. The D-V spatial information is transmitted from the oocyte to the embryo by a spatially restricted cascade of molecular events (Moussian and Roth, 2005; Stein and Stevens, 2014). This cascade of events includes the activation of Toll specifically at the ventral side of the embryo, which in turn generates a nuclear gradient of the transcription factor, Dorsal, across the D-V axis of the syncytial blastoderm. The Dorsal gradient is established during the nuclear division cycles 10 through 14, embryonic stage 4 (Roth et al., 1989). This gradient modulates a multitude of genes according to their responsiveness to Dorsal (Stathopoulos and Levine, 2002).

At embryonic stage 5, the nuclei are enveloped by the embryonic membrane, resulting in the cellularization of the embryo. At stage 6, gastrulation begins. During gastrulation, mesoderm, neurogenic ectoderm and dorsal ectoderm are formed. The development of these germ layers is orchestrated by the differential activation of downstream genes of Dorsal (Stathopoulos and Levine, 2002; 2004).

Twist (Twi), the master regulator of the mesoderm, is activated by a high concentration of Dorsal at the ventral part of the blastoderm. Twi orchestrates a complex network of genes, responsible for the mesoderm formation and subsequent sub-patterning. The activation of this complex network of genes in the ventral cells from the embryos induces the contraction of their basal side. These cells acquire then a wedge shape necessary to invaginate into the interior of the embryo. This inward movement of cells creates a furrow on the ventral side, a

developmental hallmark of *Drosophila* embryo (Leptin and Grunewald, 1990).

The secretion of Thisbe (a FGF ligand) by the overlying ectoderm orchestrates subsequently the mesodermal spreading below the ectoderm, through FGF receptor activation (Sandmann et al., 2007). As the mesoderm spreads below the overlying ectoderm, it receives ectodermal signals, which are essential for the patterning of the mesoderm (Stathopoulos and Levine, 2004; Moussian and Roth, 2005).

The anterior-posterior segmentation of the ectoderm instructs the patterning of the underlying mesoderm, by modulating the expression of *twi*. Two important molecules that modulate *twi* expression levels in the mesoderm are Wingless (Wg) and Sloppy-paired (Slp). The ectoderm secretes Wg, which in turn leads to the activation of *slp* in the mesoderm, via the transcription factor dTCF (Pangolin). Slp, in turn, inhibits a repressor of *twi*, Bagpipe, in the anterior part of each mesodermal segment. In the posterior part, Bagpipe remains active, leading to *twi* repression (Lee and Frasch, 2000). Thus, *twi* only remains expressed in the anterior mesoderm of each segment (**Figure 1.1A**). The somatic muscles originate from the region of high *twi*, whereas the visceral mesoderm and the fat body from the regions of low *twi* expression (Dobi et al., 2015).

1.1.2 Formation of the larval musculature in the embryo

The larval somatic muscles develop from the anterior region of each mesodermal hemisegment, which is composed of cells with high expression of *twi*. These cells are allocated into 18 myogenic clusters (in the case of the abdominal hemisegment) (**Figure 1.1B**), from which the progenitors of the 30 somatic muscles are specified (Carmena et al., 1995), (**Figure 1.1C-F**).

Diffusible molecules secreted by the ectoderm orchestrate within each of the 18 myogenic clusters a stepwise decrease in the number of cells that can become a muscle progenitor. The first stage of a myogenic cluster is designated competence domain. Some cells from the competence domain then acquire the potential to become a muscle progenitor, thus forming an equivalence (pro-muscular) cluster (Carmena et al., 1998). Notch inhibition assures that only one cell from the equivalence cluster acquires the progenitor fate (Rusconi and Corbin, 1998), (**Figure 1.1B, C**).

From 18 competence domains in the abdominal hemisegment, 18 muscle progenitors are specified, which in turn give rise to 30 muscle founder cells (FCs) and six adult muscle precursors (AMPs) by asymmetric division. The AMPs are quiescent cells necessary for the adult myogenesis, whose role is described later (Carmena et al., 1995). The 30 FCs within the hemisegment are organized in three groups: dorsal, lateral, and ventral, according to the spatial organization of the future muscles (Dobi et al., 2015), (**Figure 1.1D-F**).

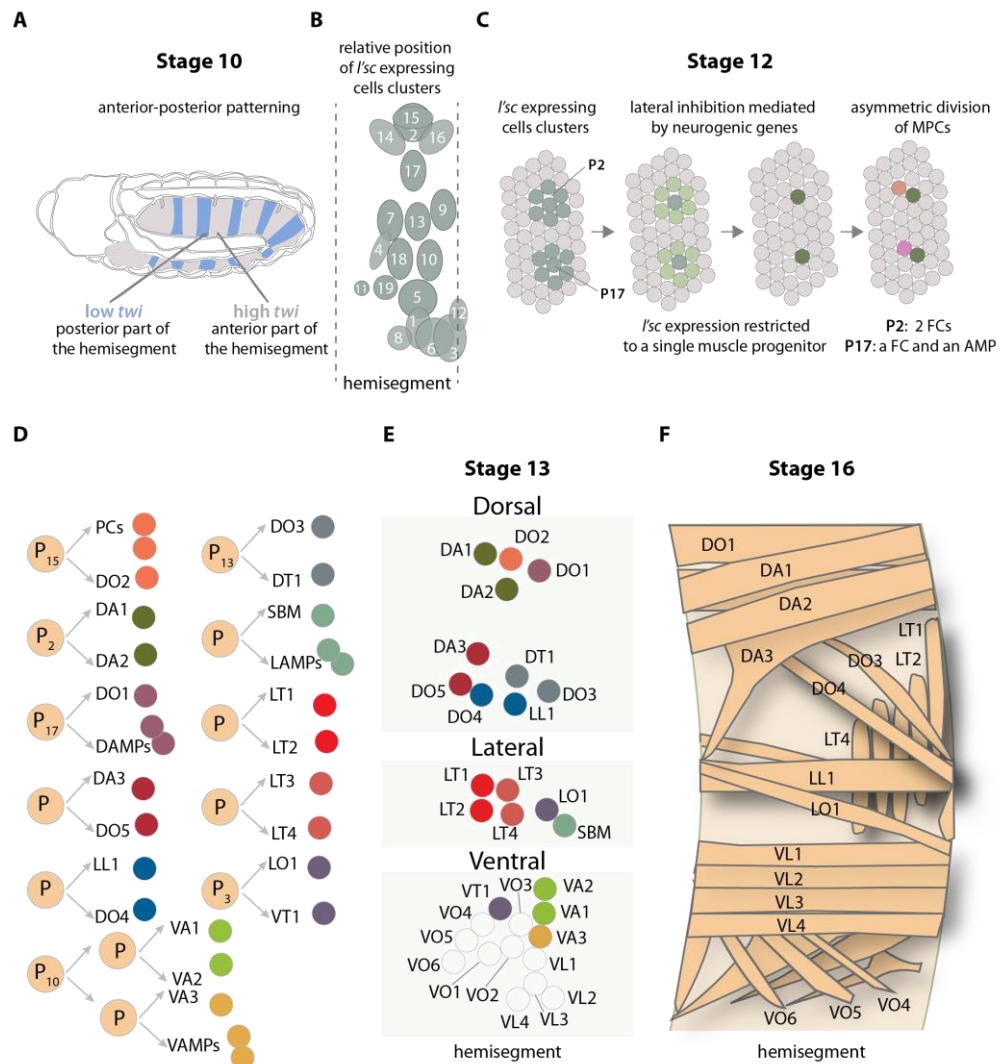


Figure 1.1. Development of the larval somatic muscles in the embryo

(A) Modulation of *twi* expression underlies mesodermal anterior-posterior patterning. Ectodermal signalling modulates *twi* expression at the mesoderm, generating a high expression region, at the anterior part, and a low expression region at the posterior part of a segment. The somatic muscles originate from the high *twi* region.

(B) Diffusible molecules secreted by the ectoderm subdivide the high *twi* region into 18 myogenic clusters throughout an abdominal hemisegment, designated competence domains. All the cells from the competence domains express *lethal of scute* (*I'sc*).

(C) The competence domains undergo a stepwise decrease in the number of cells that can become a muscle progenitor cell (MPC). The muscle progenitors divide asymmetrically. As representative examples, the cell lineage of P2 and P17 are depicted.

(D) Cell lineage generated by each muscle progenitor. Some progenitors originate only FCs, others AMPs and pericardial cells (PCs). DAMPs (dorsal AMPs), LAMPs (lateral AMPs) and VAMPs (ventral AMPs). A to E adapted from Dobi et al., 2015.

(E) The FCs of each type of larval muscles occupy the position of the future muscle.

(F) The larval somatic muscles from an abdominal hemisegment. Each muscle has a two-letters nomenclature. The first letter describes the position within the hemisegment: D (dorsal), L (lateral) and V (ventral); and the second letter the orientation of the muscle: O (oblique), A (acute), T (transverse), and L (longitudinal).

1.1.2.1 Founder Cells provide instructions for muscle development

Each FC contains the genetic instructions to form a particular muscle fiber. If fusion is blocked, some FCs are able to create mini-muscles, which can even attach to tendon cells, and express markers of the mature muscle (Rushton et al., 1995).

The identity genes, expressed by the FCs, encode the genetic instructions for the formation of each muscle fiber (Frasch, 1999), including their size and shape (Bataillé et al., 2010). The identity genes are either expressed exclusively in a single FC, such as *ladybird* (Jagla et al., 1998), or in a larger and overlapping number of FCs, such as *Krüppel* (*Kr*) (Ruiz Gomez et al., 1997), *slouch* (*slou*) (Knirr et al., 1999), *nautilus* (*nau*) (Keller, 1998), and *Pox meso* (*Poxm*) (Duan et al., 2007).

These identity genes are either activated by extrinsic factors secreted by the ectoderm, such as *Wg* activates *eve*; or by other identity genes, such as, the activation of *slou* in the VA2 muscle by *Kr* (Ruiz Gomez et al., 1997). Moreover, identity genes can also prevent the expression of other identity genes (Knirr et al., 1999). In summary, the identity genes interplay with each other, thus generating a specific expression profile of identity genes unique to each FC or forming muscle fiber. This unique profile of identity genes expression, known as combinatorial code of identity gene expression, orchestrates a multitude of downstream targets responsible for development and morphology of each muscle fiber (Dobi et al., 2015).

Once a FC-specific network of identity genes is established, how does it control muscle formation and differentiation? The comparison of the transcriptional profile from two distinct FC populations provided insights into how muscle morphology and diversity are generated by a network of identity genes (Dobi et al., 2014). The first interesting insight was that the majority of genes found to be up-regulated were

similar in the two population of FCs. This group of genes comprises the FC transcriptional core, whose genes are involved in cell morphology, cell motility, and cell adhesion, as well as microtubule cytoskeleton organization. While the diversification of the muscles is controlled only by a smaller number of genes (Dobi et al., 2014). An example of such a gene is *kon-tiki* (*kon*). *Kon* is expressed in only a subset of FCs and myotubes (Estrada et al., 2006). *Kon* is a receptor essential for myotube elongation and attachment (Schnorrer et al., 2007).

As mentioned before, the FCs have all the genetic instructions to form a muscle, but they need to increase their mass to become a mature muscle. This is achieved by the fusion of the fusion competent myoblasts (FCMs) with the FCs. The FCMs derive from the cells that had a strong Notch signal within the equivalence cluster, leading to the expression of *Lame duck* (*Lmd*), a zinc finger transcription factor (Busser et al., 2012). *Lmd* regulates in turn *Mef2*, *stick-and-stones*, and *blow*, whose activities are essential for fusion with the FCs (Duan et al., 2001; Busser et al., 2012). Interestingly, *Lmd* also activates *tramtrack69*, a zinc finger repressor, whose function is to repress FC genes in FCMs, and thus to stabilize the FCM fate (Ciglar et al., 2014).

1.1.2.2 Fusion and elongation of the larval muscles

Muscle fibers contain from four to 25 nuclei (Beckett and Baylies, 2007), thus rendering myoblast fusion a key morphogenetic process for the formation of muscles (**Figure 1.2**). The fusion of FCMs with FCs takes place in five main steps: (1) recognition and adhesion between a FCM and a FC or growing myotube, (2) cytoskeletal arrangement at the site of fusion, (3) pore formation, (4) mixture of the cytoplasmic contents and FCM nuclear reprogramming, and (5) disassemble of the fusion machinery at the site of fusion to allow subsequent fusion events (Rochlin et al., 2010; Schulman et al., 2015).

FCs and FCMs express cell-type specific transmembrane proteins containing immunoglobulin (Ig) domains, whose function is to mediate

cell-recognition and cell-adhesion (**Figure 1.2B**). The expression of two different types of adhesion proteins guarantees only heterotypic fusion events. Interestingly, identity genes also control the number of fusion events, and thus the number of nuclei per muscle (Bataillé et al., 2010). Upon each fusion event, the two cytoplasms are mixed, however the nucleus of the FCM acquires the fate of the FC/myotube. The mechanism that leads to FCM reprogramming after fusion is not yet understood.

1.1.2.3 Specification of tendon cells

During myoblast fusion, the myotube elongates towards the tendon cells to form a special type of attachment, designated myotendinous junction (MTJ), (**Figure 1.2**). The myotube elongation and attachment are partially non-autonomous processes. In these two processes, the muscles need extrinsic molecules, namely guidance cues and ECM components, secreted by the tendon cell precursors (Schweitzer et al., 2010).

The tendon cell precursors originate from ectodermal cells that express *stripe*, a master regulator of tendon cell development (Frommer et al., 1996). *Stripe* is an Early growth response (EGR)-like transcription factor (Frommer et al., 1996; Hatini and DiNardo, 2001), present in two splice variants, *stripeA* and *stripeB*. Each isoform is associated with a particular developmental status of the tendon cells: *stripeB* controls the early differentiation of ectodermal cells into tendon precursors, while *stripeA* orchestrates the steps for tendon precursor cell maturation (Volohonsky et al., 2007).

The specification of the tendon cell precursors is directed by secreted signals within the ectoderm. During stages 11-12, each ectodermal parasegment includes three territories that secrete Hedgehog (Hh), Spitz (ligand for EGF receptor) and Wg, respectively. These three secreted ligands induce expression of *stripeB* in the adjacent cells.

stripeB orchestrates subsequently the specification of these ectodermal cells in tendon precursors (Hatini and DiNardo, 2001).

Differentiation of the tendon precursors in tendon cells is triggered by the degradation of *stripeB* mRNA (Nabel-Rosen et al., 1999). The degradation of *stripeB* mRNA is mediated by the interplay of the two isoforms of a RNA-binding protein from the Star family (Signal transduction and RNA control), Held Out Wing (How): How(L) and How(S) (Nabel-Rosen et al., 2002; Volohonsky et al., 2007). StripeB induces the expression of How(L), which in turn decreases the levels of *stripeB* mRNA (Nabel-Rosen et al., 1999), thus inhibiting further differentiation until the elongating myotubes reaches the vicinity of the tendon cell precursor (Becker et al., 1997).

The growing myotubes secrete an EGFR ligand, Vein, which is essential for the maturation of the tendon cell precursor (Yarnitzky et al., 1997). Upon muscle-tendon contact, the level of How(S) increases in the tendon precursors, presumably due to Vein signalling (Nabel-Rosen et al., 1999). Subsequently, How(S) enhances the splicing of *stripeA*, thus elevating the *stripeA* mRNA levels (Volohonsky et al., 2007). StripeA in turn induces the expression of genes necessary for the maturation of the tendon cells (Subramanian et al., 2003).

1.1.2.4 Muscle attachment: formation of myotendinous junctions

Muscle and tendon cells form a stable attachment, a myotendinous junction (MTJ) (**Figure 1.2C**), which is essential to withstand the forces generated during muscle contractions. The building blocks of this junction are integrin heterodimers and a special type of ECM, tendon matrix. The tendon matrix “glues” the two cells together. Moreover, it provides elastic properties to the myotendinous junction (Brown, 2000a).

There are two types of myotendinous junctions: direct and indirect junctions. In the direct type, such as in the Lateral Transverse (LT)

muscles, a single muscle attaches to a tendon cell with little tendon matrix between them. While in an indirect type, such as in the ventral longitudinal (VL) muscles, multiple muscles, often from different directions, connect to a tendon cell with large quantities of tendon matrix in between (Brown, 2000a), (**Figure 1.2C**).

The tendon matrix is composed mainly of Thrombospondin (Tsp) and Tiggrin (**Figure 1.2C**). Tendon cells and muscles contribute differently to the assembly of this matrix: tendon cells secrete Tsp, while muscles capture Tiggrin secreted distally by other cell types (Schweitzer et al., 2010). Tsp starts to be secreted at embryonic stages 12-13, accumulating in dots around the tendon cells precursors (Subramanian et al., 2007). Because Tsp is secreted much before the myotube has reached the tendon cells, direct cell-cell membrane contact between muscle and tendon is thus unlikely to occur. At stage 16, upon myotendinous junctions formation, Tsp accumulates strongly at the MTJ (Subramanian et al., 2007). The integrin heterodimer expressed by the muscle, α PS2 β PS, binds to Tsp, attaching then the muscle to the tendon matrix (Subramanian et al., 2007).

Tiggrin is secreted into the hemolymph (insect blood) by the fat body and the hemocytes. Tiggrin diffuses through the hemolymph, and eventually reaches the muscle attachment, where it is captured. Tiggrin is also a ligand for the integrin heterodimer, α PS2 β PS, thus contributing to the attachment of the muscle to the tendon matrix (Fogerty et al., 1994). Interestingly, the recruitment of Tiggrin by the muscle appear to be independent of α PS2 β PS (Martin-Bermudo and Brown, 2000).

The myotubes and the tendon cells express different types of integrin heterodimers. The both types of heterodimers share the same β subunit, but they are composed of different α subunits: α PS1 in tendons, and α PS2 in muscles. As mentioned before, α PS2 β PS from the muscle side binds to Tsp and Tiggrin. ECM accumulation can recruit integrin at the muscle ends. In fact, the extracellular parts of

α PS2 and β PS subunits can localize at the attachment sites without their intracellular parts (integrin tails) (Brown, 2011). Conversely, the cytoplasmic tail of β PS can also localize without the extracellular part (Martin-Bermudo and Brown, 1999). This localization is independent of Talin, a cytoplasmic protein essential to link integrin tails to the cytoskeleton (Brown et al., 2002).

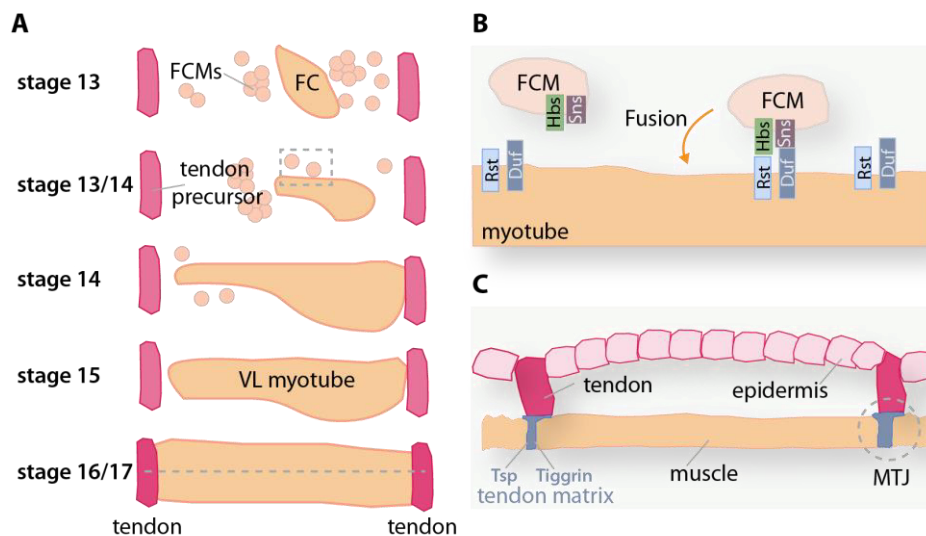


Figure 1.2. Elongation and attachment of the larval muscles in the embryo

(A) The larval myogenesis in the embryo occurs during stages 13 to 17. The formation of a ventral longitudinal (VL) muscle is described to depict the main steps of muscle formation in the embryo. The founder cell (FC), containing the genetic instructions for muscle formation, localizes at the correct position within the hemisegment. The fusion competent myoblasts (FCMs) fuse with the FCs to yield a myotube (details on 1.2B). The growing myotube elongates towards the tendon cells in response to guidance cues secreted by the tendon cells. Once the myotube reaches the tendon cells, the leading edge is remodelled in response to attachment cues to form an attachment with the tendon cells.

(B) FCs and FCMs express cell-type specific transmembrane proteins, containing immunoglobulin (Ig) domains, whose function is to mediate cell-recognition and cell-adhesion. FCs express both Dumbfounded/Kirre (Duf) and Roughest/IrreC (Rst), while FCMs express Sticks and Stones (Sns) and Hibris (Hbs). Duf interacts with Sns and Rst with Hbs. The expression of the two different set of adhesion proteins guarantees only heterotypic fusion events.

(C) Cross-sectional view (dashed line on 1.2A) of an attached VL muscle. The VL muscle attachment type is indirect, meaning multiple muscles connect to a tendon cell with large quantities of a special type of ECM, the tendon matrix, in between. The tendon matrix is composed mainly of Thrombospondin (Tsp) and Tiggrin. Tendon cells and muscles contribute differently to the assembly of this matrix: tendons secrete Tsp, while muscles capture Tiggrin secreted by other cell types.

Lack of α PS2 leads to severe detachment of the muscles during embryogenesis (Brown, 1994), whereas absence of α PS1 results in a milder phenotype (Brower et al., 1995). This phenotypic difference shows that the integrin heterodimer α PS2 β PS has an essential role in anchoring the muscles to the tendon matrix, and thus in the formation of MTJ. In contrast, the contribution of the integrin heterodimers from the tendon is less important.

1.2 Development of the somatic adult musculature

The main activities of a *Drosophila* larva are searching and eating food. The musculature formed during embryogenesis (**Figure 1.3A**) makes the larva a perfect vehicle to navigate in soft substrates, such as decomposing fruit. However, the larval musculature does not support adult movements, such as flight.

Pulses of the steroid hormone 20-hydroxyecdysone (ecdysone) control the end of the larval phase and of the onset of metamorphosis. During metamorphosis, the cylindrical larva has to be remodelled into a fly with legs, wings and an everted head. This dramatic transformation demands the destruction of almost all larval tissues by programmed cell death (PCD) (Zirin et al., 2013).

1.2.1 Formation of the adult abdominal muscles

There are three main sets of adult abdominal muscles: the dorsal, the lateral and the ventral sets. In each segment, the dorsal set is composed of 17-22 parallel longitudinal fibers; the lateral set consists of 20 parallel fibers along the dorsoventral axis; while the ventral set is composed of 5-8 fibers, localized laterally to the ventral midline (Bate et al., 1991; Currie and Bate, 1991). The development of the abdomen dorsal muscles is explained here (**Figure 1.3B**).

The adult abdominal muscles of each segment derive from abdominal adult muscle precursors (AMPs), whose specification occurs during

embryogenesis as explained before (**Figure 1.1**). AMPs are muscle-committed stem-like cells that during metamorphosis build the adult muscles. Distinct populations of abdominal AMPs (**Figure 1.3A**) originate different types of adult abdominal muscles. Similarly to the embryonic FCs, the AMPs express specific identity genes, whose role is to control the development of a particular type of adult muscle. For instance, the lateral AMPs (**Figure 1.3A**), expressing *ladybird*, form all the lateral abdomen muscles (Figeac et al., 2010), .

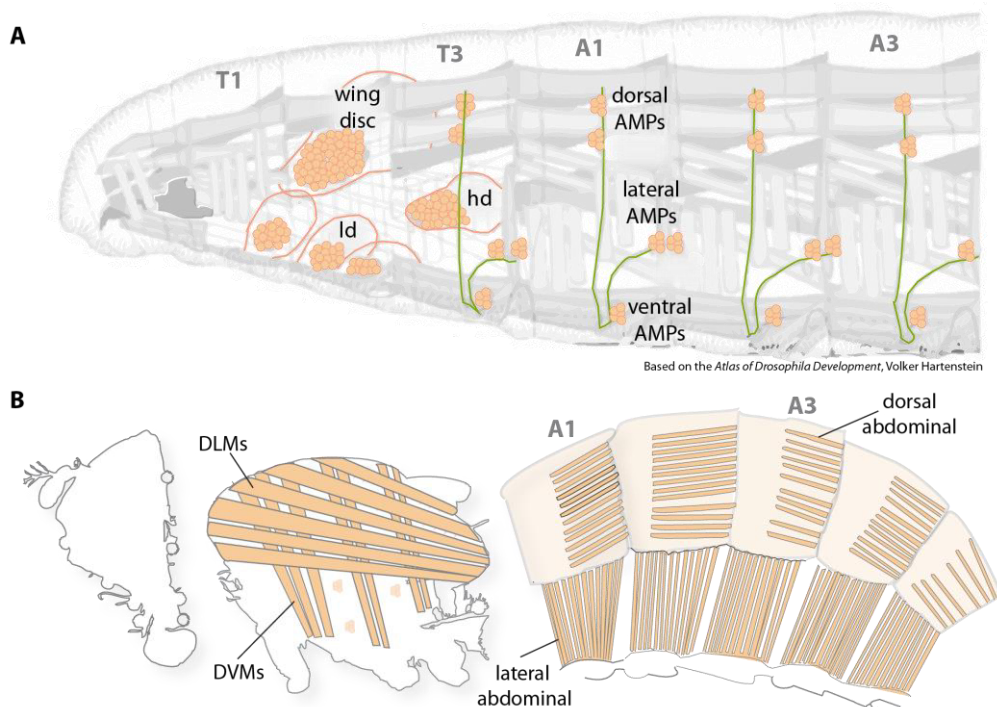


Figure 1.3. The larval and adult *Drosophila* musculatures

(A) Several populations of adult myoblast precursors (AMPs) are present in the L3 larvae. The AMPs that originate the adult abdominal muscles are located in the abdominal hemisegments, associated with nerve bundles. These abdominal AMPs are allocated into three clusters: a ventral, a lateral, and a dorsal. The AMPs that give rise to the indirect flight muscles (IFMs), are located in the thoracic segments, organized in structures called imaginal discs. Two populations of AMPs, one associated with the imaginal wing disc and other presumable with the imaginal leg disc (ld), contribute to the formation of DLMs and DVMs, respectively. The imaginal discs serve as a stem cell niche for the AMPs. Haltere disc (hd).

(B) The adult somatic musculature is composed of several types of muscles. In the abdomen, there are three distinct muscles types: dorsal, lateral and ventral types. The fly thorax contains the IFMs, which are composed of the dorsoventral muscles (DVMs) and the dorsal longitudinal muscles (DLMs). The DVMs are composed of three fiber groups: DVM-I (three fibers), DVM-II (two fibers), and DVM-III (2 fibers). The DLMs are composed of an array of six large fibers.

During the larval phase, the abdominal AMPs proliferate, giving rise to a pool of myoblasts expressing *duf*, a FC-specific gene (**Figure 1.3A**). The proliferation continues during metamorphosis, however, only a subset of these cells retains the expression of *duf*. These cells are the FCs of the adult abdominal muscles (Dutta, 2004). *Duf* is a transmembrane protein important to attract *duf* non-expressing myoblasts to fuse, and thus originating myotubes (Dutta, 2004).

At 28h APF (23-25°C), single FCs, surrounded by myoblasts that resemble the embryonic FCs, are at the positions corresponding to myotube forming sites (Dutta, 2004), (**Figure 1.4A**). Upon fusion, 17-22 myotubes start to form, along the anteroposterior axis (**Figure 1.4B**). These growing myotubes extend long cellular processes mainly towards the anterior side (Currie and Bate, 1991). Presumably, these cellular processes probe the environment for guidance cues, secreted by the tendon precursors in the overlying developing epidermis.

The adult abdominal epidermis develops from histoblasts, from which the tendon precursors are also generated. During metamorphosis, the histoblasts replace the polyploid larval epithelia cells (LECs). The adult epithelium of each abdominal hemisegment is composed of two compartments: an anterior (A) and a posterior (P) compartments. The anterior part of A originates the tendon cell precursors, which are the epidermal attachments of the dorsal abdominal muscles. The muscles attach anteriorly to the tendon cells of the same hemisegment, whereas the posterior tip of the muscle attaches to the tendon cells, located at the anterior part of A, from the next hemisegment (Krzemien et al., 2012), (**Figure 1.4C**).

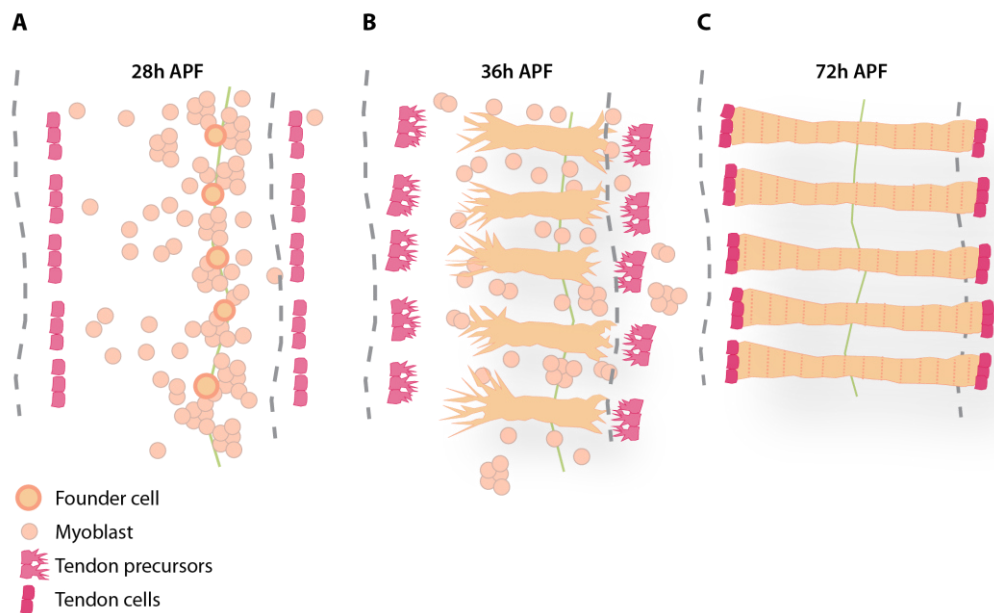


Figure 1.4. Development of the dorsal adult abdominal muscles in the pupa

(A) The FCs occupy the positions of the future muscles within the abdominal segment in the pupa. The FCMs fuse then with each of the FCs to yield a myotube.

(B) The growing myotubes elongate towards the tendon cells in response to presumable guidance cues. These cues make the myotube elongate along the anterior-posterior axis. Both myotube ends display very dynamic filopodia.

(C) The dorsal abdominal muscles attach anteriorly to the tendon cells of the same hemisegment, whereas the posterior tip of the muscle attaches to the tendon cells, located at the anterior part of A, from the next hemisegment.

Interestingly, when the histoblasts start to migrate dorsomedially (18h APF at 23-25° C), *stripe*, a pivotal gene for tendon cell specification, is detected in the most anterior histoblasts from the A compartment (Krzemien et al., 2012). *Stripe* may instruct the developing tendons to secrete molecular cues for guiding the myotubes underneath.

Interestingly, inducing the ectopic expression of *stripe* in different regions of the epithelium leads to dorsal muscles to build ectopic attachments there. This shows that *stripe*, as a master regulator of tendon cell identity, is able to induce other epithelial cells to acquire a tendon cell fate. These tendons induced ectopically are able in turn to secrete guidance cues, thus attracting the growing myotubes towards them (Krzemien et al., 2012).

The mechanisms regulating the abdominal muscle guidance towards the tendon cell are still poorly understood. However, a pivotal player in this mechanism has been identified, Kon. *kon* knockdown in the dorsal

abdominal muscles by RNAi results in a severely disorganized dorsal abdominal musculature (Perez-Moreno et al., 2014). However, how Kon helps the muscle to find the correct attachment is not clear.

1.2.2 Formation of the indirect flight muscles

Flying is a complex activity that requires very specialized muscles. The *Drosophila* adult has two sets of flight muscles: the indirect and the direct sets. Here, the formation of the indirect flight muscles (IFMs), composed of the dorsoventral muscles (DVMs) and the dorsal longitudinal muscles (DLMs), is described (**Figure 1.5**).

The IFMs are fibrillar muscles (Schönbauer et al., 2011), meaning that the sarcomeres are nonaligned. In addition, the IFMs contract asynchronously. These features among others render the IFMs perfect engines for flying. The remaining adult muscles, including the abdominal, are tubular, with laterally aligned sarcomeres. In addition, they contract synchronously (Dickinson, 2006; Wang et al., 2011b). Although the DVMs and DLMs are the unique fibrillar adult muscles, their developmental programs differ: one is formed from FCs and other uses a template-based mechanism.

Two populations of AMPs, one associated with the imaginal wing disc and other presumable with the imaginal leg disc, contribute to the formation of DLMs and DVMs, respectively (Rivlin et al., 2000; Dutta, 2004; Atreya and Fernandes, 2008), (**Figure 1.3A**). The epidermal tissue of the imaginal discs serves as a stem cell niche for the AMPs (Gunage et al., 2014).

1.2.2.1 The developmental program of the DVMs

The DVMs are composed of three groups of muscles: DVM-I (three fibers), DVM-II (two fibers), and DVM-III (two fibers), (**Figure 1.5C**). The three groups of multi-fiber arrays arise from FCs (Atreya and Fernandes, 2008), (**Figure 1.5A**). The FCs can be distinguished from the other myoblasts by the strong expression of *duf* (Dutta, 2004),

larger nuclei, and a cytoskeleton highly enriched in microtubules (Rivlin et al., 2000).

Each FC originates a single DVM fiber (**Figure 1.5B**). At 10h APF (25°C), the seven FCs of the three groups of DVMs are located in the region, where the DVM fibers are going to form. Three FCs originate the three fibers of the DVM-I, two FCs “seed” the two fibers of DVM-II, and finally, two other FCs originate the two DVM-III fibers (**Figure 1.5A**). When the fusion is impaired these FCs are able to form mini DVM fibers (Dutta, 2004).

The mechanism underlying the elongation of these muscles (**Figure 1.5B**) is not yet known. However, it is likely that molecular cues secreted by the tendon cells have a central role in DVMs guidance and attachment.

1.2.2.2 The developmental program of the DLMs

The DLMs originate from larval scaffolds named templates. These scaffolds derive from the three larval dorsal oblique muscles (LOM) in the second thoracic hemisegment (**Figure 1.5A**). These muscles undergo a series of transformations to become templates, which include the loss of the larval sarcomeres, and myotube elongation (6-13h APF at 25°C). The onset of the LOMs remodelling coincides with the beginning of the myoblast migration from the imaginal wing disc towards the LOMs (Fernandes et al., 1991).

During remodelling of the LOMs, their nuclei do not degenerate. In fact, they are transcriptionally active. The templates start to express *duf*, founder cell-specific gene, as early as 6.5 h APF (Dutta, 2004).

From 14h APF onward, the three templates begin to split generating six DLMs myotubes in a hemisegment (Fernandes et al., 1991). Concomitantly, the myotubes elongate towards the anterior and posterior sides of the thorax, where their epidermal attachments are located (Weitkunat et al., 2014), (**Figure 1.5B**). Upon continuous fusion, the DLMs keep elongating towards the epidermis. At 20h APF,

filamentous extension from the tendon cells, decorated with α PS1 β PS integrin (tendon specific integrin heterodimer), meet the extension from the DLMs, which have not yet accumulated α PS2 β PS integrin (muscle specific integrin heterodimer). At 24h APF, a band of α PS2 β PS integrin decorates the muscle ends. α PS1 β PS integrin is still present in the tendon extension, but it is also accumulated in a band, between the processes and the cellular body of the tendon cells (Fernandes et al., 1996; Weitkunat et al., 2014) .

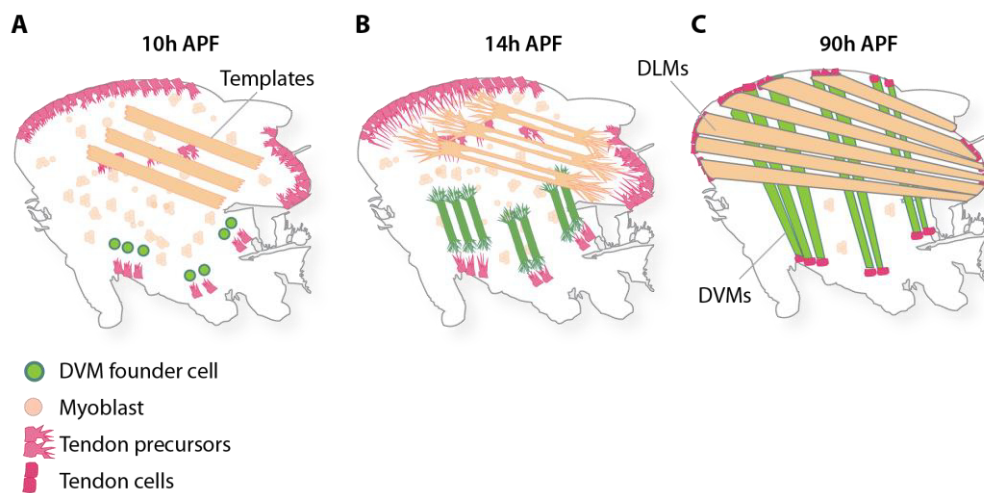


Figure 1.5. Development of the indirect flight muscles, DVMs and DLMs, in the pupa

(A) DVMs: The seven FCs of the three groups of DVMs are located in the region, where the DVM fibers are going to form. **DLMs:** The DLMs originate from larval scaffolds named templates. These scaffolds derive from the three larval dorsal oblique muscles (LOM). These muscles undergo a series of transformations to become templates, which include the loss of the larval sarcomeres, and elongation.

(B) DVMs: FCs fuse with the DVM FCs to form myotubes. These myotubes elongate presumably in response to guidance cues secreted by the tendon cells.

DLMs: The three templates begin to split generating six DLMs myotubes in a hemisegment. Concomitantly, they extend towards the anterior and posterior sides of the thorax, where their epidermal attachments are located.

(C) DVMs: The DVMs are composed of three groups of muscles: DVM-I (three fibers), DVM-II (two fibers), and DVM-III (two fibers). **DLMs:** The DLMs are composed of six fibers per hemisegment.

The tendon cells, to which DLMs attach, derive from the *stripe* expressing epithelial cells in the wing disc. From 8 h APF onwards, the four anterior patches are part of the developing dorsal epidermis from the thorax, and are located anteriorly to the templates. The tendon

cells, which attach to the anterior end of the DLMs, belong to one of the four anterior-epidermal domains-expressing *stripe* (Fernandes et al., 1996; Tiwari et al., 2015). In addition, the posterior *stripe*-expressing patch produces the tendon cells that connect with the posterior end of the DLMs. Kon is essential for the recognition of the tendon cells, and thus to form a stable myotube-tendon attachment (Weitkunat et al., 2014). However, the mechanism underpinning this process is poorly understood.

An interesting question is whether the growing DLMs need guidance cues to find the tendon cells; or if the templates, by increasing their mass in a laterally constricted fashion, elongate and subsequently arrive to their epidermal attachments. Interestingly, when the templates are ablated, the DLMs are able to form *de novo*, which includes finding and attaching to the tendon cells (Farrell et al., 1996). This ability suggests that, if it is necessary, the DLMs formed *de novo* are endowed, possibly, with receptors able to sense guidance cues secreted by the tendon cells.

1.3 Kon is essential for the two phases of *Drosophila* myogenesis

Kon participates in the formation both of larval muscles in the embryo (Schnorrer et al., 2007), and of adult muscles in the pupa (Perez-Moreno et al., 2014; Weitkunat et al., 2014), thus making Kon a pivotal player in the two phases of *Drosophila* myogenesis. The mechanism underlying Kon function is, however, poorly understood.

1.3.1 The role of Kon in the larval myogenesis, in the embryo

In the embryo, Kon has an essential role in the formation of a subset of muscles, called ventral longitudinal (VL) (Schnorrer et al., 2007). At the end of the embryogenesis, stage 17, wild-type VL muscles attach to

tendon cells, located at two opposite segment borders, while *kon* mutant VL muscles are detached and rounded. This severe phenotype results from defects, both in elongation and attachment of these muscles. During elongation, *kon* mutant myotubes do not form a normal leading edge (Schnorrer et al., 2007), which normally characterizes migrating cells (Montell, 2003; Jacquemet et al., 2015), (**Figure 1.6**). This defect suggests that in absence of Kon, the myotubes cannot organize properly the cytoskeleton to elongate.

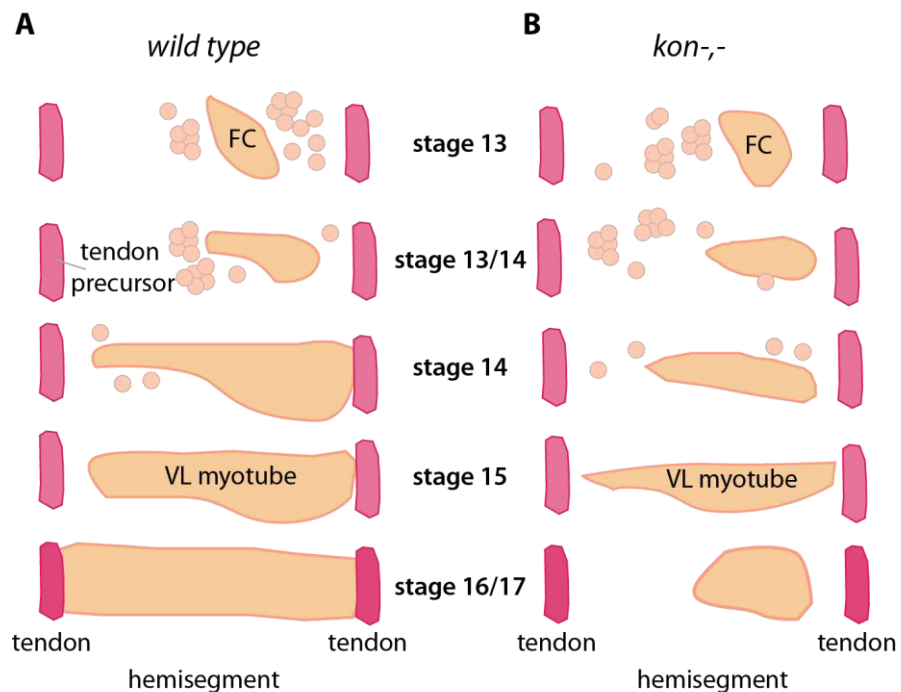


Figure 1.6. Kon is essential for the formation of the VL muscles

(A) Kon participates in the formation of the larval ventral longitudinal (VL) muscles in the embryo. The VL muscles are attached to the tendon cells located at the hemisegment borders. The FCs fuse with the VL FC to give rise to an elongating myotube. During elongation, the VL myotube forms a leading edge, which extends towards the anterior tendons, located at the hemisegment borders. Once the VL myotube reaches the tendon cells, the leading edge enlarges to form an attachment. This remodelling is presumably triggered by attachment cues.

(B) *kon* mutant myotubes do not form a normal leading edge. The VL myotubes that eventually reach the vicinity of the tendon cells exhibit a second type of defect: the underdeveloped leading edge does not enlarge to form an attachment with the tendon cells. This defect results in detached and rounded VL muscles.

A hypothesis to explain the defect observed during elongation could be that Kon functions as a co-receptor. Kon may thus assist in the enrichment of guidance cues in the vicinity of a particular receptor to facilitate its activation. A possible example of such a guidance molecule is Slit. Slit is secreted by the tendon cells, which in turn activates Robo in the VL muscles, steering the elongating myotubes towards the tendon cells (Kramer et al., 2001). Interestingly, a Kon homolog, NG2 was shown to modulate the cell responsiveness to FGF (Binamé et al., 2013), possibly by increasing the local concentration in the vicinity of the FGF receptor. In *kon* mutant embryos, which express normally Slit and Robo, it is interesting to note, that the myotubes have nonetheless problems in the formation of a normal leading edge, which is a morphological hallmark of cellular migration. This, in turn, could indicate that the myotube cannot, for example, sense properly Slit, because without Kon, the concentration of Slit in the vicinity of Robo is not optimal.

The VL myotubes from *kon* mutants that eventually reach the vicinity of the tendon cells exhibit a second type of defect: the underdeveloped leading edge does not enlarge to form an attachment with the tendon cells. This defect results in detached and rounded VL muscles (Schnorrer et al., 2007), (**Figure 1.6B**). The inability in remodelling the cytoskeleton at the leading edge possibly underlies the failure in forming an attachment. The remodulation of the leading edge is presumably necessary to increase the myotube surface, and thus the number of integrin molecules binding to the tendon matrix.

Which molecules could Kon sense that trigger attachment formation? Possible examples are ECM components secreted by the tendon cells, or molecules present at the membrane of the tendon cells, here collectively called attachment cues. These attachment cues could through Kon mediate a switch from an extending to an attaching mode. Together, it is conceivable, that Kon has a dual mode of action, long- and short range, specific for each phase of VL development: elongation

and attachment. The here proposed long- and short-range sensing activities of Kon require, however, to be further investigated.

1.3.2 The role of Kon in the adult myogenesis, in the pupa

In the pupa, Kon participates in the formation of two types of adult muscles, dorsal abdominal muscles (Perez-Moreno et al., 2014) and the DLMs (Weitkunat et al., 2014). *kon* knockdown in the dorsal abdominal muscles results in a severely disorganized dorsal abdominal musculature, consisting of muscles with different angles of orientation in respect to the A-P axis (Perez-Moreno et al., 2014). This suggests that Kon has a role in the guidance of these adult muscles to the correct attachment site. Interestingly, this phenotype also indicates an increase in the contribution of the presumable long-range function of Kon to adult muscle development, probably due to an increase in the distance between the dorsal abdominal muscles and the tendon cell, comparing to the distance between the VL muscles and the tendon cells in the embryo. Nevertheless, the mechanism underpinning Kon function in abdominal muscle is still poorly understood.

Kon also has an essential role in the DLM formation also shown by RNAi knock-down. This study showed that the DLM fibers can reach the tendon cells, however, they fail to form stable attachments, resulting in a rounding muscles similarly to the VL muscles in the embryo (Schnorrer et al., 2007; Weitkunat et al., 2014). Thus, the development of the DLM muscles seems to require more the presumable short-range function of Kon than the long-range one. Interestingly, the DLM elongating fibers may compensate for the lack of the presumable long-range role of Kon by producing very long cellular projections (Weitkunat et al., 2014), whose function could be similar to that of cytonemes. Taken together, these long projections, generated upon *kon* knockdown, could be a strategy of the DLMs to compensate for the inability of sensing guidance cues via Kon.

Nonetheless, the mechanism mediated by Kon in the DLMs remains still poorly understood.

Kon presumably recognizes molecular cues, either secreted or present at the surface of the tendon extensions. A recently published genetic screen examined the function of 1384 genes by knock-down specifically in tendon cells, using the *stripe-GAL4* driver. This RNAi screen aimed to discover new tendon players that participate in the formation and maintenance of the attachments with the DLMs. The knock-down screen yielded 21 candidates, however none of them is a suitable interaction partner of Kon. The 21 candidates identified are involved in different molecular functions, such as intracellular transport, cell adhesion, transcription factor activity, and chromatin remodelling. The gene *myspheroid* (it produces the β PS integrin subunit) and *talin* were among the candidates identified. This demonstrates that integrin and Talin are also essential at the tendon side to form the attachment with the DLM muscles (Tiwari et al., 2015).

To date, there is no particular study addressing the role of Kon in DVMs formation, however, there are preliminary evidences showing that Kon may also be important for DVMs development. These preliminary evidences came from a already mentioned study, which used a general muscles driver, *Mef2*, also expressed in the DVMs, to address the role of Kon in DLMs. *kon* RNAi driven by *Mef2* yielded an empty thorax, meaning that both the DLMs and DVMs were rounded or missing (Weitkunat et al., 2014).

1.3.3 Kon homologues and protein structure

Kon is conserved up to humans. Examples of relevant homologues include NG2, in mouse and rat, and CSPG4 in humans. NG2/CSPG4 is expressed in numerous tissues, such as in the brain (Birey et al., 2015; Dimou and Gallo, 2015), skin (Giangreco et al., 2009) and muscles (Grako et al., 1999; Petrini et al., 2003). In the human muscles, NG2/CSPG4 decorates the sarcolemma. Interestingly, the

highest level of expression in the muscles is observed after birth, although the expression levels decline with the age (Petrini et al., 2003). Thus, it is likely according to this trend that, the expression levels are even higher before birth.

The role of NG2/CSPG4 in vertebrate myogenesis is poorly understood. However, it was shown that the platelet-derived growth factor- α (PDGF α)-receptor in aortic smooth muscles from a *NG2/CSPG4* mouse knockout is unresponsive to one of its ligands, PDGF-AA. Thus, these *NG2/CSPG4* null smooth muscle cells cannot proliferate and migrate upon PDGF-AA treatment (Grako et al., 1999). A possible explanation for this impairment could be that Kon assists in the enrichment of PDGF-AA in the vicinity of its receptor, thus facilitating activation.

The role of NG2/CSPG4 in tumorigenesis (Schrappe et al., 1991; Behm et al., 1996; Shoshan et al., 1999; Chekenya et al., 2002; Wang et al., 2011a), including in metastasis (Burg et al., 1998; Benassi et al., 2009), has been receiving more attention than that in human myogenesis. NG2/CSPG4 was suggested to increase the invasiveness of the tumour, presumably by triggering cell migration via Rho activation (Paňková et al., 2012). The main cause of death by a tumour is organ failure due to invasion of healthy tissues by tumour cells. Hence, tumour cell migration underlies tumour malignancy (Paňková et al., 2009; Jacquemet et al., 2015). In fact, NG2/CSPG4 is expressed in the most malignant brain tumour, glioblastoma (GBM) (Wang et al., 2011a). Furthermore, targeting NG2/CSPG4-expressing cells from the GBM was shown to decrease tumour size as well as to improve the survival, in a mice model for GBM (Poli et al., 2013). The link among NG2/CSPG4, Rho activation and cell migration was also shown in oligodendrocyte precursors cells (OPC) (Binamé et al., 2013).

During metastasis, tumour cells require to sense cytokines secreted distally in the target-organs (Chiang and Massagué, 2008), and thus present at very low concentration in the vicinity of the tumour. A

possible function of NG2/CSPG4 in metastasis could be to concentrate cytokines, and thus facilitating the activation of other receptors important to trigger migration. Interestingly, NG2/CSPG4 was shown to modulate the responsiveness of OPCs to FGF. In OPCs, down-regulation of NG2/CSPG4 impairs FGF-dependent directional migration. However, the impairment is ameliorated upon increase in FGF concentration in the medium (Binamé et al., 2013). This could indicate that NG2/CSPG4 has a role in increasing the local concentration of FGF in the vicinity of the receptor.

The protein structure of Kon is rather complex. Kon has a very large extracellular part composed of two lamininG (LamGs) domains, and 15 chondroitin sulphate proteoglycan (CSPGs) repeats. The intracellular part of Kon is short and contains a PDZ-Binding Domain motif (PDZ-BD) (Schnorrer et al., 2007), (**Figure 1.7**). The Kon homologues are also composed of similar domain types (Staub et al., 2002). The LamG domain is found in several proteins, such as Laminin (Beckmann et al., 1998), Neurexin (Südhof, 2008; Knight et al., 2011) and Slit (Ypsilanti et al., 2010). The CSPG domains of Kon homologues, including the human one, are linked to a sulphated polysaccharide, called chondroitin sulphate (Staub et al., 2002). This modification is not, however, present in Kon (Schnorrer et al., 2007). The lack of chondroitin sulphate combined with a new Pfam classification, considering Kon CSPG domains as cadherin-like instead (Pfam database, (Finn et al., 2016)), may lead in the future to a reclassification of this domain.

How these protein domain clusters contribute to the overall activity of Kon, and thus to muscle formation? The EMS-mutagenesis screen, by which *kon* null alleles were generated, also yielded other alleles with less severe point mutations (Schnorrer et al., 2007). These alleles showed that some domain clusters contribute significantly to the overall Kon activity, and in the embryo to the formation of the VL muscles. One of those alleles, *kon*^{C41} contains a missense mutation in

a LamG domain (**Figure 1.7**). In *kon^{C41}* embryos, the majority of VL muscles were detached, resulting in embryonic lethality. However, this phenotype was not as severe as that of *kon* null embryos (Schnorrer et al., 2007). This could indicate that the residual activity of Kon^{C41} at extracellular level comes from the CSPG domains. An alternative interpretation is that Kon^{C41} could act as a dominant negative, and thus masking the actual activity of the CSPG domains. Taken together, a more conclusive approach is necessary to investigate what is the actual contribution of the LamG domains to the overall activity of Kon.

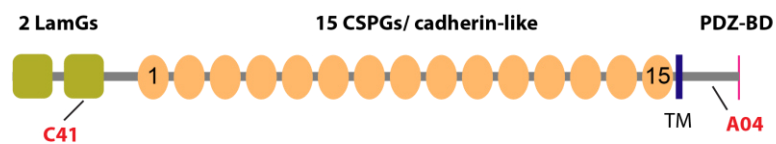


Figure 1.7. Kon protein structure

Kon has a very large extracellular part composed of two lamininG (LamGs) domains, and 15 chondroitin sulphate proteoglycan (CSPGs) repeats. The intracellular part of Kon is short and contains a PDZ-Binding Domain motif (PDZ-BD). *kon^{C41}* contains a missense mutation in a LamG domain. *kon^{A04}* has a nonsense mutation in the intracellular part, yielding a truncated version without the PDZ-BD.

A second allele, *kon^{A04}*, which contains a nonsense mutation in the intracellular part, yielding a truncated version without the PDZ-BD (**Figure 1.7**), revealed that the PDZ-BD is also essential for the overall activity of Kon. This phenotype also resulted in embryonic lethality. In *kon^{A04}* embryos, the majority of the VL muscles were also detached, although, a less severe phenotype than that of *kon* null embryos (Schnorrer et al., 2007). How the PDZ-BD of Kon participates in the formation of the VL muscles is not yet clear.

A possible mechanism is that this domain may anchor proteins that can induce cytoskeletal remodelling during leading edge and attachment formation. This is suggested by an experiment, which investigated the phenotype generated by either overexpression of *kon* or of a mutated version with an inactive PDZ-BD. Overexpressed Kon

increases the number of filopodia in the muscles, although this effect is partially prevented upon inactivation of the PDZ-BD (Schnorrer et al., 2007).

PDZ-BD was shown to interact with Glutamate receptor binding protein, Dgrip (Schnorrer et al., 2007). Dgrip has seven PDZ domains (Swan et al., 2004; 2006), which could recruit potentially up to six additional proteins. These proteins in turn could recruit (directly or indirectly) protein complexes linked to cytoskeletal dynamics. Hence, identifying Kon intracellular interactions partners is essential to understand the link between Kon and cytoskeletal dynamics. And thus, how Kon induces myotube elongation and attachment.

1.3.4 *Drosophila* myogenesis: a system to study challenges in ligand sensing

A central question in developmental biology is how a particular receptor that lies, during different developmental contexts, at various distances to the ligand source, senses efficiently its ligand. An example of such a context is the formation of muscles during the two phases of *Drosophila* myogenesis, which at the onset of their formation, lie at different distances to the ligand source. However, these different distances seem not to interfere with Kon activity.

Studying metastasis provided insights into how a particular population of receptors adapts to sense cytokines secreted distally in the target-organs, and thus present at very low concentration in the vicinity of the metastasizing tumour cell. As a strategy, these cells increase the concentration of the receptor, so that the cells are still responsive to cytokines at lower concentrations (Müller et al., 2001).

The participation of Kon in the two phases of *Drosophila* myogenesis provides a good model to study this problem during development, due to two main reasons, besides the one already mentioned. First, Kon is a putative receptor for guidance and attachment cues. Therefore, it is

likely that its ligand sensing activity is gradually challenged as the muscle increases in size. Second, Kon has a complex extracellular structure, which could be used differently according to the size of the muscle, as a mechanism to solve challenges in sensing a ligand.

1.4 The genomic fosmid library provides tools for studying Kon

The genomic fosmid library provides a source of molecular reagents with an intact cis-regulatory neighbourhood (Ejsmont et al., 2009). This collection is composed of genomic fragments carried by a fosmid vector called FlyFos. FlyFos clones serve as molecular reagents that can be manipulated through recombineering in bacteria. Examples of such manipulations include tagging, deleting and mutating. Then, the resulting construct can be introduced into the fly genome via Φ C31 mediated site-specific transgenesis, generating thus a transgenic fly line (Venken et al., 2006).

The expression of the construct in the fly is then driven by its intact close to endogenous cis-regulatory elements. These regulatory elements, like in the endogenous gene, dictate the expression levels, as well as the spatial and temporal expression patterns of the construct (Ejsmont et al., 2009). Thus, the fosmid approach circumvents possible experimental artefacts generated by overexpression, as well as expression in incorrect tissues, and at incorrect developmental stages. This strategy has been recently used to generate a genome-wide resource to study the localization of endogenous proteins in *Drosophila* (Sarov et al., 2016).

Taken together, the *Drosophila* genomic fosmid library is a suitable resource to obtain a *kon* genomic clone, from which a set of constructs can be engineered, aiming to elucidate the mechanism underlying Kon function in *Drosophila* myogenesis.

1.5 Aim and objectives of this work

The aim of this work was to unveil the mechanism underlying the function of Kon during *Drosophila* myogenesis.

The specific objectives were:

1. Developing *kon* constructs that recapitulate the expression profile of endogenous *kon*, to provide a bone fide understanding of the function of Kon during *Drosophila* myogenesis
2. Identifying the contribution of each Kon domain type to the overall activity of Kon
3. Testing whether Kon participates in myotube guidance
4. Determining which mechanism Kon uses to solve the challenges generated by a larger distance to the putative source of molecular cues, the tendon cells
5. Identifying possible Kon interactions partners

2 Results

The Results chapter is divided in five sections. In section 1, I assessed if the tendon cells precursors, the putative source of guidance cues, were present in *kon* mutant embryos. In addition, I expanded the characterization of *kon* mutant embryos by analysing the distribution of components necessary for muscle attachment. In section 2, I developed and validated a *kon* fosmid derived toolkit that recapitulates the expression profile of endogenous *kon*. In section 3, I describe how this Kon toolkit enabled me to determine which Kon domains are required for the formation of the smaller muscles of the *Drosophila* embryo. In section 4, I tested if Kon participates in myotube guidance. In addition, I assessed if the participation of Kon in muscle formation is customized according to the developmental circumstances of a particular type of muscle. Finally, in section 5, I explain how I applied the tagged constructs from the Kon toolkit to identify Kon interaction partners.

2.1 Tendon cell specification and ECM assembly in *kon* mutant embryos

Kon is essential for the formation of the larval VL muscles in the embryo. The developmental journey of these muscles is composed of a stereotyped sequence of events, which includes myotube elongation and attachment. In *kon* mutant embryos, the VL muscles have defects in cytoskeleton remodelling that are translated into defects either to reach the tendon cells or to form a stable attachment with the tendon cells (Schnorrer et al., 2007).

The VL muscle elongation and attachment are partially non-autonomous processes. In these processes, the VL muscles need extrinsic molecules, namely guidance cues and ECM components, secreted by the tendon cell precursors (Schweitzer et al., 2010). Kon may detect (directly or indirectly) extrinsic molecular information to

induce cytoskeletal remodelling, essential for myotube extension and attachment.

Before I tested this hypothesis, I verified in *kon* mutant embryos (1) if the essential source of guidance and attachment cues, the tendon cells precursors, are specified; and (2) whether components necessary for muscle attachment, such as ECM, are present.

2.1.1 Tendon cells precursors were specified in *kon* mutant embryos

To determine if the tendon cell precursors are specified in *kon* mutant embryos, I immunostained the mutant embryos with a marker for tendon precursors, Short stop (Shot) (Strumpf and Volk, 1998). In *control* embryos, the tendon cell precursors located at the segment border were decorated with Shot (**Figure 2.1A**). In *kon* mutant embryos, I observed the same pattern (**Figure 2.1B**). This pattern indicates that the tendon precursors are specified normally in *kon* mutant embryos. Thus, the VL muscles receive most likely secreted guidance cues, such as Silt (Kramer et al., 2001). Nonetheless, the *kon* mutant muscles cannot form a normal leading edge (Schnorrer et al., 2007), resulting into elongation and attachment defects of the VL muscles.

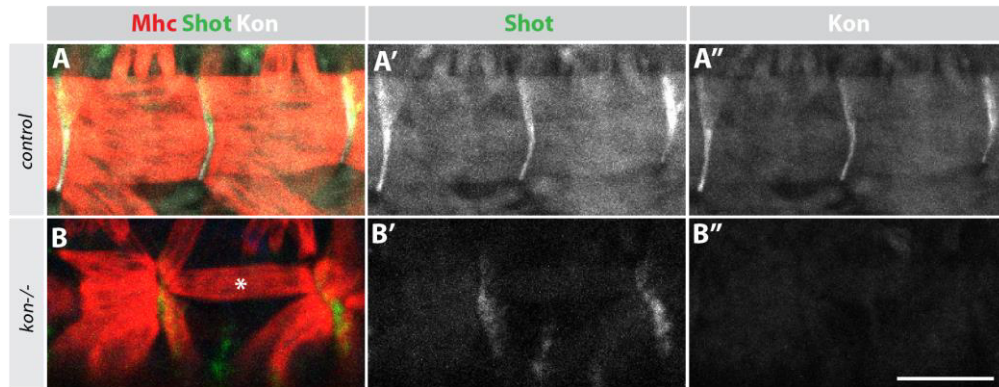


Figure 2.1. Tendon precursors are specified in *kon* mutant embryos

(A) Shot decorates the tendon cell precursors located at the segment borders. In stage 17 *control* embryos (*kon+/-*), the VL muscles attach to those cells.

(B) In stage 17 *kon* mutant embryos (*kon-/-*), the tendon cell precursors, marked by Shot, are specified. The asterisk marks a VL muscle attached. Scale bar = 30 μ m

2.1.2 Tendon matrix components were present in *kon* mutant embryos

The VL muscles attach indirectly to tendon cells via tendon matrix, forming a myotendinous junction (MTJ). This matrix includes ECM components that are for example secreted by the tendon cells (Schweitzer et al., 2010). To form this attachment, the myotubes undergo morphological changes. One of the initial changes is the remodelling of the leading edge. The tips of the myotube enlarge, leading to an increase in surface area contacting with the tendon matrix. This morphological change is part of the transition from a growing to an attaching myotube (Schnorrer and Dickson, 2004). At this stage, integrin is also recruited to the myotube tips to mediate the direct attachment of the muscle to the ECM components, which comprise the tendon matrix (Hynes and Zhao, 2000; Charvet et al., 2012).

I analysed whether the components necessary for attachment are present in *kon* mutant embryos. For this purpose, I analysed the distribution of: (1) the main ECM components of the tendon matrix, Tsp and Tigrin (Fogerty et al., 1994; Bunch et al., 1998; Brown, 2000b; Subramanian et al., 2007); (2) the main ECM receptor, integrin (Brown

et al., 2000), and its cytoskeletal linker, Talin (Brown et al., 2002; Klapholz et al., 2015); (3) as well as the main components of the muscle basement membrane, Laminin and Collagen IV (Borchiellini et al., 1996; Urbano et al., 2009; Pastor-Pareja and Xu, 2011).

Tsp is secreted locally by the tendon cell precursors as early as embryonic stage 12. Lack of Tsp causes muscle defects at embryonic stage 16 (Subramanian et al., 2007). Tsp is localized at the attachment sites (**Figure 2.2A**), as previously reported (Subramanian et al., 2007). In *kon* mutant embryos, Tsp was still localized at the remaining MTJ (**Figure 2.2B**), however its level seemed lower. This requires to be further investigated.

Tiggrin is synthesized distally by other embryonic tissues and recruited by the muscles through a process independent of integrin, the main Tiggrin receptor. *tiggrin* mutants show defects in the muscles during embryonic (Borchiellini et al., 1996) and larval phases (Bunch et al., 1998). Tiggrin was highly enriched at the attachment sites of the VL muscles, at stage 17, the end of larval muscle myogenesis (**Figure 2.2C**), as previously reported (Fogerty et al., 1994; Bunch et al., 1998). In *kon* mutant embryos, Tiggrin was still localized both at the remaining MTJ and at ectopic muscle-muscle attachments, formed by clustering of tendon-detached *kon* mutant-VL muscles (**Figure 2.2D**). This result indicates that the *kon* mutant muscles can still recruit Tiggrin.

In *control* embryos, β PS integrin accumulated at the muscle attachment sites (**Figure 2.2E**), as previously reported (Brown, 1994; Devenport et al., 2007; Pines et al., 2012). In *kon* mutant muscles, β PS integrin was enriched in ectopic attachments between detached neighboring muscles (**Figure 2.2F**). However, it was also present at the remaining MTJs of attached muscles (data not shown). This suggests that Kon is not essential for β PS integrin recruitment at the remaining MTJs.

In *control* muscles, Talin accumulated at the muscle attachment sites (**Figure 2.2G**) similarly to β PS integrin, as previously reported (Brown

et al., 2002; Klapholz et al., 2015). In *kon* mutant muscles, Talin was both at the remaining MTJ and at the ectopic muscle-muscle attachments (**Figure 2.2H**). This can be explained in light of published data showing that ECM components, such as Tsp (**Figure 2.2B**), at ectopic muscle-muscle attachments can recruit integrin, and thus Talin (Brown et al., 2002).

Besides the ECM at the muscle-tendon junction, another layer of ECM, called the basement membrane, is also important for the formation of muscles. The basement membrane surrounds the entire muscle and enables it, for example, to slide smoothly against other muscles, during larval movement (Brown, 2011). The basement membrane is mainly composed of Laminin and Collagen IV (Kalluri, 2003). To analyse the distribution of Laminin on the VL muscles, I used a tagged, fully functional *LanB1-GFP* fosmid obtained from the *Drosophila* TransgeneOme project (Sarov et al., 2016). *LanB1* encodes the β chain, which is incorporated in both Laminin trimers (Urbano et al., 2009).

In *control* muscles, Laminin enveloped the VL muscles with a slight enrichment at the MTJs (**Figure 2.2I**), as previously described (Urbano et al., 2009). In *kon* mutant muscles, Laminin also enveloped the VL muscles, although they were rounded and detached (**Figure 2.2J**). Collagen IV, as a component of the basement membrane, also surrounded *control* VL muscles with a prominent enrichment at MTJs (**Figure 2.2K**), as well as the rounded and detached mutant muscles (**Figure 2.2L**). This result indicates that, in *kon* mutant embryos, the components of the basement membrane are present in comparable levels to those in *control* embryos.

Taken together, these data show that the tendon cell precursors are specified in *kon* mutant embryos. In addition, the ECM components from the tendon matrix, as well as integrin, are present at comparable levels to those of *control* embryos. However, in the absence of Kon, the VL myotubes most presumably do not respond properly to them,

leading to defects during myotube extension and attachment, and subsequently to rounded VL muscles and embryonic lethality (Schnorrer et al., 2007).

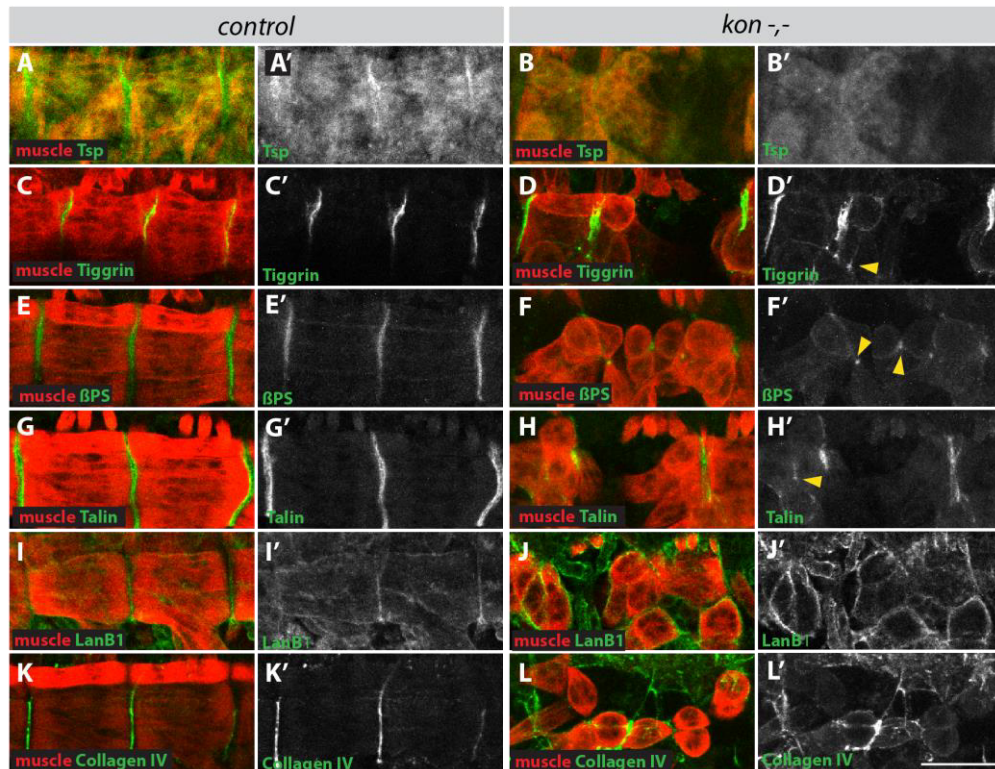


Figure 2.2. Attachment components are present in *kon* mutant embryos

- (A) Tsp accumulates at the attachment sites in *control* embryos (*kon*^{+/-}).
- (B) Tsp localizes at the remaining MTJs from *kon*^{-/-} embryos, however at lower levels.
- (C) Tiggrin accumulates at the attachment sites in *control* embryos.
- (D) Tiggrin localizes at the remaining MTJs, as well as at the ectopic muscle-muscle attachments (yellow arrowhead), in *kon* mutant embryos.
- (E) β PS localizes at the attachment sites in *control* embryos.
- (F) β PS accumulates at the ectopic muscle-muscle attachments (yellow arrowheads) in *kon* mutant embryos.
- (G) Talin accumulates at the attachment sites in *control* embryos.
- (H) Talin is present at the remaining MTJs, as well as at the muscle-muscle ectopic attachments (yellow arrowhead), in *kon* mutant embryos.
- (I) LanB1 is incorporated in both Laminin trimers. Laminin envelops the larval muscles in *control* embryos.
- (J) Laminin encloses the VL muscles, although they are rounded and detached in *kon* mutant embryos.
- (K) Collagen IV envelops the larval muscles. In addition, Collagen IV accumulates at the muscle attachments in *control* embryos.
- (L) Collagen IV envelops the VL muscles, although they are rounded and detached. In *kon* mutant embryos, some ectopic muscle-muscle attachments still contain high levels of Collagen IV. Scale bar = 30 μ m. All embryos are stage 17.

2.2 Development and validation of molecular tools to study the functional domain types of Kon

Kon participates in the formation of muscles with very different sizes (Schnorrer et al., 2007; Perez-Moreno et al., 2014; Weitkunat et al., 2014). Often larger muscles start to develop further away from their attachment sites, the tendon cells, than smaller muscles do. Nevertheless, both type of muscles have to be able to sense tendon-derived ligands, independently of the distance that they have to diffuse to reach the muscles. The distance of diffusion may, however, impose some challenges to the receptors, namely a decrease in concentration of the ligand in their vicinity.

Kon protein has a complex and large extracellular part, composed of two LamG and 15 CSPG domains (Schnorrer et al., 2007). These two domain clusters could be used differently according to the size of the muscles, as a mechanism to respond efficiently to a decrease in ligand concentration, generated by longer distances of diffusion.

To elucidate how the individual Kon domains participate in the formation of the *Drosophila* muscles, I generated a toolkit using as a starting material, a genomic *kon* clone. This clone was provided by the *Drosophila* genomic fosmid library (Ejsmont et al., 2009). A particular gene present in one of those clones can be, for example, tagged through recombineering in bacteria. This tagged gene can be subsequently integrated into the *Drosophila* genome, thus generating a transgenic fly expressing a tagged version of that particular gene.

The workflow to create such a fly line includes a multitude of steps, such as tagging through recombineering; injecting the tagged fosmid in *Drosophila* embryos for genomic integration; screening the resulting flies to identify the ones that have incorporated successfully the fosmid in their genome; and finally, characterizing the expression and functionality of the tagged protein.

As a proof of principle, I have tested the entire workflow using a small group of fosmid clones. From this work, two fly lines of tagged sarcomeric proteins, Stretchin-GFP and Obscurin-GFP, were applied to study how a RNA-binding protein Arrest (Aret, also known as Bruno) controls splicing of IFM specific isoforms (Spletter et al., 2015).

Numerous conditions were tested to establish an efficient workflow for the generation of the fly lines from the TransgeneOme project. I have contributed to the design and optimization part of this workflow, as well as to test the functionality of the tags. These tested tags and the optimized workflow were applied to generate 880-tagged transgenic fly lines, which are available for the entire scientific community (Sarov et al., 2016).

Finally, I have also applied this workflow to generate tools for studying the functional domains of Kon.

2.2.1 Validation of the *kon* fosmid

To engineer deletions and mutations in *kon*, as well as to add tags, I selected the clone FlyFos021621 from the genomic fosmid library (Ejsmont et al., 2009). This clone carries an approximately 44 kb genomic fragment, which includes the complete known *kon* locus. The *kon* locus comprises about 14 kb (**Figure 2.3A**), with an 8,276 nucleotides long mRNA, distributed in twelve exons. The majority of the signal sequence is harboured in the second exon, however the last amino acid of the signal sequence is encoded by the third exon (Schnorrer et al., 2007).

To verify the functionality of *kon* harboured in the genomic fragment from the FlyFos021621 clone, I performed a functional assay. I introduced the genomic clone into the fly genome, and then crossed it into a *kon* mutant background (see Material and Methods), to test for rescue of this phenotype. A *kon* mutant embryo has rounded VL1 muscles, which were labelled by 5053-Gal4/UAS-GMAGFP (Schnorrer et al., 2007) (**Figure 2.3B, C**). Because of these defects, *kon* mutants

die during embryogenesis (Schnorrer et al., 2007). Upon expression of *kon* derived from the FlyFos021621 clone, the rounded muscle acquired a normal morphology and attachment pattern (**Figure 2.3D**), indistinguishable from those of control embryos (**Figure 2.3B**). In addition to the full rescue of the embryonic phenotype, the animals carrying this clone reached adulthood, and could be maintained as a homozygous stock.

This functional assay demonstrated that the FlyFos021621 clone contains a functional copy of *kon*, and it is thus suitable as a molecular reagent to engineer constructs to characterize the function of the Kon domains.

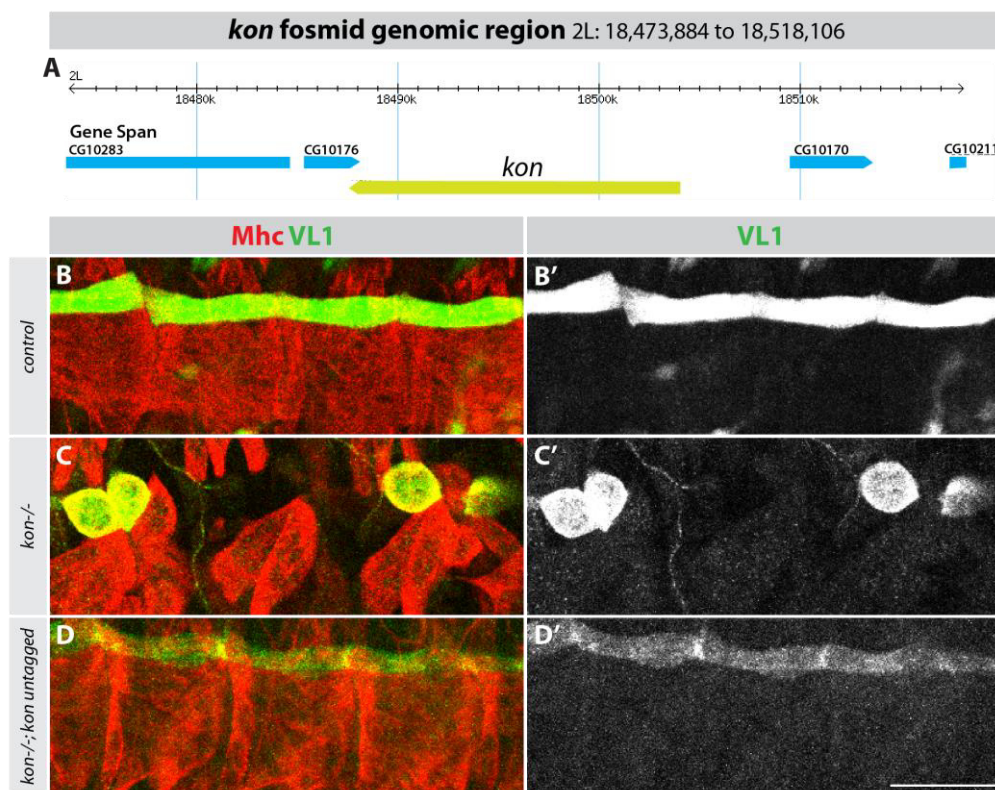


Figure 2.3. *kon* from FlyFos021621 clone is completely functional

(A) The genomic fragment from the FlyFos021621 clone.

(B) Stage 17 embryo expressing GMA-GFP using the VL1 muscles-specific 5053-GAL4 driver in *wild-type* background.

(C) Stage 17 embryo expressing GMA-GFP using the VL1 muscles-specific 5053-GAL4 driver in a *kon* mutant background. The VL1 muscles are completely rounded and detached.

(D) Stage 17 embryo expressing Kon derived from FlyFos021621 clone in a *kon* mutant background. Kon provided from the fosmid clone rescues the *kon* mutant phenotype. Scale bar = 30 μ m

2.2.2 Generation of tools to detect the localization of Kon during myogenesis

Using the functional *kon* fosmid (FlyFos021621), I generated a set of tagged clones that allow *in vivo* localization studies of the tagged Kon protein.

In growing myotubes, the polarized localization of Kon at the attachment sites (Schnorrer et al., 2007) is, presumably, important for the detection of molecular cues, necessary to orchestrate myotube elongation and attachment. Therefore, I expected that at least one of the domains of Kon mediates Kon enrichment at the tips of the muscles. Testing this hypothesis requires the detection of the engineered Kon proteins after deletion or mutation of a particular domain or domain cluster. A good way to detect the localization of proteins is using a tag. It is essential, however, to preserve the biological activity of the protein upon tagging. For that purpose, I tested two variables: (1) the size of the tag and (2) the location of the tag within the protein.

To address both issues, I tested three cassettes, containing three different tag sequences: (1) a GFP-containing cassette (38 kDa), (2) a HA cassette (4 kDa), and (3) a V5-containing cassette (13 kDa). The GFP- and the V5-containing cassettes also include 3xFLAG and 2xTY1 sequences (see Material and Methods). These three cassettes were introduced at two different locations within the coding sequence of Kon: (1) immediately after the signal sequence; and (2) at the intracellular part of Kon, immediately after its transmembrane domain. In this way the C-terminal PDZ-BD is left intact.

I applied bacterial recombineering technology to insert the different tags into FlyFos021621 clone (see Material and Methods). The tagged clones were next integrated into the fly genome by site-specific transgenesis into VK00033 on chromosome 3. I tested four tagged proteins, Kon-GFPaSS (after signal sequence), Kon-HAaSS, Kon-

GFP_{intra}, and Kon-V5_{intra} (**Figure 2.4A, D, G, J**). All of them localized at the tips of the VL muscles, in *wild-type* background, similarly to the endogenous protein (**Figure 2.4B, E, H, K**). Thus, the tags do not interfere with the localization ability of the Kon protein.

To test functionality of these constructs, I crossed them in a *kon* mutant background. The VL muscles expressing exclusively Kon-GFPaSS were either partially attached or rounded (**Figure 2.4C**), whereas the muscles expressing Kon-HAaSS were fully attached (**Figure 2.4F**). This result may suggest (1) that the large GFP tag obstructs the interaction between the two LamGs at the N-terminus with a putative ligand; and (2) that the two LamG domains have an essential role in Kon activity during myogenesis. In contrast, the small HA tag after the signal sequence resulted in a fully functional Kon. In addition to the full rescue of the embryonic phenotype, the animals carrying this clone reached adulthood, and can be maintained as a homozygous stock.

Interestingly, both the GFP as well as the V5 tag, within the Kon intracellular part, produced VL muscles with wild-type morphology (**Figure 2.4I, L**), indicating that these two-tagged versions of Kon are fully functional. Moreover, these two-tagged constructs yielded adult flies, which can be maintained as a homozygous stock. Because *kon-V5intra* was smaller than *kon-GPFintra*, and thus easier to modify through recombineering, I decided to use *kon-V5* fosmid in the following experiments, as the parent construct to delete or modify the various domains of Kon.

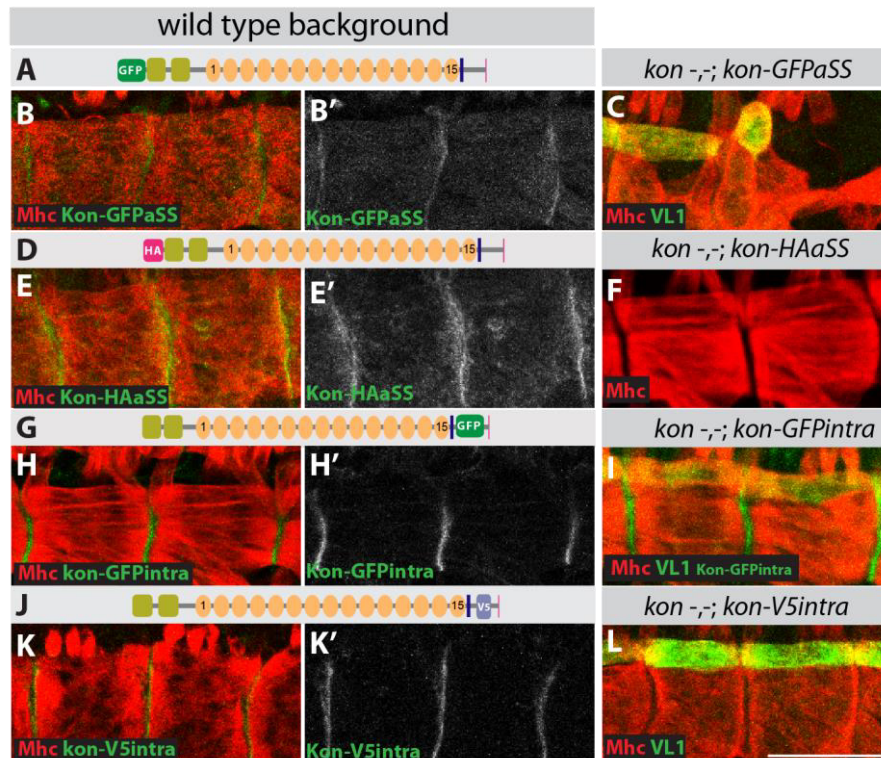


Figure 2.4. Tagging the intracellular part of Kon preserves its biological activity
 (A-C) Kon containing (A) a GFP tag (38 kDa) after the signal sequence expressed in (B) *wild-type* background or (C) in a *kon* mutant background. This GFP tagged version of Kon cannot rescue the mutant phenotype.
 (D-F) Kon containing (D) a HA tag (4 kDa) after the signal sequence expressed in (E) *wild-type* background or (F) in a *kon* mutant background. This HA tagged version of Kon produced VL muscles with wild-type morphology.
 (G-I) Kon with (G) an intracellular GFP tag (38 kDa) expressed in (H) *wild type* or (I) in a *kon* mutant background. The VL muscles have wild-type morphology.
 (J-L) Kon with (J) an intracellular V5 tag (13 kDa) expressed in (K) *wild type* or (L) in a *kon* mutant background. The *kon* mutant phenotype was fully rescued. Scale bar = 30 μ m

2.3 The role of Kon domains during myogenesis of the larval somatic muscles in the embryo

2.3.1 Expression levels of the Kon fosmid derived constructs

The Kon protein can be divided into three major domain types: two N-terminal LamGs, 15 extracellular CSPGs, and a C-terminal intracellular part terminating in a PDZ-binding domain (PDZ-BD). To study the role of each domain of Kon, I engineered a set of *kon* deletion constructs.

This set of constructs is derived from *kon-V5intra*, which is fully functional (**Figure 2.4L**). Using this construct, I deleted either (1) the two LamGs (*kon-V5 ΔLamGs*), or (2) the 15 CSPGs (*kon-V5 ΔCSPGs*). In addition, I (3) mutated the PDZ-BD (*kon-V5 PDZ-BD mutated*) by replacing the last amino acid, valine, by glycine (see Material and Methods) (**Figure 2.5A**).

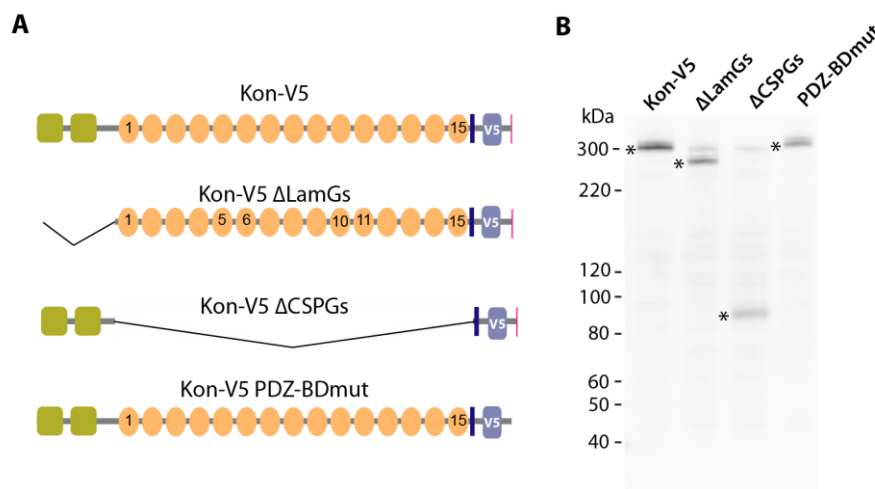


Figure 2.5. Kon-V5 derived toolkit

(**A**) Schematic representation of the Kon-V5 derived toolkit. The main domain types of Kon were either deleted or mutated.

(**B**) The proteins levels of Kon-V5, Kon-V5 ΔCSPGs, Kon-V5 ΔLamGs and Kon-V5 PDZ-BD mutated were assessed. The four proteins were expressed in *wild-type* embryos. The embryos were then lysated and the proteins were pulled down with a V5 antibody. The four proteins are expressed at comparable levels.

Before assessing the contribution of each domain type to the overall activity of Kon, I first compared the level of protein expression of each of the constructs by Western blot analysis. Either deletions or mutation of the main domain types of Kon did not interfere with the protein stability (**Figure 2.5B**).

The following section describes the applications of these tools to assess the contribution of each Kon domain type to the larval muscle formation in the embryo.

2.3.2 The LamG domains and the PDZ-BD of Kon are essential for the formation of the VL muscles

To pinpoint the contribution of each Kon domain to the formation of the VL muscles, I performed a functional genetic rescue assay by expressing *kon-V5* (positive control), *kon-V5* Δ LamGs, *kon-V5* Δ CSPGs and *kon-V5* PDZ-BDmut in a *kon* mutant background. In this functional assay, the biological activity of each construct was then quantified, at embryonic stage 17, by scoring two variables: the length and attachment site size of the VL1 muscle. For scoring attachment site, I stained the muscles with Talin, the protein that links the integrin to the cytoskeleton (Brown et al., 2002).

The two phenotypic extremes in this assay were the *kon* mutant embryos, with mostly rounded and detached VL1 muscles (**Figure 2.6B, H**), comparing to the wild-type or Kon-V5 embryos, with fully attached VL1 muscles (**Figure 2.6A, C, H**).

I observed that the VL muscles expressing exclusively *kon-V5* Δ LamGs were 25 percent shorter (median value) and had attachment sites 50 percent smaller (median value), (**Figure 2.6E, H**). Although the lack of the two LamGs produced VL muscles with severe defects, this phenotype was less severe than that of the *kon* null situation (**Figure 2.6B**). By contrast, the VL1 muscles expressing *kon-V5* Δ CSPGs exhibited wild-type morphology (**Figure 2.6D, H**). Taken together, the extracellular domains of Kon had different roles in VL muscle formation. This striking difference indicates that the two LamGs are essential for VL muscle formation, while the 15 CSPG domains are dispensable at embryonic stage. This difference also suggests that the two LamG domains are important to interact with a putative extracellular ligand. However, the lack of the LamG domains did not generate a *kon* null phenotype, suggesting that the CSPG domains could also interact with the extracellular ligand.

Finally, to assess the role of the PDZ-BD, as most likely the only domain that conveys intracellularly the activation signalling from the extracellular part of Kon, I evaluated the biological activity of the *kon-V5 PDZ-BDmut* construct. I observed that the VL muscles expressing Kon-V5 PDZ-BDmut were 37 percent shorter (median value) and had attachment sites 50 percent smaller (median value), than wild-type muscles (**Figure 2.6F, H**). This indicates that the C-terminal PDZ-BD is also essential for Kon function and thus for VL muscles formation.

The essential roles of the two LamGs and the PDZ-BD were additionally confirmed by the inability of Kon-V5 Δ LamGs, and Kon-V5 PDZ-BDmut to rescue the embryonic lethality of *kon* mutants (**Figure 2.7A**). Together, these data yielded the main conclusion that, Kon consisting of the LamG domains, the transmembrane domain (TM), and the intracellular part with its PDZ-BD comprises a “compact” version of Kon, which is sufficient for the formation of the VL muscles in the embryo. In addition, this compact version of Kon generated viable larvae (**Figure 2.7A**).

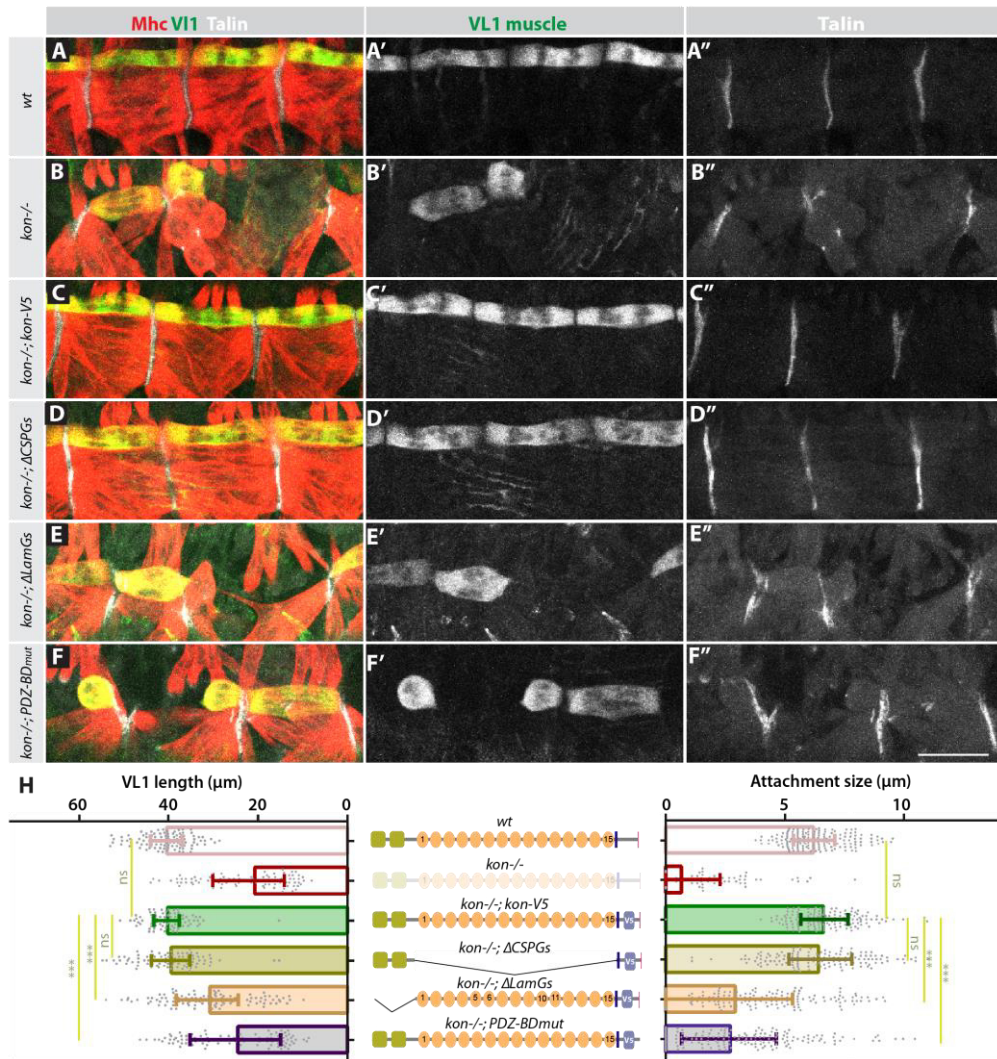


Figure 2.6. A compact version of Kon is sufficient for the formation of VL muscles in the embryo

(A) VL1 muscles in *wild-type* background. The muscles are fully attached.

(B) VL1 muscles in a *kon* mutant background.

(C) Expression of *kon-V5* in a *kon* mutant background. The VL muscles are fully attached.

(D) Expression of *kon-V5* Δ CSPGs in a *kon* mutant background. The VL muscles are fully attached.

(E) Expression of *kon-V5* Δ LamGs in a *kon* mutant background. The VL muscles are shorter and rounded. Talin accumulates at the remaining MTJs.

(F) Expression of *kon-V5* PDZ-BDmut in a *kon* mutant background. The VL muscles are shorter and detached. Talin accumulates at the remaining MTJs.

(H) The VL1 length and attachment size quantification of all the genotypes above mentioned. Stage 17 embryos, expressing all GMA-GFP in the VL1 muscle. Median and the interquartile range (IQR). $n = 60$ -120 VL muscles, number of embryos = 20-30 per condition. ns (not significant), *** $p < 0.001$. Scale bar = 30 μ m

2.3.3 The 15 CSPG domains have a minor role in attachment formation

The attachment sites are essential to withstand the tension generated upon muscle contraction. The muscles at stage 17, at the end of embryogenesis, are already under tension, although this tension is supposedly lower than the tension generated upon larval movement (Yuan et al., 2010; Pines et al., 2012). This leads to the question, whether this “compact” version of Kon produces attachments that are able to withstand the forces generated during larval movement.

Analysing the VL muscle morphology at third instar larval stage (L3) provides the opportunity to directly test if the attachments are completely functional, and thus able to withstand forces generated during larval movement. To test whether the lack of the 15 CSPGs impacts the ability of the attachment sites to bear force upon larval movement, I analysed the morphology of the VL muscles in *kon-V5* Δ CSPGs L3 larvae. These muscles experienced more than 72 hours of intense activity. The VL muscles in wild-type L3 larvae were attached to the hemisegment border, like observed at the end of embryogenesis (**Figure 2.7B, D**). Around 25% of the VL muscles from *kon-V5* Δ CSPGs larvae were however lost, supposedly due to detachment (**Figure 2.7C, D**), thus showing that those attachment sites were not able to bear the forces generated upon larval movement. This indicates that 15 CSPGs have a minor role in generating stable VL attachments, possibly through sensing a particular attachment cue.

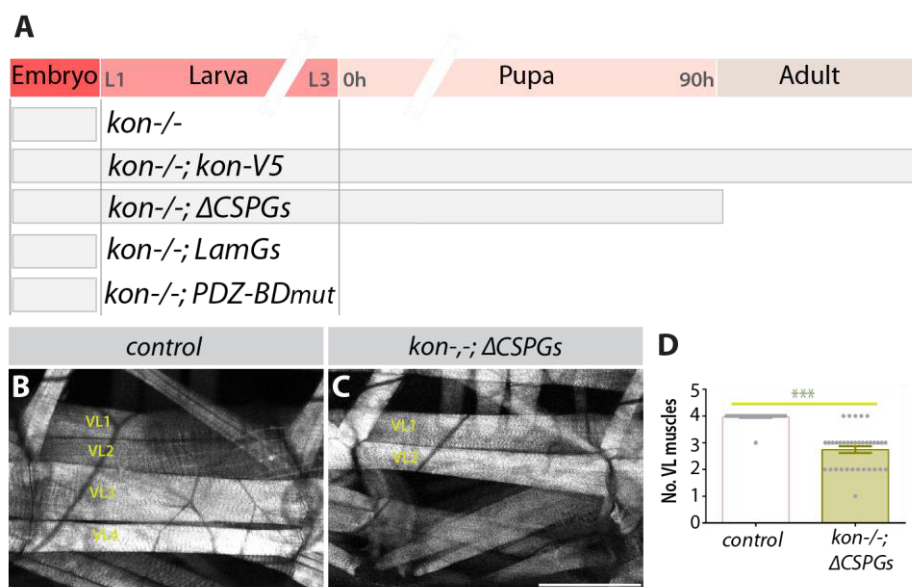


Figure 2.7. The 15 CSPG domains have a minor role in generating stable VL attachments

(A) The viability of the fly lines expressing exclusively *kon-V5*, *kon-V5 ΔCSPGs*, *kon-V5 ΔLamGs* or *kon-V5 PDZ-BDmut*. Either deleting the two LamG domains or mutating the PDZ-BD causes embryonic lethality. Deleting the CSPGs domains results in pupal lethality.

(B) A representative live image from a L3 larva hemisegment expressing GMA-GFP driven by *Mef2-GAL4*. The VL muscles are fully attached.

(C) A representative live image from a L3 larva expressing *Kon-V5 ΔCSPGs* together with GMA-GFP driven by *Mef2-GAL4*, in *kon* mutant background. Some VL muscles are missing. Scale bar = 200 μm

(D) Quantification of the number of VL muscles per hemisegment (Means ± SEM. n = 20-30 hemisegments, per 10-20 larvae per condition. ****p* < 0.001).

Interestingly, the 15 CSPGs are conserved up to humans (Schnorrer et al., 2007), arguing that these domains are likely to have an important function. However, the data, presented so far, indicated that the 15 CSPG domains have a minor role in VL attachment. A possible explanation is that *Kon-V5 ΔLamGs* may not localize as well as the other mutated versions of *Kon*. In other words, *Kon* may require the two LamGs to localize at the attachment site, and thus to participate in the VL development.

2.3.4 Kon requires the LamG domains to localize at the muscle attachment site

To determine if a particular domain is important for Kon localization, I measured the enrichment ratio of Kon-V5, Kon-V5 Δ LamGs, Kon-V5 Δ CSPGs, and Kon-V5 PDZ-BDmut proteins at muscle attachment sites, during stages 15-17, in a wild-type background. The enrichment ratio was calculated by normalizing the fluorescence intensity of the V5 staining, from a representative area at the attachment site, with the fluorescence intensity of the adjacent cytoplasmic area.

All three mutated proteins, Kon-V5 Δ LamGs, Kon-V5 Δ CSPGs, and Kon-V5 PDZ-BDmut localized significantly less than Kon-V5 protein at the tips of the VL muscles, throughout stages 15-17 (**Figure 2.8**). This result indicates that all the three domain types contribute to a normal localization of Kon at the tips of the VL muscles.

In addition, I observed that Kon-V5 Δ CSPGs localized similarly to Kon-V5 PDZ-BDmut, whereas Kon-V5 Δ LamGs localized the least at the attachment sites (**Figure 2.8F, L, R**). This indicates that the two LamGs play a major role in localizing the Kon protein to the attachment sites.

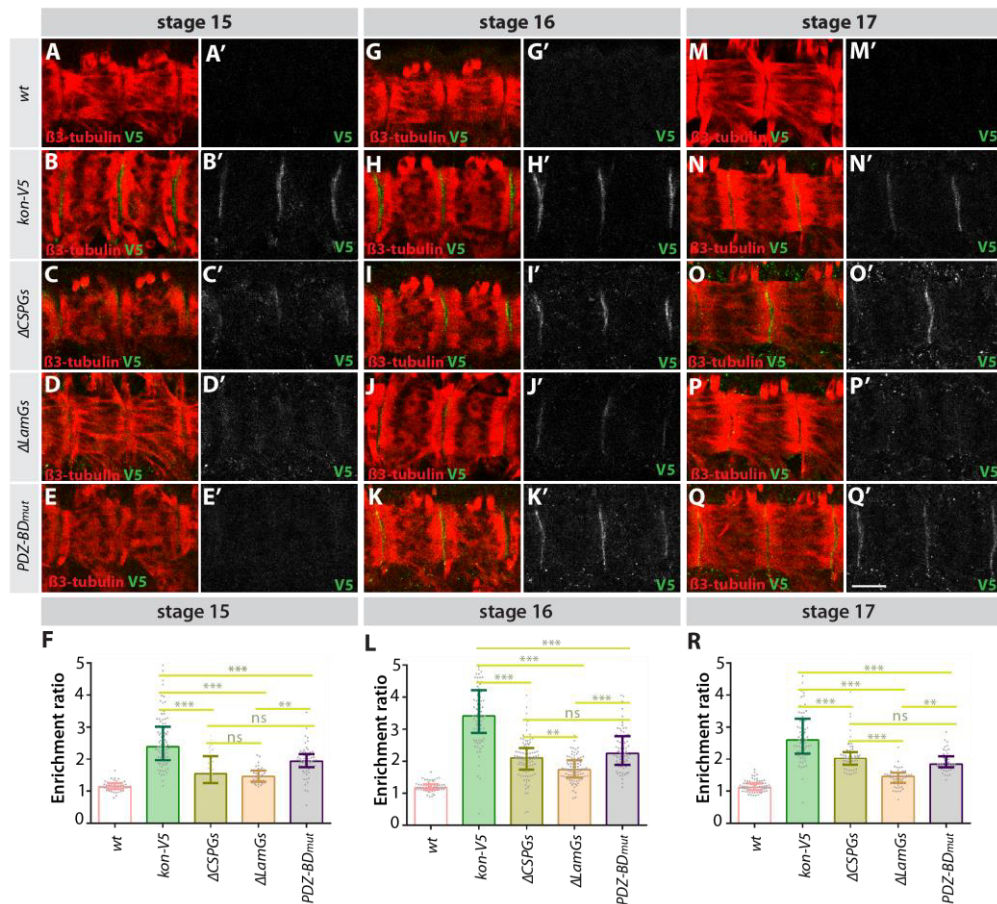


Figure 2.8. Kon requires the LamG domains to localize at the attachment site
 (A-E) Stage 15 embryos stained with V5 antibody to reveal the localization of the Kon-V5 derived constructs in *wild-type* background. (A) Wild-type embryos. This condition was a control for the specificity of the V5 antibody. (B) Kon-V5. (C) Kon-V5 Δ CSPGs. (D) Kon-V5 Δ LamGs. (E) Kon-V5 PDZ-BDmut.
 (F) Enrichment ratio of the Kon-V5 derived constructs, expressed in *wild-type* background, at stage 15.
 (G-L) Stage 16 embryos stained with V5 antibody. (G) Wild-type embryos. (H) Kon-V5. (I) Kon-V5 Δ CSPGs. (J) Kon-V5 Δ LamGs. (K) Kon-V5 PDZ-BDmut.
 (L) Enrichment ratio of the Kon-V5 derived constructs expressed in *wild-type* background at stage 16.
 (M-R) Stage 17 embryos stained with V5 antibody. (M) Wild-type embryos. (N) Kon-V5. (O) Kon-V5 Δ CSPGs. (P) Kon-V5 Δ LamGs. (Q) Kon-V5 PDZ-BDmut. Scale bar = 20 μ m
 (R) Enrichment ratio of the Kon-V5 derived constructs expressed in *wild-type* background at stage 17. Median and the interquartile range (IQR). n = 50-120 attachment sites, number of embryos = 25-35 per condition. ns (not significant), ** $p < 0.01$, *** $p < 0.001$.

2.3.5 The CSPG domains synergize with the LamG domains

Kon-V5 Δ LamGs protein cannot localize properly at attachment sites (**Figure 2.8**), thus defects in localization may underlie the problems in VL formation shown before (**Figure 2.6**). To assess the biological activity of the extracellular domains independently of their concentration at the attachment site, I overexpressed *kon* Δ LamGs and *kon* Δ CSPGs using a *UAS* promoter, instead of the endogenous *kon* cis-regulatory elements, present in the fosmid-derived constructs. These *UAS-constructs* were exclusively overexpressed in a single VL1 muscle, per hemisegment, in a *kon* mutant background, using a *5053-GAL4* driver. The two overexpressed proteins, Kon Δ CSPGs and Kon Δ LamGs, were highly enriched at the attachment sites (**Figure 2.9D, E**). Their protein levels were higher than the levels of endogenous Kon (**Figure 2.9A**). Therefore, the attachment sites of the VL1 muscles were fully saturated with each of the overexpressed Kon mutated proteins.

To quantify the biological activity of the two overexpressed mutated proteins, Kon Δ LamGs and Kon Δ CSPGs, I scored the length and attachment site size of the VL1 muscles. Remarkably, overexpression of Kon Δ LamGs resulted in VL muscles with length and attachment site size (**Figure 2.9E, H**) similar to the ones, observed upon overexpression of Kon Δ CSPGs (**Figure 2.9D, H**). This indicates that when Kon Δ LamGs is expressed at high levels, leading to sufficient localization of the mutated protein to the myotube tips, the 15 CSPGs are as functional as the LamG domains. This prompted me to test, if the CSPG domain can synergize extracellularly with the LamG domains, when they are expressed together. To test this, I overexpressed *kon* full length in VL1 muscles, in a *kon* mutant background.

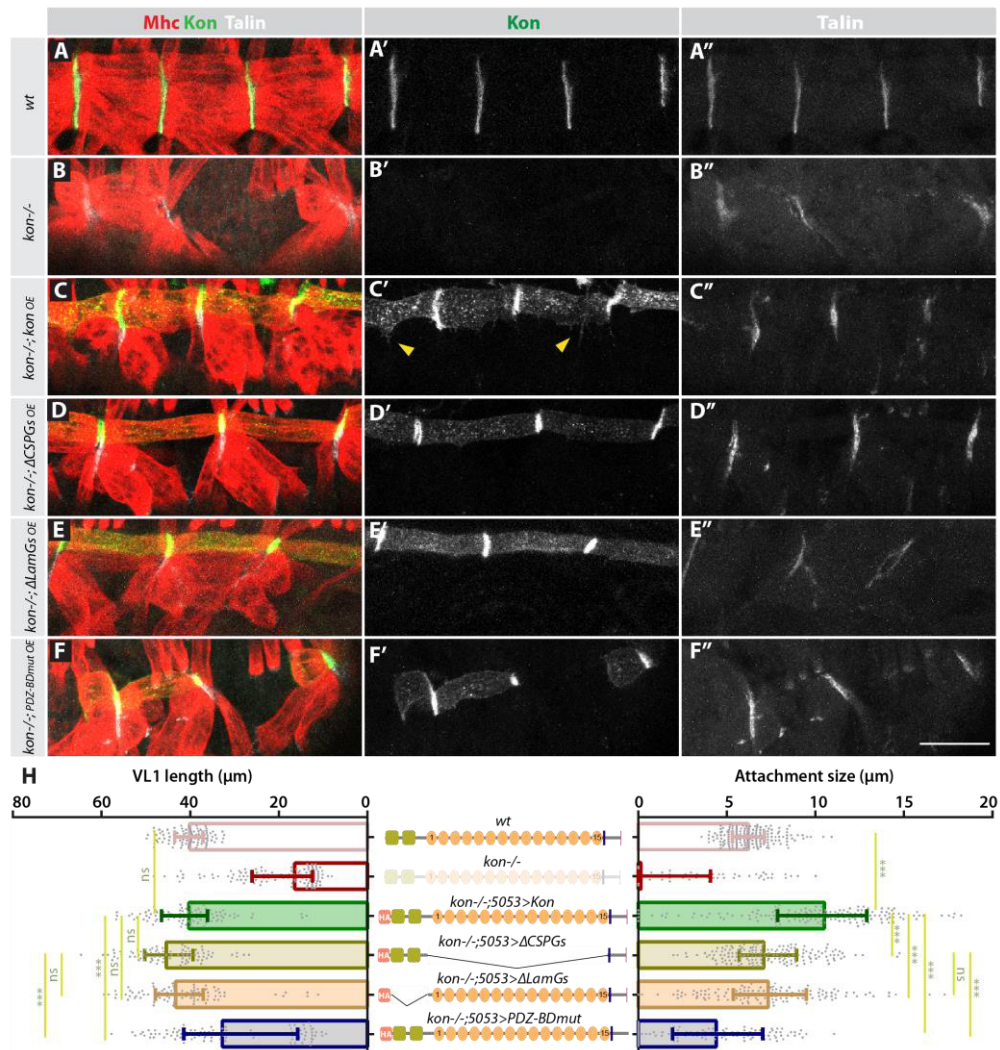


Figure 2.9. The CSPG domains synergize with the LamG domains

(A-F) Stage 17 embryos were stained with Mhc, Kon, and Talin.

(A) Kon and Talin localize at the attachment sites of the VL1 muscles in *wild-type* embryos.

(B) In *kon* mutant embryos Talin localizes at the remaining muscle attachments.

(C) Overexpression of Kon using 5053-GAL4 driver (VL1 muscles) in a *kon* mutant background. The yellow arrowheads pointed to filopodia at the lateral side of the VL1 muscles.

(D) Overexpression of Kon Δ CSPGs driven by 5053-GAL4 in a *kon* mutant background. The VL1 muscle displays wild-type morphology.

(E) Overexpression of Kon Δ LamGs driven by 5053-GAL4 in a *kon* mutant background. The construct enrichment at the attachment site is higher than the enrichment of Kon in wild-type attachments. This high enrichment boosted the rescue ability of Kon Δ LamGs.

(F) Overexpression of Kon PDZ-BDmut driven by 5053-GAL4 in a *kon* mutant background. Increasing the levels of the construct does not lead to a boost of the rescue ability of Kon PDZ-BDmut. Scale bar = 30 μ m

(H) Quantification of the VL1 length and the attachment site size, detected here by Talin staining. Median and the interquartile range (IQR). $n = 60$ -120 VL muscles, number of embryos = 20-35 per condition. ns (not significant), *** $p < 0.001$.

Kon overexpression resulted in larger attachment sites (**Figure 2.9H**), and in filopodia formation at the lateral sides of the VL1 muscles (**Figure 2.9C**), while the overexpression of Kon Δ CSPGs resulted in VL1 muscles with wild-type morphology (**Figure 2.9D, H**). Comparing the two phenotypes suggests that the 15 CSPGs can synergize with the LamG domains, thus leading to an increase in actin dynamics and to the modulation of the attachment site architecture.

In contrast to the two proteins with a single type of extracellular domain, the overexpression of Kon PDZ-BDmut yielded shorter VL1 muscles with smaller attachment sites (**Figure 2.9F, H**). Therefore, an increase of Kon protein levels with mutated PDZ-BD, at the attachment site, did not increase its overall biological activity. This result indicates that the two types of extracellular domains cannot compensate for the intracellular PDZ-BD. In fact, the PDZ-BD is the only predicted intracellular domain of Kon, and thus the only domain that can participate in signalling transductions upon extracellular activation.

Together, these experiments yielded two main conclusions: (1) Kon consisting of the two LamG domains, TM domain, and the intracellular part with its PDZ-BD comprises a “compact” version of Kon, sufficient for the formation of the VL muscles in the embryo, and for survival until pupal stage. (2) The CSPG domains can serve as a booster of the LamG domain, which could be required at later stages in development, namely adult myogenesis in pupa.

2.4 An essential role of the CSPG domains in adult myogenesis

The distance that the muscles have to elongate to reach the tendon cells is larger during adult myogenesis. How do receptors, which participate in both phases of myogenesis, cope with an increase in distance to the tendon cell, presumably the major source of guidance and attachment cues?

During the formation of the larval VL muscles in the embryo, whose length is approximately 40 μm , a compact version of Kon, missing the CSPG domains, is sufficient (**Figure 2.6**). However, during the development of the adult muscles, the 15 CSPGs may be essential to synergize with the LamG domains, as a potential mechanism to cope with a distant source of molecular cues. Three arguments encouraged me testing this hypothesis.

First, the 15 CSPGs are conserved up to human, suggesting an important role for these domains (Schnorrer et al., 2007). Second, when the localization problem of Kon-V5 ΔLamGs was circumvented by overexpression, the 15 CSPGs could produce VL muscles with wild-type morphology (**Figure 2.9**). This suggests that the 15 CSPGs may boost the activity mediated by the two LamGs, which in turn may be necessary for the development of larger muscles. Finally, all the *kon-V5 ΔCSPGs* pupae died during metamorphosis (**Figure 2.7A**), indicating that the 15 CSPGs are likely to play a major role during adult myogenesis.

To test this hypothesis, I analysed two types of adult muscles, dorsal abdominal muscles and the dorsoventral muscles (DVMs, indirect flight muscles), which similarly to the larval VL muscles, derive from founder cells. Both muscle types are larger than the VL muscles, approximately seven and twenty times, respectively.

2.4.1 The 15 CSPGs are essential for guidance of the dorsal abdominal muscles

To investigate if the 15 CSPG domains participate in the formation of the adult dorsal abdomen muscles, I analysed at 72h APF the mature morphology of abdominal muscles from *wild-type*, and *kon-V5 ΔCSPGs* pupae, using immunohistochemistry.

At 72h APF, the wild-type dorsal longitudinal abdominal muscles were connected to the hemisegment borders, along the A-P axis (**Figure**

2.10A, C). In contrast, in absence of the Kon CSPG domains, the abdominal musculature was composed of muscles with different angles of orientation (**Figure 2.10B, C**). This indicates that 15 CSPGs have an essential role in the formation of the dorsal abdominal muscles.

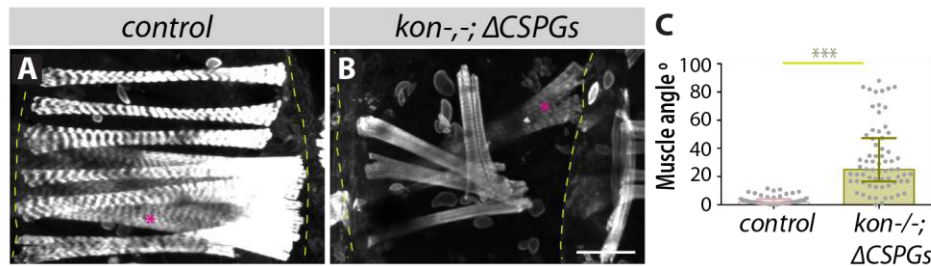


Figure 2.10. The CSPGs have a pivotal role during adult dorsal muscles formation

(A) The abdominal muscles in *wild-type* background at 72h APF. The muscles are parallel to the A-P axis. The asterisk marks larval muscles that at 72h APF were still present.

(B) The abdominal muscles expressing Kon-V5 Δ CSPGs in *kon* mutant background at 72h APF. The abdominal musculature is highly disorganized with muscles oriented with different angles. The asterisk marks larval muscles that at 72h APF were still present. Scale bar = 50 μ m

(C) Quantification of the angles from the muscles composing the dorsal abdominal musculature. 0° orientation angle corresponds to muscles parallel to the A-P axis. Median and the interquartile range (IQR). $n = 60$, number of pupae = 9 per condition. *** $p < 0.001$.

To identify how the lack of the 15 CSPGs affects the development of the dorsal abdominal muscles, I monitored the abdominal myogenesis in *kon-V5* Δ CSPGs pupae, by live imaging. The abdominal muscles emerged from a cluster of myoblasts located at the posterior border of the hemisegment. This cluster was organized like a string along the hemisegment, perpendicular to the A-P axis (**Figure 2.11A, B**). This string of cells is composed of founder myoblasts, at the positions corresponding to future fiber forming sites, and fusion competent myoblasts (Dutta, 2004). The string of myoblasts started then to fuse, yielding myotubes oriented along the anterior-posterior axis (**Figure 2.11C-F**). These myotubes elongated mainly towards the anterior end, although both ends possessed very active filopodia (**Figure 2.11C-F**).

This is consistent with the view that the myotubes actively probe the environment (Jacquemet et al., 2015).

In absence of the 15 CSPGs at 27h APF, I could not detect myotubes elongating out of the myoblast cluster (**Figure 2.11H**), as I observed in wild type (**Figure 2.11C**). However the borders of the cluster were decorated with filopodia. These filopodia were likely from the forming myotubes, whose growth orientation was random, instead of in the anterior-posterior direction (**Figure 2.11G-J**). Later, I could detect within this cluster, clumps of myotubes that elongated almost perpendicular to the A-P axis (**Figure 2.11K**), instead of along this axis like in the wild-type muscles (**Figure 2.11C-E**). This indicates that the abdominal myotubes cannot respond properly to guidance information without the 15 CSPGs, and thus they elongate along the wrong direction. Ultimately, these myotubes managed to attach, but at incorrect positions within the hemisegment. Some of these attachments were likely to be ectopic muscle-muscle connections (**Figure 2.11L**).

Together, these data show that when the muscles surpass a certain size, the LamG domains are not sufficient to sense guidance cues, but rather they require the 15 CSPGs as a booster.

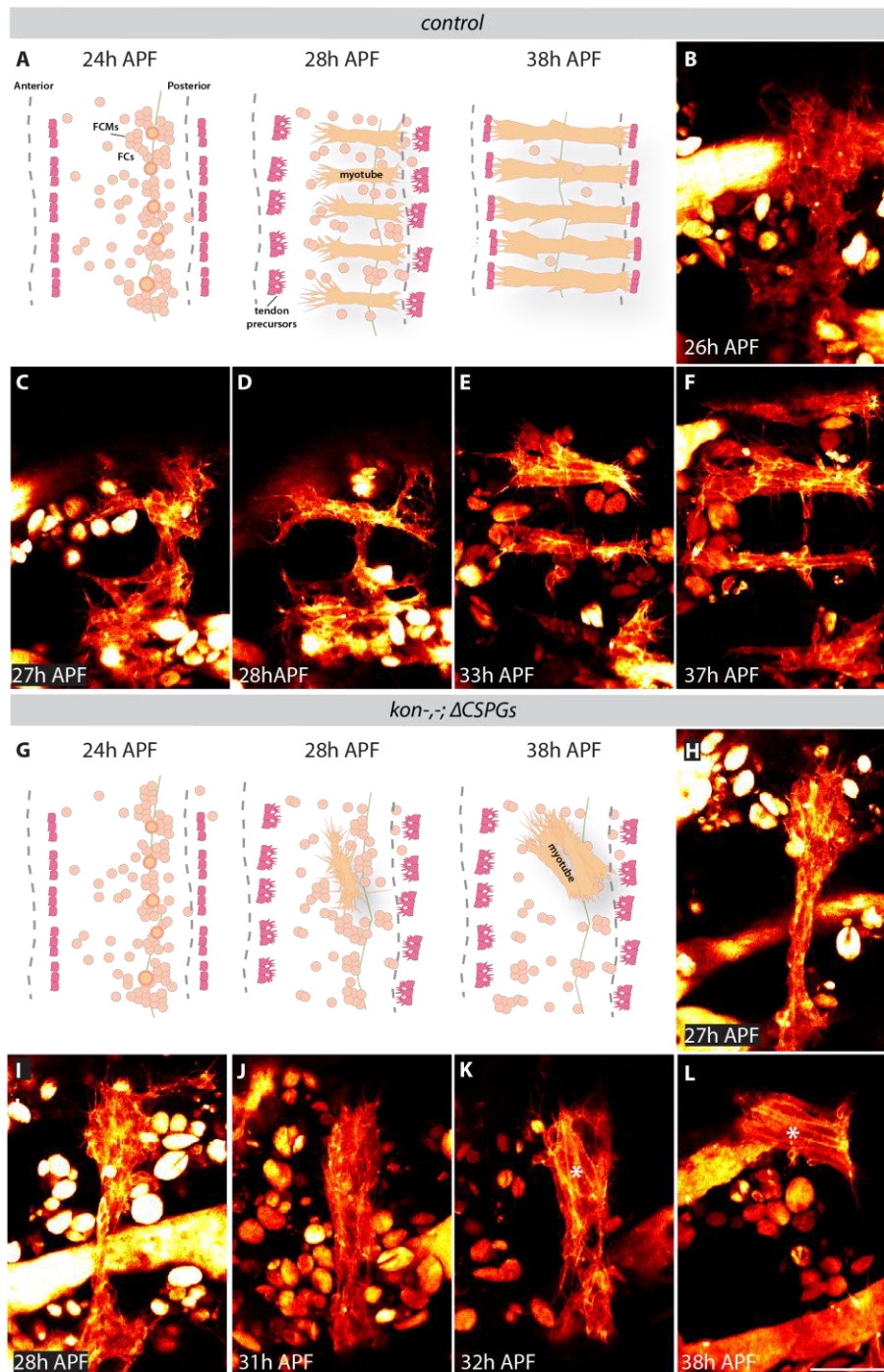


Figure 2.11. The CSPGs are essential for guidance of the adult dorsal muscles
 (A) Depiction of the adult dorsal abdominal muscle development in pupa. (B-F) Wild-type muscles were imaged from 26h APF on. (B) From the myoblast cluster, (C-F) myotubes started to grow oriented along the anterior-posterior axis. The myotubes display filopodia laterally as well as at the anterior and posterior tips.
 (G) Depiction of the *kon-5* Δ CSPGs dorsal abdominal myotubes development. (H-L) *kon-5* Δ CSPGs muscles were imaged from 27h APF on. (H-J) The borders of the myoblast cluster were decorated with filopodia. These filopodia were likely from the forming myotubes. (K) The myotubes grow with wrong direction. (L) The myotubes clump all together, probably due to ectopic muscle-muscle attachments. Scale bar = 50 μ m

2.4.2 The 15 CSPGs are essential for guidance of the DVMs

To examine whether the lack of 15 CSPGs also affects the DVM formation, I followed the development of the DVMs by live imaging (**Figure 2.12**). The DVMs, similarly to the abdominal muscles, derive from founder cells. The DVMs are composed of three distinct muscle groups spanning the thorax, approximately along the dorsoventral axis: DVM I (3 fibers), DVM II (2 fibers) and DVM III (2 fibers) (Fernandes et al., 1991).

The DVMs begin to form at the ventral side of the thorax. There, the myoblast clusters start to fuse yielding myotubes, similarly to the abdominal muscles (Dutta, 2004). This developmental stage is very difficult to image, because the myoblast cluster is located very deep in thorax. Thus, the DVM imaging started at the myotube stage, when the DVMs are closer to the dorsal part. From 17-18 h APF, I could detect the two DVM II myotubes. Their width was similar to the width of the DLMs, located below them. The dorsal leading edge contained filopodia that grew towards the dorsal attachment site, while the ventral side was not possible to visualize clearly (**Figure 2.12A-C**). The development of the DVMs shares key aspects with that of other type of indirect flight muscles, the dorsal longitudinal muscles (DLMs). Next, the fibers underwent compaction. In this process, the two DVM fibers gradually became shorter and thicker (**Figure 2.12D, E**).

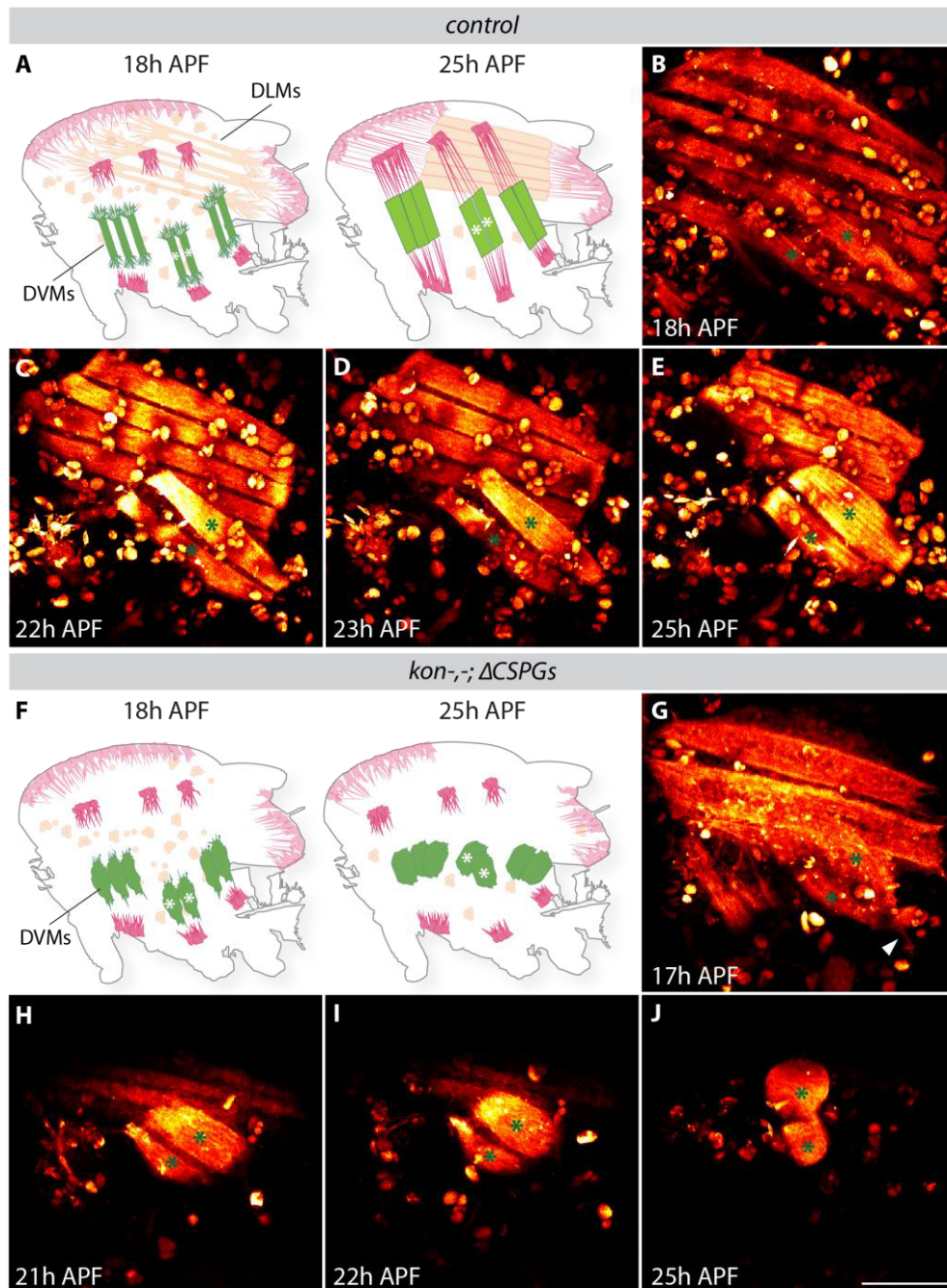


Figure 2.12. The CSPG domains are essential for the guidance of the DVMs
 (A) Depiction of DVM development, which corresponds to B-E.
 (B-E) Wild-type DVM muscles were imaged from 18h APF on. (B-C) The elongation of the DVM myotubes (asterisks) is followed by (D-E) their compaction.
 (F) Depiction of the developmental problems of *kon-V5* ΔCSPGs DVM myotubes, corresponding to G-J.
 (G-J) *kon-V5* ΔCSPGs muscles were imaged from 17h APF on. (G) The DVMs (asterisks) are not elongating, but rather rounding-up. The leading edges were very thin (white arrowhead). (H-J) Gradually, the DVM myotubes round, until becoming completely spherical. Scale bar = 100 μm

In absence of the 15 CSPGs, the two DVM II myotubes formed, however, they displayed severe morphological defects (**Figure 2.12F, G**). First, the lateral sides of the myotubes had a clear curvature, indicating that the myotubes were not elongating, but rather rounding-up (**Figure 2.12G**). Second, the leading edges were very thin (**Figure 2.12G**), in contrast to those of a wild-type myotube (**Figure 2.12B**). These two types of defects suggest that the DVMs cannot correctly elongate, probably due to problems in sensing guidance cues, which trigger cytoskeletal changes leading the myotube to elongate towards their attachments sites.

Gradually, the DVM myotubes rounded, and eventually they became two spherical myotubes (**Figure 2.12H-J**). This severe phenotype indicates that the 15 CSPGs are essential for the DVMs to elongate, possibly by helping the myotubes to access guidance information.

2.4.3 The CSPG domains have a minor role in DLM attachment (template-based)

The CSPG domains have an essential role in guidance of the dorsal abdominal muscles and of the DVMs. I could not assess, however, if the 15 CSPGs also play a pivotal role during attachment. To clarify this point, I tested the role of the 15 CSPGs in the attachment of the DLMs, a second type of indirect flight muscles.

The DLMs derive from larval templates. These templates constitute a substantial proportion of the mature DLMs (Fernandes et al., 1991; Fernandes and Keshishian, 1996). Hence, the DLMs elongate substantially less than the DVMs. To date, the mechanism underpinning the DLM elongation is not known. Nevertheless, I believe that three models are conceivable.

The first model of DLM elongation is increasing the mass of the templates through fusion, in a laterally constricted fashion. This model does not require guidance cues, because the templates provide the

direction of elongation. A second model is elongation driven by guidance cues secreted by the tendon cells, similarly to the muscles described before. A third model combines the two models mentioned before. In this model, the contribution of the guidance cues to DLM elongation is however substantial less than in the second model.

I favour the first and the third models, because, as it was suggested before (Fernandes et al., 1996), the templates are not only a source of mass, but also a structure that potentially provides an orientation for DLM elongation.

To determine if the DLMs develop normally in the absence of the 15 CSPGs, I analysed the mature morphology of these muscles in *kon-V5* Δ CSPGs pupae, at 90h APF by immunohistochemistry.

At 90 APF, the wild-type DLMs spanned the thorax along the anterior-posterior axis (**Figure 2.13A**). In absence of the 15 CSPG domains, most of the DLMs also spanned across the thorax, however, some minor defects were visible (**Figure 2.13B**), possibly due to detachment.

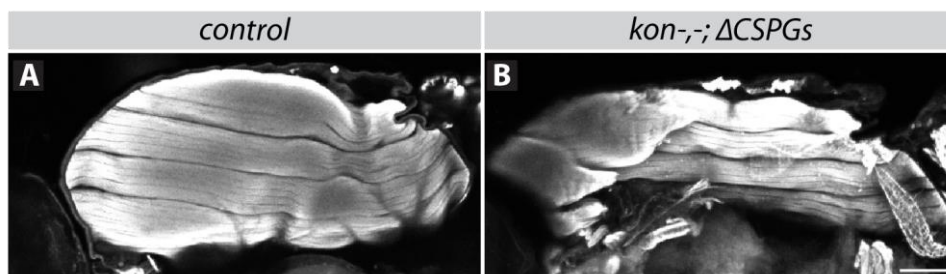


Figure 2.13. The 15 CSPG domains have a minor role the DLM formation
 (A) The DLMs fibers in the control at 90h APF. They span the entire thorax.
 (B) The *kon-V5* Δ CSPGs DLMs fibers in *kon* mutant background at 90h APF. Some fibers are missing, possibly due to detachment. Scale bar = 100um

To understand the origin of those minor defects, I monitored the early developmental hallmarks of the DLMs by live imaging. As described before (Fernandes et al., 1991; Fernandes et al., 1996), the DLMs originate from three larval dorsal oblique muscles (LO), which resist histolysis. These three larval muscles dedifferentiate into three

templates (**Figure 2.14A, B**). Next, each template split in two myotubes (**Figure 2.14C**). Those myotubes elongated along the A-P axis, towards the attachment sites, located near the cuticle of the thorax (**Figure 2.14D**).

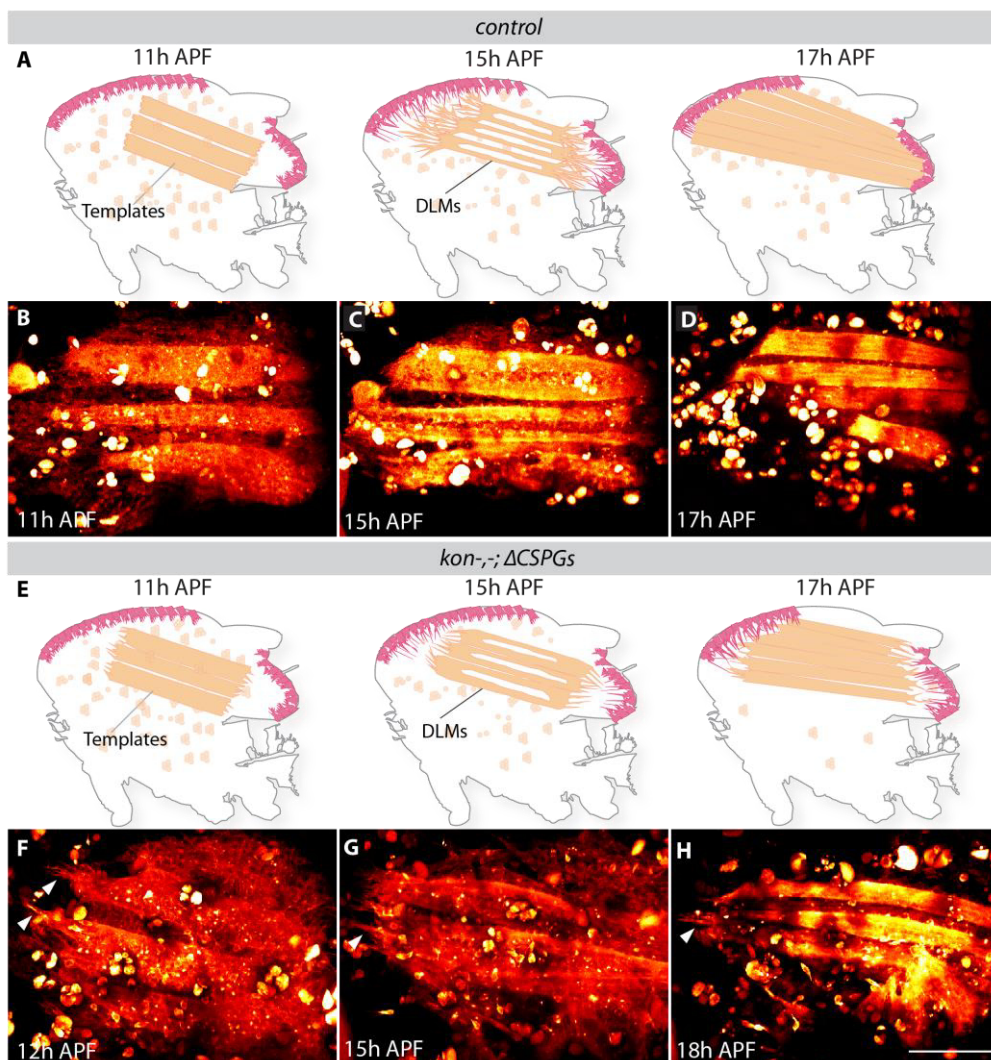


Figure 2.14. The CSPG domains have a minor role in DLM development

(A) Depiction of the DLM development, corresponding to B-D.

(B-D) Wild-type DLM muscles were imaged from 11h APF on.

(C) Each template split in two myotubes.

(D) The DLM myotubes elongate along the A-P axis, towards the attachment sites.

(E) Depiction of the developmental problems of *kon-5* Δ CSPGs DLM myotubes, corresponding to F-H.

(F) *kon-5* Δ CSPGs pupae had a normal number of templates, but their leading edges have abnormally long and thin protrusions (white arrowheads).

(G-H) *kon-5* Δ CSPGs templates split, and the myotubes elongate. The leading edges are, however, abnormal, composed of very long and thin protrusions (white arrowheads). Scale bar = 100 μ m

kon-V5 Δ CSPGs pupae had a normal number of templates, but their leading edges had abnormally long and thin protrusions (**Figure 14E, F**), similarly to the DVM myotubes (**Figure 2.12**). In absence of the 15 CSPGs the templates split nevertheless, and the majority of the muscles continued to elongate towards the tendon cells. The leading edges were, however, abnormal, composed of very long and thin protrusions (**Figure 2.14G, H**).

In summary, lack of the 15 CSPGs caused cytoskeletal defects at the leading edges of the DLM muscles, which could indicate that those muscles do not respond properly to possible guidance cues. Because guidance cues may play a secondary role in DLM elongation, they could reach nonetheless the tendon cells, by most likely increasing template mass, in a laterally constricted fashion. During attachment initiation, the two LamG domains were sufficient to sense attachment cues, and thus triggering the attachment formation. However, as demonstrated by analysing the *kon-V5* Δ CSPGs DLMs at 90h APF (**Figure 2.13**), the attachments did not appear entirely normal.

Analysing the function of the 15 CSPG domains during adult myogenesis yielded two main conclusions: (1) the CSPG domains are essential in the formation of larger muscles, which depend heavily on guidance cues to find their attachment sites; and (2) the activity of the CSPG domains is primarily required during guidance. Together, these data suggest that for the formation of adult muscles, the LamG domains require to be boosted by the CSPG domains.

2.5 Strategies to identify Kon interactions partners

To date, besides Dgrip, no other Kon interaction partner was identified (Schnorrer et al., 2007). The identification of other interaction partners is central to understand the molecular mechanism underpinning the activity of Kon during the two phases of myogenesis. To shed light on

which guidance and attachment molecules Kon recognizes, I performed immunoprecipitation of Kon using lysates from embryos and pupae, followed by label free mass spectrometry analysis.

One of the strategies to identify protein complexes, namely affinity purification mass spectrometry (AP-MS), requires several purification steps, including fractionating the eluate by gel electrophoresis, followed by analysing each gel band by mass spectrometry. Here, I used another strategy, affinity enrichment mass spectrometry (AE-MS). With AE-MS the purification steps can be minimized, which includes using mild buffers and a single-step of affinity enrichment of the tagged protein, and its interactors. This process yields an eluate with a large amount of unspecific binders, regarded as background. However, the true interactors, defined as significantly enriched proteins, are extracted by analysing their intensity profile across the samples with generic statistical testing (Keilhauer et al., 2014; Hein et al., 2015).

2.5.1 Kon interactions partners during larval myogenesis

To identify the interaction partners of Kon during embryonic myogenesis, I used as baits two different fosmid-derived tagged versions of Kon, Kon-V5 and Kon-HA. I performed single-step affinity enrichment of endogenously expressed V5 or HA-tagged Kon. These two baits had the potential to yield binding partners of the two LamGs, the 15 CSPGs and the PDZ-BD. Kon-V5 and Kon-HA are expressed at endogenous levels and are completely functional (**Figure 2.4**). Furthermore, the two tagged version of Kon localized specifically at the tips of the VL muscles (**Figure 2.4**), and therefore artefacts generated by Kon mislocalization, due to overexpression (**Figure 2.9**), were less likely to occur.

The proteins identified by mass spectrometry were given with their LFQ values (label free quantification), which were depicted in a volcano plot. On the x-axis of the volcano plot, the variable Log (LFQ

bait- LFQ control) indicates the enrichment level of a particular protein, thus proteins that have higher values on the x-axis are more enriched in the sample. On the y-axis, the variable $-\text{Log}(\rho \text{ value})$ indicates whether the enrichment of a particular protein was statistically significant. The level of statistic significance increases along y-axis.

Using either Kon-V5 or Kon-HA as baits yielded eluates in which Kon was significantly enriched (**Figure 2.15A, B**), indicating that the immunoprecipitation and in principle the mass spectrometry analysis worked. The Kon-V5 derived eluate contained significantly enriched levels of Sallimus (Sls), the fly Titin homologue (**Figure 2.15A**). However, if the interaction was real, it would not be biological relevant, because the *s/s* mutant phenotype (Hakeda et al., 2000) is not similar to the one of *kon*.

Taf10b, RpL36, CG5343 and Actin 57B were almost significantly enriched in Kon-V5 derived eluate (**Figure 2.15A**). Taf10b is a transcription initiation factor (Georgieva et al., 2000), RpL36 a ribosomal protein (Voelker et al., 1989; Rugjee et al., 2013), and CG5343 was inferred to have a role in RNA splicing (Herold et al., 2008). Because these three proteins do not have a reported role in ECM recognition/interaction, actin dynamics or in myogenesis in general, I excluded them for further validation experiments.

Interestingly Actin 57B is one of the actins present in the muscles, however according to literature it plays only a role in actin dynamics in the postsynaptic side. Moreover, the *actin 57B* mutant phenotype is not similar to the one of *kon* (Blunk et al., 2014).

The Kon-HA derived eluate did not yield any potential interaction partner (**Figure 2.15B**). The poor yield of these two experiments could be due to the low abundance of the putative ligand of Kon. Alternative experiments to circumvent these problems are suggested in the Discussion chapter.

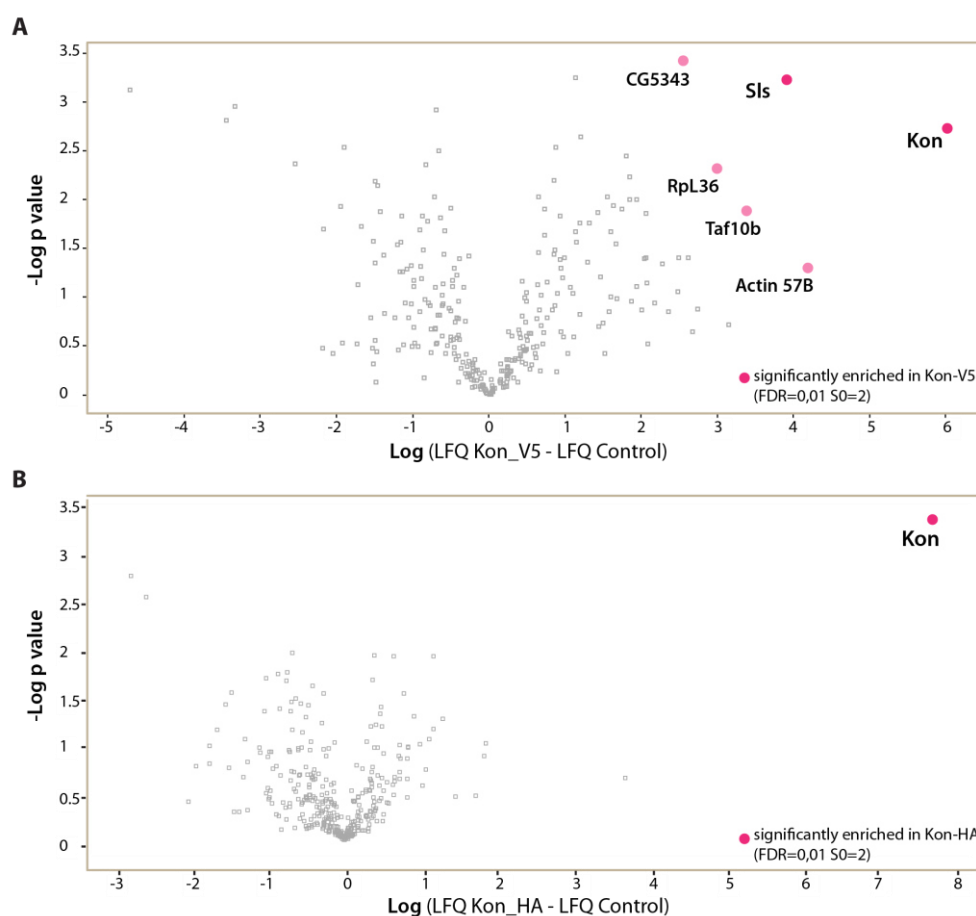


Figure 2.15. Kon interaction partners in the embryo

(A) Eluates from *kon-V5* embryos were analysed by mass spectrometry. Kon was significantly enriched, indicating that the immunoprecipitation and in principle the mass spectrometry analysis worked. Sallimus (Sls), the fly Titin homologue, was also significantly enriched. On the x-axis of the volcano plot, the variable Log (LFQ bait-LFQ control) indicates the enrichment level of a particular protein. On the y-axis, the variable -Log (p value) indicates whether the enrichment of a particular protein was statistically significant. FDR (False discovery rate) = 0.01

(B) Eluates from *kon-HA* embryos were analysed by mass spectrometry. Kon was significantly enriched. FDR (False discovery rate) = 0.01

Using the full length of Kon as bait to identify Kon interaction partners in the embryo was unsuccessful, likely because of the large size of Kon and the lability of the interactions. Therefore, I decided to use smaller bait. The smallest functional domain of Kon is the PDZ binding domain (PDZ-BD). A PDZ domain recognizes short peptides with a COOH-terminal hydrophobic residue and a free carboxylate group. (Pawson and Scott, 1997). The last residues from the C-terminal sequence of the PDZ-BD bind to the β strand from the flanking peptide-binding groove, thus forming an antiparallel β sheet (Doyle et

al., 1996). Protein domains that recognize short and unstructured sequences can be successfully identified using peptides as baits (Schulze and Mann, 2004). This approach was already successfully applied, for instance, to identify interaction partners of the cytoplasmic tail of $\beta 1$ integrin (Meves et al., 2011; Böttcher et al., 2012).

To identify proteins that interact with the PDZ-BD from Kon, I used synthetic peptides composed of 25 amino acids as baits in pull-down experiments (see Material and Methods), followed by mass spectrometry analysis. I used two peptides as baits. The “active” peptide included the complete PDZ-BD sequence from Kon, whereas the “inactive” peptide had its COOH-terminal hydrophobic residue valine, replaced by glycine, which leads to the disruption of the PDZ-BD activity (Beuming et al., 2005; Schnorrer et al., 2007; Tonikian et al., 2008). I used a similar strategy to inactivate the PDB-BD from the *kon* fosmid. I performed two biological replicates, each one with technical triplicates for each of the peptides. This approach yielded a longer list of proteins, which were significantly enriched in the eluate produced with the active peptide (**Figure 2.16**). The proteins that were significantly enriched in the two independent experiments (biological replicates) were PALS1-associated tight-junction protein (Patj), Polychaetoid, (Pyl or ZO-1), Stardust (Std), Protein tyrosine phosphatase Meg (Ptpmeg) and Myosin heavy chain-like (Mhcl). All these proteins contain PDZ domains, and with the exception of Mhcl, they are all known polarity components.

In the embryo, Mhcl is expressed in founder cells (FC) of the somatic mesoderm, and it localizes at the contact site between the fusion competent myoblast (FCM) and the FC during fusion. However, in the absence of Mhcl the musculature of the embryo is normal (Bonn et al., 2013), indicating that, even if the interaction was real, it would not be functionally relevant.

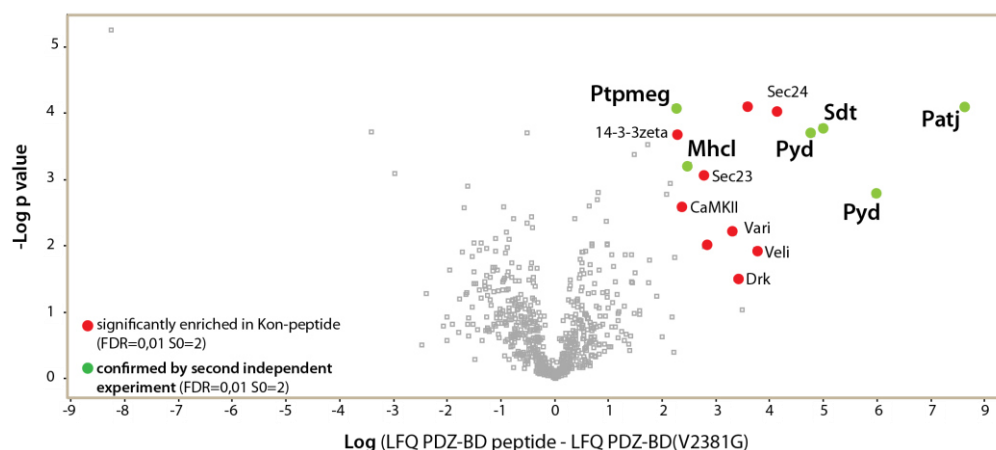


Figure 2.16. PDZ-BD peptide as bait to identify PDZ containing interaction partners

Two synthetic peptides (an “active” and an “inactive”) were used as baits in pull-down experiments with *w-* embryos, followed by mass spectrometry analysis. The “active” peptide included the complete PDZ-BD sequence from Kon, whereas the “inactive” peptide had its COOH-terminal hydrophobic residue valine, replaced by glycine, which leads to the disruption of the PDZ-BD activity. Two biological replicates yielded six proteins significantly enriched: PALS1- associated tight-junction protein (Patj), Polychaetoid, (Pyd or ZO-1), Stardust (Std), Protein tyrosine phosphatase Meg (Ptpmeg) and Myosin heavy chain-like (Mhcl). All these proteins contain PDZ domains, and with the exception of Mhcl, they are all known polarity components. FDR (False discovery rate) = 0.01

The remaining candidates have a well known role in the morphogenesis of the epithelium (Tepass, 2012), however, to my knowledge a role in myotube polarization and growth has not been yet reported. On the other hand, there is some indication given by work done with the mouse homolog of Kon, NG2, which prompted me to further consider a possible interaction between Kon and Patj.

NG2 interacts with MUPP1 (Barritt et al., 2000). This protein is very similar to its homologue, Patj (Adachi et al., 2009). Work done in the polarization and migration of oligodendrocytes implied that NG2 may interact with Patj, and that Patj, in turn, would recruit Pals (Binamé et al., 2013), an homologue of Stardust (Roh and Margolis, 2003).

To test whether Kon interacts with Patj in *Drosophila*, I cloned the four PDZ domains of Patj and overexpressed them together with the intracellular part of Kon in S2 cells. These initial experiments failed to validate this interaction (data not shown), however, this requires further analysis.

2.5.2 Kon interaction partners during adult myogenesis

To identify Kon interaction partners in pupae, I tried, in collaboration with Dr Marco Hein (Mann department, MPI of Biochemistry), to circumvent possible technical problems, which could explain the poor results from the embryo experiments. During sample processing, namely immunoprecipitation, the composition of each replicate can vary, without any biological cause, but rather due to human error, such as inaccurate pipetting. This source of variability of human origin decreases the replicability among triplicates, which in turn decreases the significance values for the enrichment of each particular protein in the sample. Thus, to minimize the sources of variability during immunoprecipitation, this procedure was fully automatized using an IP robot (Hein et al., 2015). Part of the workflow as well as the bioinformatics analyses used in this set of experiments was originally developed to characterize the human interactome (Hein et al., 2015).

To identify Kon interaction partners that have a role in the myogenesis of adult muscles, I used pupal lysate and as baits, the fosmid-derived Kon-GFP, which is completely functional (**Figure 2.4**), or the overexpressed Kon-YFP under *Mef2-GAL4* driver (general muscle driver). In theory, this approach could yield interaction partners that assist Kon during the formation of DLMs, DVMs and abdominal muscles.

Using either Kon-GFP or Kon-YFP as baits yielded eluates in which Kon was significantly enriched (**Figure 2.17A, B**), indicating that the immunoprecipitation followed by the mass spectrometry analysis worked. Both eluates were also significantly enriched for other proteins, although the two baits yielded two different lists of significantly enriched proteins (**Figure 2.17A, B**).

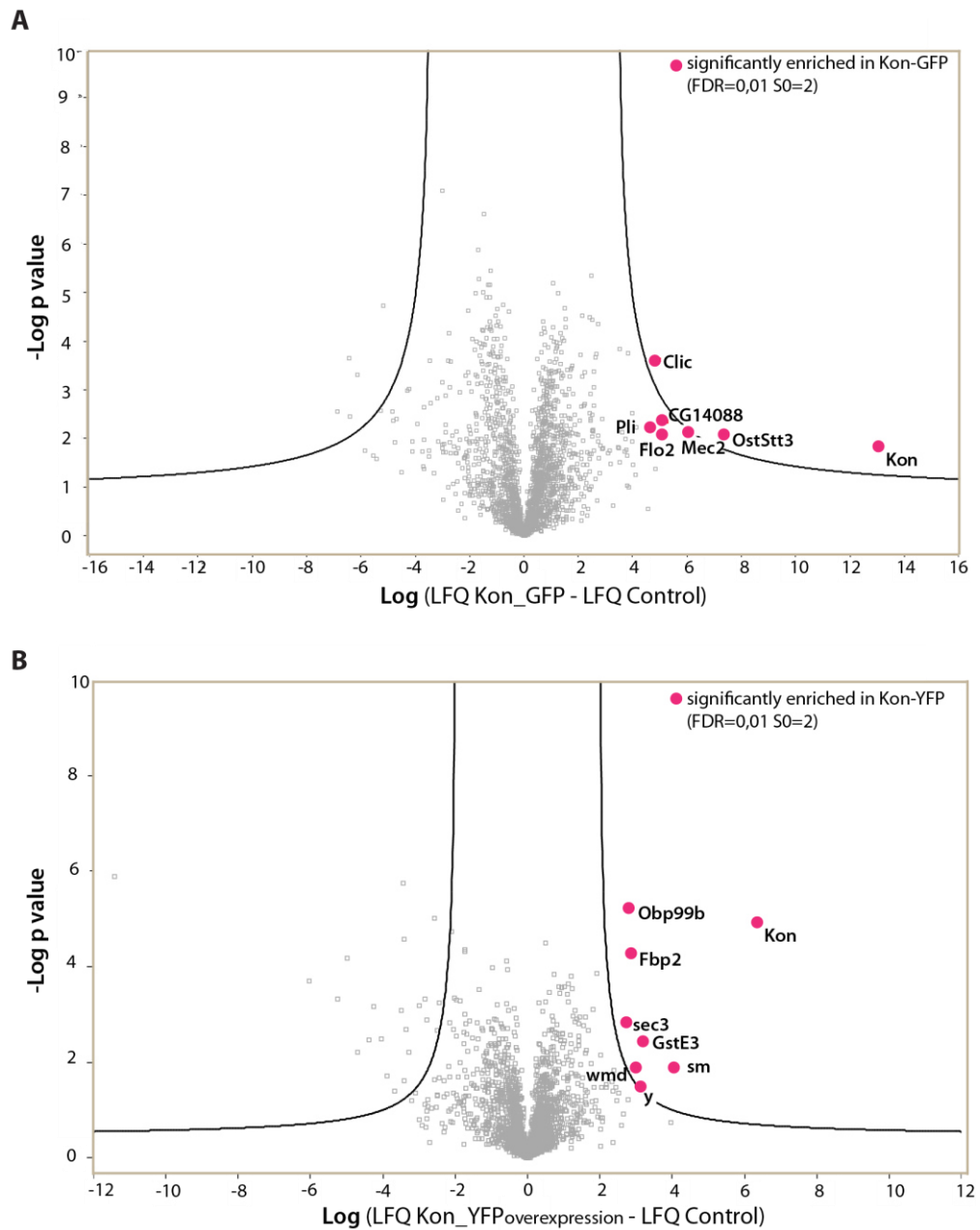


Figure 2.17. Kon interaction partners in pupae

(A) Eluates from *kon-GFP* pupae were analysed by mass spectrometry. Kon was significantly enriched, indicating that the immunoprecipitation and in principle the mass spectrometry analysis worked. The eluates yielded by Kon-GFP were significantly enriched for Pellino (Pli), Mec2, Oligosaccharyltransferase (OstStt3), CG14088, Chloride intracellular channel (Clic), and Flotillin-2 (Flo2). FDR (False discovery rate) = 0.01

(B) Eluates from overexpressed *kon-YFP* pupae were analysed by mass spectrometry. Kon was significantly enriched. The eluates yielded by overexpressed Kon-YFP were significantly enriched for yellow (y, probably cuticle contamination), Glutathione S Transferase E3 (GstE3), Odorant-binding protein 99b (Obp99b), wing morphogenesis defect (wmd), Fat body protein 2 (Fbp2), smooth (sm), and Sec3. FDR (False discovery rate) = 0.01

Before I performed further validation experiments, I checked whether these potential Kon interaction partners met two criteria: (1) having a role in ECM recognition/interaction, actin dynamics or in myogenesis in general, and (2) if the mutant alleles were at least pupal lethal.

The eluates yielded by Kon-GFP were significantly enriched for Pellino (Pli, participates in innate immune signalling (Ji et al., 2014)), Mec2 (biological activity in nephrocytes filtration (Zhang et al., 2013)), Oligosaccharyltransferase (OstStt3, involved in the biological process of protein glycosylation (Yamamoto-Hino et al., 2015)), CG14088 (a serine protease without known function, however the mutants are viable), Chloride intracellular channel (Clic, biological role in ethanol tolerance (Bhandari et al., 2012)), and Flotillin-2 (Flo2, participates in spread of morphogens, but the mutant is viable (Katanaev et al., 2008)) (**Figure 2.17A**). Because these proteins did not fulfil the two criteria necessary for continuing with further validation, I did not proceed with further experiments.

The eluates yielded by overexpressed Kon-YFP were significantly enriched for yellow (y, participates in the melanin biosynthetic process (Wittkopp et al., 2002), probably cuticle contamination), Glutathione S Transferase E3 (GstE3, involved in glutathione metabolic process (Saisawang et al., 2012)), Odorant-binding protein 99b (Obp99b, an pheromone binding protein (Hekmat-Scafe et al., 2002)), wing morphogenesis defect (wmd, it participates in the morphogenesis of the wing (Dworkin and Gibson, 2006)), Fat body protein 2 (Fbp2, it has alcohol dehydrogenase activity (Guruharsha et al., 2011)), smooth (sm, role in RNA processing (Lasko, 2000)), and Sec3 (it belongs to the exocytosis complex, and it has a role in asymmetric distribution of receptor during cell polarization (Wan et al., 2013), however the knockdown in muscles is viable (data not shown), (**Figure 2.17B**). Because these proteins did not fulfil the two criteria mentioned before, I did not proceed with further analysis.

Taken together, these approaches revealed to be unsuccessful to identify Kon interaction partners that may play a role during Kon mediated myogenesis. Alternative approaches are suggested in the Discussion chapter.

3 Discussion

The main objectives of this study were, first, identifying the contribution of each domain type to the overall activity of Kon; second, determining if Kon, as putative receptor, has a role in myotube guidance; and finally, identifying how Kon customizes its activity in two distinct developmental scenarios: one in the embryo, in which the formed larval muscles are rather small, and another in the pupae, in which the formed adult muscles are larger. My results suggest that Kon functions according to two modes, which mediate either muscle elongation (guidance) or attachment. These two modes are particularly distinguishable in adult myogenesis. These two modes are not however linked exclusively to a particular extracellular domain type, because the two types of domains are partially redundant. In addition, I showed that a compact version of Kon, missing the long CSPG domains was sufficient for the formation of smaller muscles, during larval myogenesis. However, during formation of larger muscles, in the adult myogenesis, this compact version is not sufficient, requiring thus to be synergized by the CSPG domains. In the absence of the CSPG domains, the adult muscles had severe defects, similarly to the *kon* RNAi phenotype (Perez-Moreno et al., 2014), showing that the CSPG domains have an essential role during adult myogenesis. Together, Kon CSPG domains boost the sensing activity of the LamG domains, so that Kon maintains an efficient ligand sensing activity in the two developmental scenarios, including across long distances in pupae.

3.1 Unveiling the function of the three Kon protein domain types

The first homolog of Kon was identified in human melanoma cells over 30 ago (Harper and Reisfeld, 1983). However, numerous aspects of the role of Kon and its homologues are poorly understood, including how the three types of protein domains, which compose Kon and their homologues, interplay to mediate a multitude of biological processes. This study shed light on this question, using *Drosophila* myogenesis as a model system. This model system can emulate certain aspects of human pathologies, in which the Kon homologues were shown to play a relevant role, namely in metastasis (Burg et al., 1998; Benassi et al., 2009). This is the first *in vivo* study, which establishes a link between guidance and Kon, thus providing insights how NG2/CSPG4 may increase the metastatic potential of, for example, melanomas and soft tissue sarcomas (Burg et al., 1998; Benassi et al., 2009). Furthermore, this study also explained how the two types of extracellular domains of Kon, which are conserved up to humans (Staub et al., 2002), contribute to myotube guidance. Testing if similar mechanism underlies the activity of the Kon homologues, NG2/CSPG4, could pave the way toward designing better therapeutically solutions to decrease the metastatic potential of, for example, melanomas.

The contribution of the extracellular domain types of Kon to myotube guidance varies according to the distance that the myotube has to elongate to reach the tendon cells. To note that with the exception of the DLMS, the size of the muscle reveals approximately the distance that the myotube has to elongate. A compact version of Kon, missing the long CSPG domains was sufficient for the formation of smaller muscles, during larval myogenesis. Investigating further the functional difference between the two types of extracellular domains showed that, what renders the LamG domains particularly distinguishable from the CSPG domains is their essential role in Kon localization at the tips of

the myotubes (**Figure 2.8**). However, when Kon Δ LamGs was overexpressed, this protein could accumulate at the tips of the VL muscles (**Figure 2.9**). In this context, Kon Δ LamGs could also yield VL muscles with wild-type morphology. Hence, when the localization problem of Kon Δ LamGs was circumvented by overexpression, both LamG and CSPG domain types could generate wild-type VL muscles without its counterpart type (**Figure 2.9**). Remarkably, overexpression of full length Kon resulted in more filopodia dynamics and larger attachment sites (**Figure 2.9**). This indicates that the two extracellular domain types synergize with each other, possibly by rendering the myotube more responsive to guidance and attachment cues.

The role of guidance cues in adult myogenesis has been so far not investigated. However, during the formation of the adult muscles, the tendon cells, like in the larval myogenesis in the embryo (Kramer et al., 2001; Schweitzer et al., 2010), are also likely to secrete guidance cues. Hence, Kon may mediate myotube guidance by helping the elongating myotube to sense guidance cues, presumably secreted by the tendon cells. Taken together, I propose that Kon has a long-range sensing activity, which is defined here as the ability to sense cues secreted distally. In fact, Kon homologues were shown in vitro to mediate cell chemotaxis in response to a PDGF source (Binamé et al., 2013), demonstrating that Kon homologues are also endowed with a long-range sensing activity.

The participation of Kon in myotube attachment suggests that Kon also senses attachment cues. These cues, in contrast to the guidance ones, require to be exclusively localized in vicinity of the tendon cells, thus only triggering attachment formation when the myotube reaches the tendon cells. Taken together, Kon is likely to function according to two different modes, which are characterized by long- and short-range sensing activities. The long-range sensing activity contributes to myotube elongation through sensing guidance cues secreted presumably by the tendon cells (**Figure 3.1**). Thus, this mode is mainly

required during the formation of adult muscles, whose elongation needs to be guided. In contrast, short-range sensing activity contributes to myotube attachment through sensing attachment cues (**Figure 3.1**). This mode is essential for all the muscles that require Kon for their development, independently of their size and developmental program (founder cell- or template-based). Although, the LamG domains appear to be the most important extracellular type for the short-range sensing mode, the overexpressed Kon Δ LamGs was also able to mediate VL muscle attachment (**Figure 2.9**). This suggests that 15 CSPGs can also sense attachment cues, which direct the myotube to form an attachment.

The synergy between the LamG and the CSPG domains are mainly required during adult myogenesis. Analysing the myogenesis of *kon-V5 Δ CSPGs* pupae provided evidences that the CSPG domains are essential for the formation of larger muscles, which depend heavily on guidance cues to find their attachment sites. In addition, the synergetic activity of the CSPG domain is primarily required during myotube guidance. A similar synergy could also underlie NG2/CSPG4-expressing tumours metastasis.

The study of each domain type of Kon also showed that they contribute differently for Kon localization at the myotube tips. Although the three domain types influence Kon localization, the LamG domains are the most important (**Figure 2.8**). An explanation for the higher contribution of the LamG domains to Kon localization could be the affinity strength with which this extracellular domain type binds to the ligand.

Interestingly, accumulation of a Kon homolog, NG2/CSPG4, at the membrane is controlled by PDGF, a proposed co-ligand. NG2/CSPG4 was proposed to serve as a co-receptor for a PDGF receptor, as a strategy to potentiate PDGF signalling (Feutlinske et al., 2015). This piece of evidence could support the hypothesis that interaction with the ligand controls the turnover rate of NG2/CSPG4, as well as that of

Kon. If the affinity to the ligand is a way to control the persistence of Kon at the membrane, this may explain why eliminating each extracellular domain type resulted in a decrease of the protein localization ability (**Figure 2.8**). Because the decrease in localization was more pronounced upon deletion of the two LamG domains (**Figure 2.8**), this would mean that the two extracellular domain types interact with the ligand with different levels of affinity.

A possible experiment to test the affinity hypothesis is to characterize the mobility of Kon Δ LamGs and Kon Δ CSPGs, both tagged with GFP, by FRAP (Fluorescence recovery after photobleaching). If the affinity hypothesis was valid, the turnover of Kon-GFP Δ CSPGs would be lower than the turnover of Kon-GFP Δ LamGs.

Given the resemblance of the CSPG domains with the cadherin repeats, an alternative mechanism to control Kon localization at the membrane could be through homophilic interactions between CSPG domains of neighbour Kon molecules, at the muscle tips. However, this would not be the main mechanism for Kon localization, because the contribution of the LamG domains for Kon localization is higher than that of the CSPG domains (**Figure 2.8**). An additional hypothesis to explain the different levels of enrichment upon mutation or deletion of Kon domains (**Figure 2.8**) is that these Kon domain types interact with components necessary for Kon trafficking, and delivery at the muscle tips. Hence, lack of some of these domains would result that the protein could not be normally delivered at the tips of the muscles.

On the other hand, endocytosis may be a process to prevent excessive accumulation of Kon at the membrane. A tight control is necessary, because excessive Kon can lead to excessive filopodia (**Figure 2.9**). In fact, NG2/CSPG4 concentration at the membrane is controlled by endocytosis via Stonin1, an endocytic adaptor. Lack of Stonin1 results in higher NG2/CSPG4 concentration at the cell membrane, leading to an enhancement in cell migration directionality (Feutlinske et al., 2015). Because NG2/CSPG4 is considered an oncogene (Feutlinske

et al., 2015; Schrappe et al., 1991; Behm et al., 1996; Wang et al., 2011a; Poli et al., 2013), controlling its concentration at the membrane is of extreme relevance to prevent tumour metastasis. It was suggested by a biochemical experiment that Stonin1 interacts indirectly with the PDZ-BD to mediate endocytosis (Feutlinske et al., 2015), however this presumable interaction was not functionally validated. My data show, however, that the mutation of the Kon PDZ-BD did not increase Kon concentration at the membrane (**Figure 2.8**). This could argue that either Kon level is not controlled by endocytosis, or the interaction between NG2/CSPG4 PDZ-BD and Stonin1 was an artefact. Hence, the interaction between NG2/CSPG4 and Stonin1 via PDZ-BD requires to be functionally validated to demonstrate its biological role.

3.2 Challenges to find interaction partners and new strategies

Identifying Kon interactions partners is central to complement the mechanistic knowledge discussed above. To identify Kon interactions partners I have applied enrichment purification followed by mass spectrometry (EP-MS) (Keilhauer et al., 2014). This approach was used for instance to generate large-scale protein interactions studies, such human Interactome (Hein et al., 2015). Similarly to this study, I have also used as baits, three different tagged versions of Kon expressed at endogenous levels (**Figure 2.4**), thus recapitulating the *in vivo* conditions. In addition, I have tested embryos and pupa to identify potential Kon interactors from the two phases of *Drosophila* myogenesis. However, these sets of experiments were unsuccessful to find Kon stable interactors (**Figure 2.15**).

A recent study showed that obligate protein complexes are rare among a multitude of interactions in the cell. The majority of the interactions are weak and non-obligatory as well as at substoichiometric levels (Hein et al., 2015). Numerous variables govern protein-protein

interactions in the cell, including biophysical affinity, kinetics exchange, spatiotemporal overlap of interactors, and cellular abundance. A stable complex contains components of equal cellular abundance, which are constitutively bound to each other. Strong complexes have also other features: the members of the complex are co-regulated across cell types, and they are present at stoichiometric levels, which is in turn predictive of the biophysical stability of an interaction (Hein et al., 2015).

Low biophysical affinity, high kinetics exchange, limited spatiotemporal overlap of interactors, or cellular abundance could explain why identifying Kon interaction partners is very challenging (**Figure 2.15**). For example, during myotube elongation, Kon may function as a co-receptor to help to increase the local concentration of guidance cues, and thus facilitating the counterpart receptor activation. In this context, the interaction between Kon and the putative co-ligand are likely to have low biophysical affinity and high kinetics exchange. An additional problem is the low cellular abundance of Kon in the embryo and in the pupa. On the top of that, source of variability, such as technical problems generated during the preparation of the eluates, can decrease replicability, and thus the probability of identifying weak interactors. When the enrichment values of a particular protein fluctuate dramatically among technical replicates, the statistic significance of the enrichment for this particular protein decreases, and the protein is likely to be discarded after the statistical analysis.

To increase the reproducibility among technical replicates a full-automatized procedure was used. This yielded significant improvements, shown by an increase in the number of significantly enriched proteins identified (**Figure 2.17**), however none could be considered as a biologically relevant interactor of Kon, during myogenesis. Of note, the Kon bait with an endogenous expression profile yielded a completely different list of proteins, compared to that of the overexpressed counterpart (**Figure 2.17**). Overexpressed baits

can yield different protein lists according to the stoichiometry of the bait and the prey in the cell. When the bait is more abundant than the prey, a small part of the bait population is in theory engaged with the prey, whereas the remaining bait is free. This free bait can then interact with other molecules, however with lower affinity. This could also explain the results obtained with the PDZ-BD peptides pull-downs (**Figure 2.16**).

Using a high quantity of the Kon PDZ-BD peptide to pull down PDZ containing proteins, which in this context were present at substoichiometric levels, most likely resulted that a small population of peptides interacted with the obligatory PDZ-containing protein. The rest of Kon PDZ-BD peptides was, however, free to interact with other PDZ-containing proteins, according to the stoichiometry and affinity levels. In fact, Dgrip, an interaction partner of the PDZ-BD of Kon (Schnorrer et al., 2007), was not identified in this assay (**Figure 2.16**).

A strategy to identify weak interaction partners with a high kinetic exchange, presumable like the interactors of Kon, is to label all the protein that interact at a particular time point with the bait, through biotinylation. A suitable technique to biotinylate protein complexes is BioID (Roux et al., 2012). To identify potential interactors, this technique can be combined with standard biotin-affinity capture, followed by mass spectrometry (Roux et al., 2012; Kim et al., 2014).

BioID is a technique based on a mutated version of the *E. coli* BirA biotin protein ligase, called BirA*. BirA* is a promiscuous version of the original BirA, which releases prematurely the intermediate product, biotinoyl-5'-AMP (bioAMP). Once released, bioAMP reacts immediately with primary amines within a 10 to 20 nm radius (Roux et al., 2012). Thus, BirA* requires to be in the proximity of the protein domains, which are likely to interact with other proteins. BioID was applied successfully to map protein complexes, such as nuclear pore complexes (Kim et al., 2014). BirA* is specially recommended to fuse

with transmembrane proteins, thus the localization of bioAMP is then restricted. Hence, Kon is a suitable protein for this technique.

To yield potential interactors of Kon, either extracellular or intracellular, BirA* requires to be integrated in at least two locations within Kon protein. To identify intracellular partners, BirA* has to be introduced within the Kon intracellular part, nearby the PDZ-BD at the C-terminus. To identify extracellular partners, a good position may be between the second LamG domain and the first CSPG domain, because a potential extracellular ligand may bind to both types of domains, as discussed before. In addition, BirA* cannot be integrated at the N-terminus of Kon due to its size, which is similar to that of GFP. Thus, its N-terminal localization will most likely disrupt Kon activity, as a N-terminal GFP tag did (**Figure 2.4**). An additional challenge in using BioID *in vivo* may be to supply the enzyme BirA* with enough biotin.

3.3 Possible mechanisms underlying the dual function of Kon during myogenesis

3.3.1 Myotube guidance via a secreted ligand

To fulfil a dual role in myotube elongation and attachment, Kon may act under certain circumstances as a co-receptor. Interestingly, NG2/CSPG4 was shown to modulate the responsiveness of OPCs to FGF. In OPCs, downregulation of NG2/CSPG4 impairs FGF-dependent directional migration. However, the impairment is ameliorated upon increase in FGF concentration in the medium (Binamé et al., 2013). This could indicate that NG2/CSPG4 has a role in increasing the local concentration of FGF in the vicinity of the receptor. A link between NG2/CSPG4 and PDGF signalling was also shown. Increasing NG2/CSPG4 concentration at the membrane synergizes the PDGF signalling, by making the receptors more responsive to the ligand in the medium (Feutlinske et al., 2015). In

similar fashion, Kon may render Robo more responsive to Slit by increasing the local concentration in the vicinity of the receptor.

Slit is essential for VL muscles guidance (Kramer et al., 2001). However, a role of Slit in the formation of adult muscle has not yet been investigated. A recently published genetic screen examined the function of 1384 genes by RNAi-mediated knock-down, specifically in tendon cells using the *stripe-GAL4* driver (Tiwari et al., 2015). However, Slit was not tested in this screening. Further experiments are required to elucidate if Slit and Robo have a role in the formation of adult muscles. If so, it would be highly interesting to test whether Kon potentiates Slit-mediated signalling via Robo.

3.3.2 Myotube attachment via a tendon cell-bound ligand

Cell-cell adhesion may be a mechanism to trigger muscle attachment formation. The transition from an elongating to an attaching myotube could be triggered by the interaction between Kon at the myotube and a particular protein at the tendon cell. To form a stable muscle attachment, these transient protein-protein interactions would be then replaced by a stronger integrin-tendon matrix binding. In fact, both LamG and CSPG domains can mediate cell-cell interactions. For example, LamG domains are present in Neurexin. Neurexin, at the presynaptic side, interacts with Neuregulin, at the postsynaptic side, to form a synapse (Dean and Dresbach, 2006). While Kon CSPG domains resemble cadherin domains (Staub et al., 2002), which are required, for example, to form epithelial junctions (Harris and Tepass, 2010). The direct muscle-tendon contact, as the first step to form an attachment, may however be unlikely. Tendon cells secrete Tsp, a component of the tendon matrix, since stage 12 (Subramanian et al., 2007), which is likely to prevent direct contact between Kon at the muscles and a tendon-bound ligand.

3.3.3 Myotube attachment via integrin modulation

An alternative hypothesis how Kon controls attachment, could be indirectly by modulating the binding properties of the integrins to the tendon matrix, as Kon homologues do (Iida et al., 1998). This could also explain why in the absence of the CSPG domains, some VL attachment cannot withstand the force generated during larval movement (**Figure 2.7**). Further experiments are necessary to clarify the link between Kon and integrin activity.

3.3.4 Myotube attachment with Kon homologues

Do the Kon homologues have also a role in muscle attachment? Apparently, the musculature from a *NG2/CSPG4* null mouse is normal (Grako et al., 1999). If *NG2/CSPG4* has a role in myotube attachment may be, however, redundant, or it is only detectable when the muscle homeostasis is compromised, such as during myopathies. Interestingly, it was suggested that *NG2/CSPG4* has a compensatory role in human myopathies, including Duchenne muscular dystrophies (DMD). It was shown that regenerating fibers from DMD patients up-regulate *NG2/CSPG4*. This may be a strategy to compensate the absence of the Dystroglycan complex, whose function is to mediate the connection between the muscular cytoskeleton and the extracellular matrix. *NG2/CSPG4* could promote additional anchoring between the DMD regenerating muscle and the ECM, either directly or by recruiting other attachment components, such as integrin (Petrini et al., 2003).

3.3.5 Cytoskeleton remodelling necessary for myotube elongation and attachment

The link between Kon and cytoskeletal dynamics was shown by an increase in filopodia formation upon overexpression of Kon (**Figure 2.9**), (Schnorrer et al., 2007), which presumably leads to hyper-activation of pathways linked to actin dynamics. This means that Kon is

able to recruit intracellular components that control actin dynamics, which in turn contribute to leading edge formation, myotube elongation, and attachment.

The PDZ-BD is presumably the only obvious conserved functional domain present in the intracellular part of Kon. The PDZ-BD interacts with one of the PDZ domains of Dgrip (Schnorrer et al., 2007), the *Drosophila* homolog of Grip. The other six remaining PDZ domains of Dgrip can potentially recruit other proteins (Swan et al., 2004; 2006), which in turn could induce cytoskeletal remodelling during leading edge and attachment formation.

Interestingly, the human homologue of Kon, NG2/CSPG4, is involved in the activation of the Rho family GTPases Rac and Cdc42 (Eisenmann et al., 1999). These molecules are involved in the formation of stress fibers, lamellipodia and filopodia (Nobes and Hall, 1995). Thus, Kon is likely to also interact with similar type of Rho family GTPases to modulate the actin cytoskeleton.

The challenge in studying proteins linked to actins dynamics during muscle elongation is that the majority of those molecules are also involved in myotube fusion, another essential mechanism for muscle formation (Rochlin et al., 2010). Mutations of those molecules prevent increase in muscle mass, thus masking their role in muscle elongation and attachment. Nevertheless, studying the downstream components of Kon is essential to understand the mechanism underlying the activity of Kon.

Attachment cues also trigger cytoskeleton remodelling, necessary to mediate the transition from a leading edge with filopodia to a stable and force resistant attachment site. Kon also participates in this process. A direct evidence for that is the formation of larger attachment sites upon overexpression of Kon (**Figure 2.9**). This suggests that together, the both Kon extracellular domain types render the myotube more responsive to attachment cues. Probably without these attachment cues, Kon cannot mediate the transition from an elongating

to an attached muscle. This could explain why upon Kon overexpression, the attached muscles still had filopodia laterally (**Figure 2.9**), although they were presumably absent from the attachment sites. The reason could be lack of attachment cues at the lateral sides of the muscles, and thus Kon may still there stimulate actin dynamics required for elongation.

3.4 A compact and a full version of Kon: adjustments to two myogenic phases

A pivotal question in developmental biology is how cells and tissues optimize variables that influence the diffusion of signalling molecules, such as the distance and the speed required for a secreted molecule to efficiently reach a particular receptor. Diffusion-related variables, as the two mentioned before for example, are optimized according to the type of cell or tissue by several mechanisms, involving modifications of the cell membrane, the ligand or the receptor.

A mechanism involving the cell membrane is the generation of cytonemes, which serve to facilitate the communication between distant cells. Cytonemes are very long cellular projections, which function as bridges between the receiving cell with the receptor, and the sending cell, the source of the ligand (Ramírez-Weber and Kornberg, 1999; Hsiung et al., 2005; Roy et al., 2011; Bischoff et al., 2013). An alternative mechanism is to escort the ligand with lipoproteins to facilitate the diffusion, increasing thus the distance that a ligand can potentially diffuse (Panáková et al., 2005). The number of receptors at the membrane can also increase, as a strategy to keep the cells responsive to the ligand at lower concentrations (Müller et al., 2001).

Here, I described a new strategy, centred on the protein domains of the receptor. This strategy is less drastic than the expression of different Kon isoforms according to the size of the muscle would be. To

note that with the exception of the DLMs, the size of the muscle indicates approximately the distance that the muscle had to elongate to reach the tendon cells. Kon participates in the formation of muscles that can vary up to 20 times in size (**Figure 3.1**). While a compact version of Kon, missing the long CSPGs domains (**Figure 2.6**), was sufficient for the formation of smaller muscles, the adult muscles do require this domain type (**Figure 2.11**, and **Figure 2.12**). How do the CSPG domains boost the activity of the LamG domains? The LamG domains may sense an increase in the concentration of the secreted ligand, because the 15 CSPGs move the LamG domains further away from the muscle (Tillet et al., 1997), and thus closer to the source of the ligand, the tendon cells. Thus, without the 15 CSPG domains, the concentration of the ligand in the vicinity of the shorter LamGs may not reach the critical value for receptor activation.

Although, I believe that the length of the 15 CSPG domains contributes to increase the concentration of ligand reaching the two LamGs, this is unlikely to be the main function of the CSPG domains. This is supported by two pieces of evidence. First, when Kon missing the LamG domains was localized at the attachment sites by overexpressing it, the CSPG domains were able to mediate the formation of VL muscles without the two LamG domains (**Figure 2.9**). Most strikingly, the two extracellular domains could trigger the same intracellular signalling, which led to remodelling of the leading edge, necessary for myotube extension and attachment. Second, when both extracellular domain clusters were overexpressed together, they caused excessive filopodia and enlarged attachment sites (**Figure 2.9**).

Taken together, I hypothesize that the ligand interacts with both extracellular domain types, and the strongest interaction occurs when the LamGs and CSPGs bind simultaneously to the ligand. Thus, the 15 CSPGs may strengthen the binding to the ligand, which is essential in a large muscle milieu, such as the fly thorax.

Interestingly, the boosting activity of the CSPG domains is mainly required for the long-range sensing activity of Kon, which underlies myotube elongation from adult muscles formed from a FC (**Figure 2.11**, and **Figure 2.12**). In the case of the DVM muscles, a FC measuring about 15 μm (Dutta, 2004) gives rise then to a muscle, which is up to 50 times larger. This FC, and the subsequent myotube require to access guidance cues secreted at large distance. The CSPG domains have an essential role in this function, possibly by increasing the probability of a successful interaction between the ligand and Kon. The adult muscles may also use other strategies to increase the probability of a successful interaction, such as increasing the density of Kon at the muscles leading edge.

The role of the CSPG domains differs between the two types of indirect flight muscles, DVMs and DLMs (**Figure 2.12**, and **Figure 2.14**). A possible explanation for this difference is the role of guidance molecules in the development of these two muscle types. The DLMs derive from templates, which could provide a direction for elongation. Therefore, the DLMs may not need guidance cues to reach the tendon cells. Thus, this could explain why in absence of the CSPG domains, the DLM had only minor defects (**Figure 2.13**, and **Figure 2.14**), compared to *kon* knock-down by RNAi (Weitkunat et al., 2014). Long cell projections were, however, still detected (**Figure 2.14**). These cell projections could be a compensatory response to lack of the long-range sensing activity of Kon. Moreover, these cell projections may be cytoneme-like structures, aiming to bridge the space between the elongating myotube and the tendon cell. Taken together, these cytoneme-like structures, generated upon CSPG domains deletion, may be a strategy of the DLMs to compensate for the inability in sensing guidance cues.

Interestingly, when the templates are ablated, the DLMs are however able to form *de novo*, which includes finding and attaching to the tendon cells (Farrell et al., 1996). I hypothesize that, when the

templates are ablated, the CSPG domains will have an essential role in the DLMs guidance, as they have in the DVMs.

The human and rat homologues of Kon, NG2/CSPG4, have also a role in migration and adhesion (Feutlinske et al., 2015; Eisenmann et al., 1999; Paňková et al., 2012; Binamé et al., 2013), including in tumour cells (Burg et al., 1998; Benassi et al., 2009). NG2/CSPG4 is present both in primary and in metastatic tumour (Cattaruzza et al., 2013; Nicolosi et al. 2015). In fact, targeting NG2/CSPG4 in glioblastoma (GBM) and in melanoma was shown to slow down tumour growth and angiogenesis (Wang et al., 2011a). The transition between a primary and a metastatic tumour may require the use of the CSPG domains to sense the cytokines secreted distally from the target-organs, and thus present at very low concentration in the vicinity of the metastasizing cancer cell.

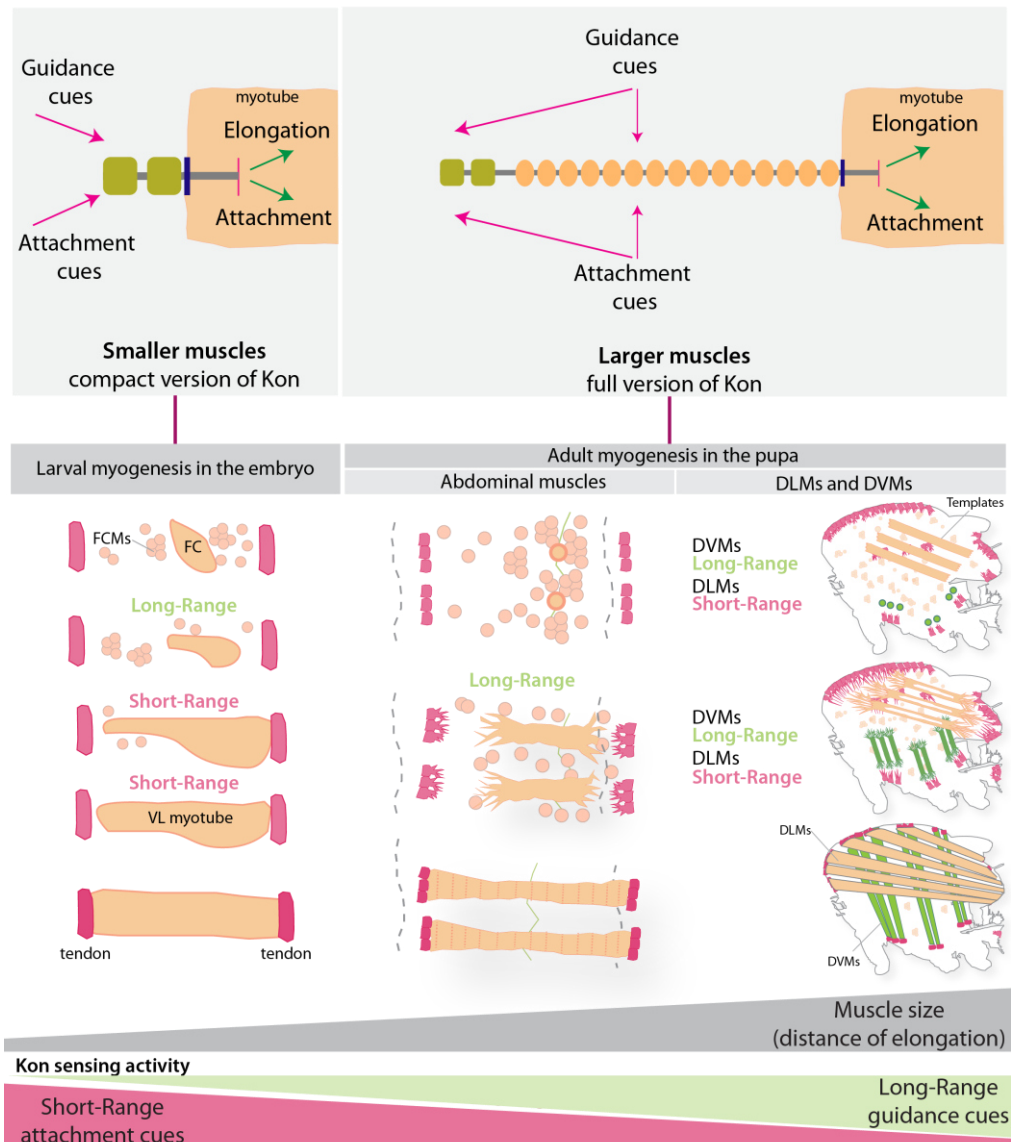


Figure 3.1. Model for the activity of Kon during *Drosophila* myogenesis

Kon customizes its activity according to the distance that the myotube has to elongate to reach the tendon cells. A compact version of Kon, missing the long CSPG domains was sufficient for the formation of smaller muscles, during larval myogenesis. However, during formation of larger muscles, in the adult myogenesis, this compact version is not sufficient, requiring thus to be synergized by the CSPG domains. Kon is likely to function according to two modes, which are characterized by long- and short-range sensing activities. These two modes are particularly distinguishable in adult myogenesis. To note that with the exception of the DLMs, the size of the muscle indicates approximately the distance that the myotube has to elongate to reach the tendon cells. The Kon long-range sensing activity is defined here as the ability to sense guidance cues secreted distally by the tendon cells. Thus, this mode is mainly required during the formation of adult muscles, whose elongation needs to be guided. In contrast, Kon short-range sensing activity contributes to myotube attachment through sensing attachment cues. These cues are exclusively in vicinity of the tendon cells, thus triggering attachment formation only when the myotube reaches the tendon cells. This mode is essential for all the muscles that require Kon for their development.

4 Conclusion

This study showed that Kon is essential for myotube guidance, thus unveiling a novel function of Kon during *Drosophila* myogenesis. Furthermore, this study identified the extracellular domain type, which renders Kon able to mediate myotube guidance, the CSPG domains. I envision that Kon mediates guidance through sensing guidance molecules secreted by the tendon cells.

The second major contribution of the study was determining for the first time how the three types of Kon protein domains interplay to mediate muscle formation in the two phases of *Drosophila* myogenesis. This study demonstrated that the participation of Kon in muscle formation is customized according to the developmental circumstances of a particular type of muscle. A compact version of Kon, missing the long CSPG domains is sufficient for the formation of smaller muscles, during larval myogenesis. However, during formation of larger muscles, in the adult myogenesis, this compact version is not sufficient, requiring thus to be synergized by the CSPG domains. Because these domain types are conserved up to humans, this study can help to understand how NG2/CSPG4 increases the metastatic potential of NG2/CSPG4 expressing tumours.

5 Material and Methods

5.1 Materials

5.1.1 General reagents

NaCl (Roth), KCl (Merck), Na₂HPO₄ (Merck), KH₂PO₄ (Merck), Triton-X (Roth), Tween (Sigma-Aldrich), MgSO₄·7H₂O (Merck), methanol (Sigma-Aldrich), n-heptane (VWR), formaldehyde 37 % v/v stock, methanol free (Roth), ethanol (Sigma-Aldrich), Tris base (Sigma-Aldrich), glycine (Sigma-Aldrich), NP-40 (Fluka), Nipagin (Sigma-Aldrich), sucrose (Merck) and SDS pellets (Sigma-Aldrich).

5.1.2 Molecular biology reagents and equipments

5.1.2.1 General reagents

Deoxynucleotides (dNTP) solution mix (NEB), Phusion polymerase (NEB), 5xPhusion buffer (NEB), Taq polymerase (NEB), 10x Taq buffer (NEB), ultra-pure agarose (Thermo Fisher Scientific), bacto-agar (Roth), tryptone (Roth), yeast extract (Roth), hygromycin 50 mg/ ml in H₂O (Hgr, Sigma-Aldrich), chloramphenicol (Cm, Sigma-Aldrich), kanamycin (Kan, Sigma-Aldrich), L-rhamnose (Sigma-Aldrich), *DpnI* (NEB), and dithiothreitol (DTT, Sigma-Aldrich).

5.1.2.2 Kits

DNA QIAquick Gel Extraction kit (Qiagen), MinElute PCR Purification Kit (Qiagen), and PureLink HiPure Plasmid Miniprep (Thermo Fisher Scientific).

5.1.2.3 Equipments

C1000 Thermal cycler (BioRad), NanoDrop (Thermo Fisher Scientific), cell electroporator (Eppendorf 2510), electroporation cuvettes 1mm

(Eppendorf), benchtop centrifuge 5424 (Eppendorf), and Minitron incubator (Infors HT).

5.1.2.4 Recombineering using *kan* resistance for selection

5.1.2.4.1 Bacteriological reagents

Arabinose (Sigma-Aldrich) and anhydrotetracycline 0.2 mM in ethanol (Clontech).

5.1.2.4.2 Solutions and media

Lysogeny broth (LB): 10 g tryptone, 5 g yeast extract, and 10 g NaCl were dissolved in ddH₂O to make a total of 1 L. The mixture was then autoclaved.

LB agar: 10 g tryptone, 5 g yeast extract, 10 g NaCl, and 15 g bacto-agar were dissolved in ddH₂O to make a total of 1 L. The mixture was then autoclaved. Next the medium was let to cool down until approximately 55 °C, and antibiotics were added to yield the following combinations: LB plates Cm15 µg/ ml, LB plates Cm15/ Hgr20 µg/ ml, and LB plates Cm15/ Hgr50/ Kan30 µg/ml.

5.1.2.4.3 Bacterial strains, plasmids and oligonucleotides

Fosmid clone *FlyFos021621*. The genomic fragment from this clone contained the *Drosophila* genomic region 2L: 18,473,884 to 18,518,106. EPI300 *E. coli* strain (Epicentre) hosted the fosmid. The resistance gene from the *FlyFos* vector is *cat* (chloramphenicol resistance). The *Flyfos* is a single copy plasmid. In presence of arabinose, there is shift to high copy number (Ejsmont et al., 2009; 2011).

Plasmid *pRedFLp4* contains a λ -derived Red α,β,γ operon, which is inducible by L-rhamnose. The operon is composed of three enzymes: Red α , 5'-3' exonuclease, Red β , a DNA annealing protein, and Red γ , an inhibitor of the major *E. coli* exonuclease and recombination complex, RecBCD. This plasmid also contains a flippase, Flp70L,

under the control of the *tetP* promoter and inducible by anhydrotetracycline. This plasmid is thermosensitive, and thus it is not replicated when the bacteria are incubated over 30 °C (Ejsmont et al., 2009; 2011).

Plasmid *pR6K* carries either *GFP* or *V5* tag sequences between *2xTY1* and *3xFLAG* sequences. *pR6K* contains *amp* and *kan*. The *pR6K* can only be amplified in a *pir+* host strain. The *GFP* and *V5* tags were amplified with oligonucleotides that were 70-bp long and HPLC purified (**Table 5.1**).

Table 5.1. List of oligonucleotides for recombineering using *kan* resistance

Oligos	Sequence
<i>GFPaSS1</i>	TCTCAATTTGCCCATACCCATGTCTATGTCTATCCTATCCACCCACAG TTGAAGTGCATACCAATCAGGACCCGC
<i>GFPaSS2</i>	ATCTTGGCCTCCTGCAGCGGCATCGATACGTAGCCATCGCCGAAGA GGGACTTGTGTCGTCATCCTTGTAGTCA
<i>V5intra1</i>	TGCTGTTGATATTAAGATCAGGAAACTGAGAAAGCACAAGGCAGA TATA GAAGTGCATACCAATCAGGACCCGC
<i>V5intra2</i>	ACAGAAGTCAAGTCTGGTGGACACGGTAGCGCCGGCGGCTGATCC TTGGA CTTGTCGTCGTCATCCTTGTAGTCA

5.1.2.5 Recombineering using *galk* selection

5.1.2.5.1 Bacteriological reagents

D-biotin (Roth), galactose (Sigma-Aldrich), 2-deoxy-galactose (DOG, Sigma-Aldrich), glycerol (Sigma-Aldrich), L-leucine (Sigma-Aldrich), and MacConkey mixture (Roth).

5.1.2.5.2 Solutions and media

Aqueous solutions: 0.2 mg/ ml D-biotin, 20% m/v galactose, 20% m/v 2-deoxy-galactose, 20% m/v glycerol, 10 mg/ ml L-leucine, and 1 M MgSO₄·7H₂O.

1x M9 buffer: 6 g Na₂HPO₄, 3 g KH₂PO₄, 1 g NH₄Cl, and 0.5 g NaCl, were dissolved in ddH₂O to a final volume of 1 L and autoclaved.

5X M63: 10 g $(\text{NH}_4)_2\text{SO}_4$, 68 g KH_2PO_4 , and 2.5 mg $\text{FeSO}_4 \cdot 7\text{H}_2\text{O}$, were dissolved in ddH₂O to a final volume of 1 L, followed by adjusting the pH with KOH to 7 and autoclaving.

M63 minimal plates with galactose: 20 g agar was dissolved in 800 ml ddH₂O and autoclaved. Then 200 ml 5x M63 medium and 1 ml 1M $\text{MgSO}_4 \cdot 7\text{H}_2\text{O}$ were added together with 10 ml 20% m/v galactose (final concentration 0.2%), 5 ml 0.2 mg/ml biotin (1 mg), 4.5 ml 10 mg/ml L-leucine (45 mg), 1 ml 15 mg/ml chloramphenicol (final concentration 15 $\mu\text{g}/\text{ml}$) and 1 ml 50 mg/ml hygromycin (final concentration 50 $\mu\text{g}/\text{ml}$).

M63 minimal plates with 2-deoxy-galactose (DOG): 20 g agar were dissolved in 800 ml ddH₂O and autoclaved. Then 200 ml 5x M63 and 1ml 1M $\text{MgSO}_4 \cdot 7\text{H}_2\text{O}$ were added together with 10 ml 20% m/v glycerol (final concentration 0.2%), 10 ml 20% 2-deoxy-galactose (final concentration 0.2%), 5 ml 0.2 mg/ml biotin (1 mg), 4.5 ml 10 mg/ml L-leucine (45 mg) and chloramphenicol (final concentration 15 $\mu\text{g}/\text{ml}$).

MacConkey indicator plates: 50 g MacConkey mixture was autoclaved in 1 L ddH₂O. Then chloramphenicol (final concentration 15 $\mu\text{g}/\text{ml}$) and hygromycin (final concentration 50 $\mu\text{g}/\text{ml}$) were added.

5.1.2.5.3 Bacterial strains, plasmids and oligonucleotides

SW102 bacterial strain and the *galk* plasmid were generated by Warming and his colleagues (Warming et al., 2005). The *galk* cassette was amplified with oligonucleotides that were 70-bp long and HPLC purified (**Table 5.2**).

Table 5.2. List of oligonucleotides for recombineering using *galk* selection

Oligos	Sequence
<i>galkLamG1</i>	TCTCAATTTGCCCATACCCATGTCTATGTCTATCCTATCCACCCACA GTTCTGTGGACAATTAATCATCGGCA
<i>galkLamG2</i>	ATGGGTGAGACATAGAGCAGCTCTAGCTCTGGACTGGTTTCTGTGA AGATTCAGCACTGTCCTGCTCCTT
<i>galkCSPG1</i>	TCATCTGCTACTGCGATCAGTCTACTGCATCAAGGCCGATTTTCAG GGACCTGTGGACAATTAATCATCGGCA
<i>galkCSPG2</i>	TTAATGGATAATCCTGCACTGCCAAATGAACCGTCTCGGTTTCCTC AACTCAGCACTGTCCTGCTCCTT
<i>galkPDZ-BD1</i>	ATGCCTCTGTGCCACAAAGTATTTCCGGATCGGTACAGCTCACCGCC CTCGCCTGTGGACAATTAATCATCGGCA
<i>galkPDZ-BD2</i>	AATAACCTAGGACTAATTCGGATCGAATTGGAAACGTTGTATTGAT CCCTCAGCACTGTCCTGCTCCTT
<i>HAaSS1</i>	TCTCAATTTGCCCATACCCATGTCTATGTCTATCCTATCCACCCACA GTTCTGTGGACAATTAATCATCGGCA
<i>HAaSS2</i>	ATCTTGGCCTCCTGCAGCGGCATCGATACGTAGCCATCGCCGAAGA GGGATCAGCACTGTCCTGCTCCTT
<i>GFPintra1</i>	TGCTGTTGATATTAAGATCAGGAAACTGAGAAAGCACAAAGGCAGA TATACCTGTGGACAATTAATCATCGGCA
<i>GFPintra2</i>	ACAGAAGTCAAGTCTGGTGGACACGGTAGCGCCGGCGGCTGATCC TTGGATCAGCACTGTCCTGCTCCTT

5.1.3 Fly reagents

5.1.3.1 List of fly lines

The fosmid were injected into embryos from the fly line, *y[1], w[*], P{nos-phiC31\int.NLS}X; PBac{y+-attP-3B}VK00033 (BL-32542)* (Venken et al., 2006). The resulting F0 generation was crossed with *y,w; Ly/TM3, Sb*.

To do the functional assay, the constructs were crossed into a *kon* mutant background (*kon* null alleles *c1139* and *c25* (Schnorrer et al., 2007)).

Fly lines for visualization of the muscles: *y,w; Mef2-GAL4, UAS-Gma-GFP/TM3,Sb*, and *y,w; Mef2-GAL4, UAS-Gma-mCherry/TM3,Sb*.

5.1.4 Food for maintenance of fly stocks and collection of embryos

All fly stocks were grown on standard cornmeal medium at 25 °C.

Plates for the collection of embryos: 17.5 g agar and 25 g sucrose were dissolved in 750 ml of dH₂O and autoclaved. The mixture was let to cool down until 55 °C, followed by the addition of 250 ml apple juice and 10 ml 15 % m/v Nipagin (in ethanol).

5.1.4.1 Dissection tools and materials

Oil Voltalef 10S (Lehmann & Voss), FemtoJet set-up 805 (Eppendorf 5247), forceps No 5 (Fine Science Tools), scissors No. 15000-02 (Fine Science Tools), and double-sided tape (Tesa).

5.1.5 Immunofluorescence reagents

5.1.5.1 General solutions

1xPBS: 8 g NaCl, 0.2 g KCl, 1.42 g Na₂HPO₄, and 0.24 g KH₂PO₄ in 1 L ddH₂O.

50% bleach (Danklorix) in ddH₂O, 1x PBS 0.1% Triton-X, 1x PBS 0.2% Triton-X, 70% methanol in 1x PBS, 50% methanol in 1x PBS. 3.7 % formaldehyde in 1x PBS.

Heat fixation solution for embryos: 3 ml Triton-X and 40 g NaCl were dissolved in ddH₂O up to the final volume of 1L.

Fixation solution for adult muscles: 4 % paraformaldehyde in 1x PBS.

5.1.5.2 Antibodies

Primary antibodies: mouse anti-Collagen IV (gift from Lisa Fessler), rabbit anti-GFP 1:1000 (Amsbio), mouse anti-GFP 1:500 (Millipore-Merck), rabbit anti-Kon (Schnorrer et al., 2007), anti-Integrin βPS 1:200 (DSHB), rat anti-Mhc 1:200 (Babraham Institute), mouse anti-Shot 1:10 (DSHB), mouse anti-Talin A22A 1:200 (DSHB), mouse anti-

Talin E16B 1:200 (DSHB), mouse anti-Tiggrin 1:500 (gift from Lisa Fessler), rat anti-Thrombospondin 1:500 (gift from Talila Volk), rabbit anti- β 1-tubulin 1:1000 (gift from Detlev Buttgereit), rabbit anti- β 3-tubulin 1:1000 (gift from Renkawitz-Pohl) and mouse anti-V5 1:500 (Thermo Fisher Scientific).

Secondary antibodies: anti-mouse IgG Alexa Fluor 488, anti-mouse IgG Alexa Fluor Alexa 633, anti-rabbit IgG Alexa Fluor 488, anti-rabbit IgG Alexa Fluor 633, anti-rat IgG Alexa Fluor 488, anti-rat IgG Alexa Fluor 568 and rhodamine phalloidin. All the secondary antibodies were diluted 1:500 and purchased from Thermo Fisher Scientific.

5.1.5.3 Mounting materials and solutions

Glass slides (Thermo Fisher Scientific), cover glasses #1.5 (Marienfeld-Superior), plastic scaffolds (MPI workshop), Vectashield mounting medium with DAPI (Vector laboratories), and 50 % glycerol in ddH₂O,

5.1.6 Biochemical reagents

5.1.6.1 Western blot analysis

5.1.6.1.1 Solutions

Running buffer: 1x NuPage Tris-acetate SDS running buffer (ThermoFisher Scientific).

Towbin buffer without methanol (transfer buffer): 3.03 g Tris base and 14.4 g glycine were dissolved in 1 L ddH₂O.

Washing solutions: 0.1% Tween in 1x PBS.

Blocking solution: 5 % nonfat dry milk (Bio-Rad) in 1x PBS 0.1% Tween.

5.1.6.1.2 Antibodies

HRP conjugates: Goat anti-rabbit IgG (H+L)-HRP conjugated and Goat anti-mouse IgG (H+L)-HRP conjugated (Jackson ImmunoResearch Laboratories), dilution 1:10,000.

5.1.6.1.3 Materials and equipments

Tissue grinder 1 ml (Wheaton), NuPageTris-acetate 3-8% precast gels (Thermo Fisher Scientific), PageRuler Plus Prestained Protein Ladder (Thermo Fisher Scientific), MagicMark XP Western Protein Standard (Thermo Fisher Scientific), PVDF transfer membrane, pore size 0.45 μm (Millipore-Merck), Whatman cellulose chromatography paper 3 MM Chr (GE Healthcare), Immobilon Western chemiluminescent HRP substrate (Millipore-Merck), XCell SureLock Mini-Cell electrophoresis chamber (Thermo Fisher Scientific), DynaMag-Spin Magnet (Thermo Fisher Scientific), and ImageQuant LAS 4000 (GE Healthcare).

5.1.6.2 Immunoprecipitation

5.1.6.2.1 Buffers

1x Basic buffer (Hubner et al., 2010): 150 mM NaCl, 50 mM Tris-HCl and 5 % glycerol

Lysis buffer (Hubner et al., 2010): 150 mM NaCl, 50 mM Tris-HCl, 5 % glycerol, 1% NP-40, 1 MgCl₂ and 1x Protease inhibitor, EDTA free (Roche)

Washing buffer I (Hubner et al., 2010): 150 mM NaCl, 50 mM Tris-HCl, 5 % glycerol and 0.05% NP-40

Washing buffer II (Hubner et al., 2010): 150 mM NaCl, 50 mM Tris-HCl and 5 % glycerol

Elution buffer: 50mM Tris-HCl (pH 6.8), 1% SDS and 1mM DTT

I-PER Insect cell protein extraction buffer (Thermo Fisher Scientific)

5.1.6.2.2 Antibodies, peptides and immunoprecipitation beads

Rabbit anti-Kon antibody 1:10,000 (Schnorrer et al., 2007) and mouse anti-V5 (Thermo Fisher Scientific) 4 µg per 50 µl of magnetic beads.

Peptides with the N-terminal coupled with biotin (synthesized in the core facility of the MPI of Biochemistry), (**Table 5.3**).

Dynabeads coupled with G protein (ThermoFisher Scientific), Magnetic beads coupled with GFP antibody or HA antibody (Miltenyi Biotec) and Dynabeads MyOne Streptavidin C1 (ThermoFisher Scientific).

Table 5.3. PDZ-BD peptides used for pull-down experiments

Peptides	Sequence
Kon PDZ-BD	ISGSVSSPPSAPPTNPLLRRNQYW V
Kon PDZ-BDmutated	ISGSVSSPPSAPPTNPLLRRNQYW G

5.1.7 Software packages

Fiji (Eliceiri et al., 2012), Adobe Illustrator CS5, and GraphPad Prism.

5.2 Methods

5.2.1 Generating *kon* constructs and transgenic flies

5.2.1.1 Engineering tagged versions of *kon*

The following protocol was adapted from a liquid culture system optimized to tag genes from the *Drosophila* genomic fosmid library (Ejsmont et al., 2009; 2011), (**Figure 5.1**).

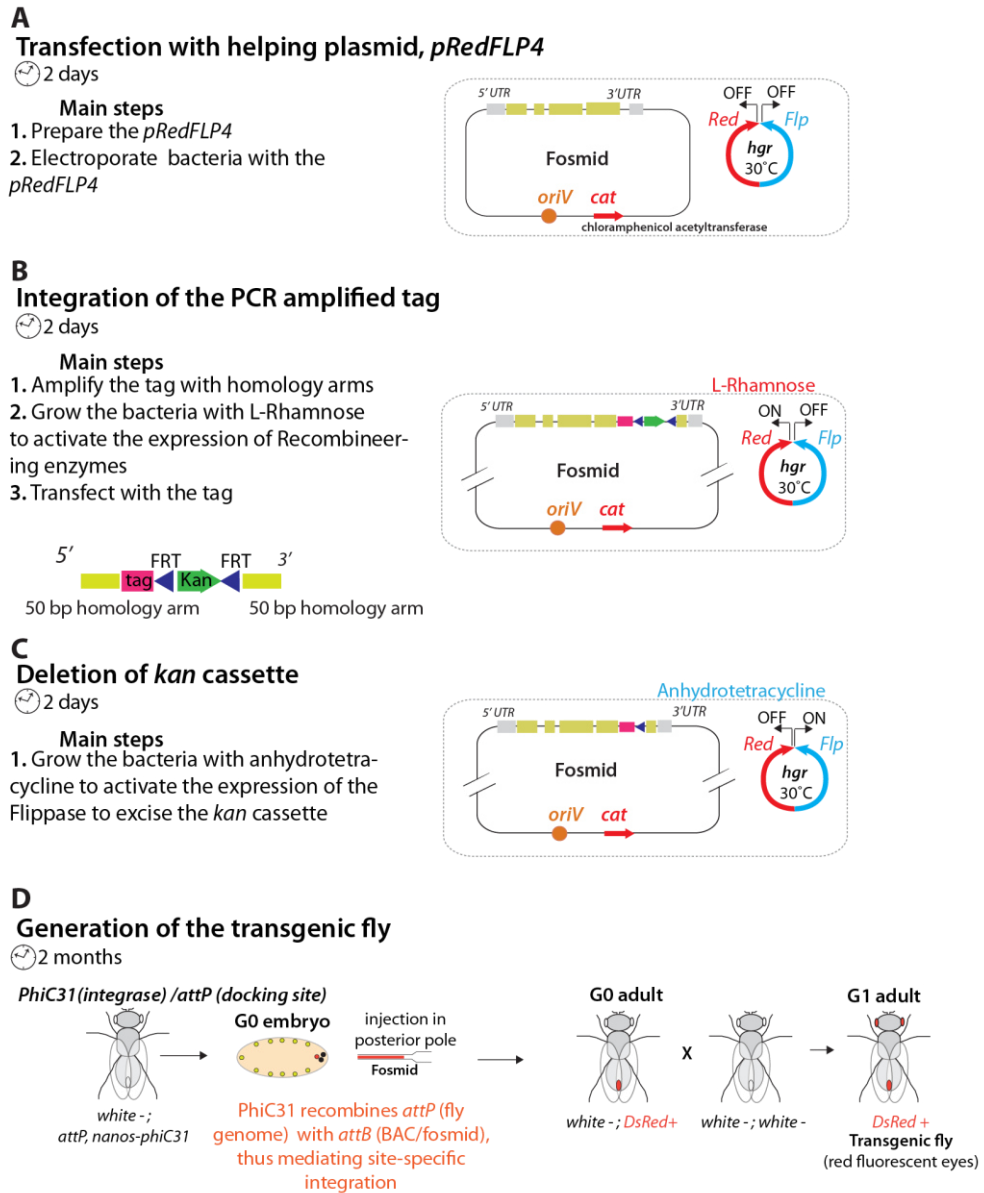


Figure 5.1. Workflow for generating a tagged version of *kon* (FlyFos021621)

(A) The fosmid is tagged through recombineering in bacteria (Ejsmont et al., 2009). The fosmid clone FlyFos021621 is hosted by EPI300 *E. coli* strain (Epicentre). The resistance gene from the *FlyFos* vector is *cat* (chloramphenicol resistance). The *Flyfos* is a single copy plasmid. EPI300 *E. coli* are electroporated with the helping plasmid *pRedFLP4*, whose resistance is *hygromycin*.

(B) The expression of the recombineering enzymes from *pRedFLP4* is induced with L-rhamnose. These enzymes induce the integration of the cassette with the homology arms into the *FlyFos021621*. Integration of the cassette confers resistance to kanamycin.

(C) The expression of *FLP4* flippase from *pRedFLP4* is induced with anhydrotetracycline. *FLP4* mediates *kan* cassette excision.

(D) The tagged fosmid is injected into *PhiC31 (integrase) / attP (docking site)* embryos for generating a transgenic fly line.

The tag is inserted through homologous recombination mediated by enzymes expressed from a helping plasmid, *pRed/Flp4*. The tag cassette, in addition to *GFP* or *V5*, contains a *kan* resistance gene. *kanamycin* resistance is rendered by successfully integrating the tag (**Figure 5.2**).

I applied this workflow to insert either a *V5* or a *GFP* tag in *kon*, included in the clone *FlyFos021621* from the genomic fosmid library (**Figure 5.2**).

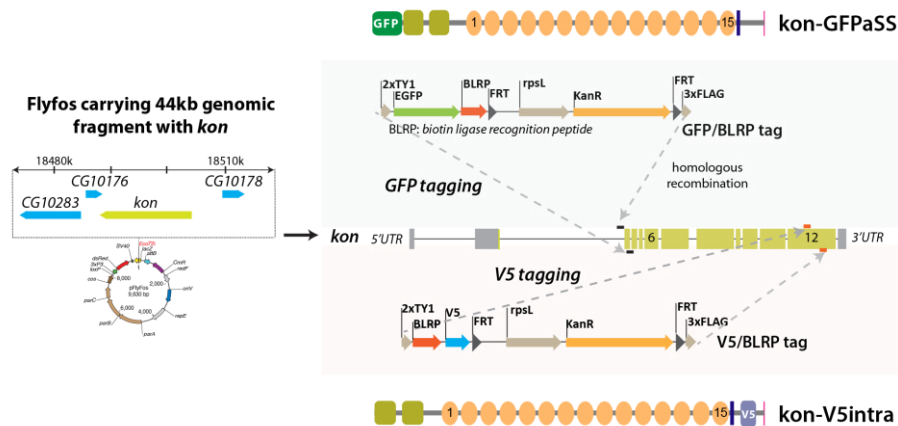


Figure 5.2. Tagging *kon* (FlyFos021621) either with a *GFP* or a *V5* tag

The *GFP*-containing tag is composed of *2xTY1*, *EGFP*, *BRLP* (biotin ligase recognition peptide), *kanR* (kanamycin resistance) flanked by two *FRTs*, and *3xFLAG*. This cassette was amplified with homology arms for the region after the signal sequence (SS). The *V5*-containing tag is composed of *2xTY1*, *BRLP*, *V5*, *kanR* (kanamycin resistance) flanked by two *FRTs*, and *3xFLAG*. This cassette was amplified with homology arms for the region after the transmembrane domain.

5.2.1.1.1 Amplifying a *GFP* tag and a *V5* tag for homologous recombination

The *GFP* and *V5* tags were amplified with oligonucleotides that were 70-bp long and HPLC purified (**Table 5.1**). Each oligonucleotide included a 20-bp sequence that pairs with the tag cassette and a minimal homology arm of 50-bp that recombines with the loci where the tag was inserted (**Figure 5.2**). Phusion polymerase amplified both the *GFP* and the *V5* tags. The PCR program: 95 °C 3 min; 98 °C 30 sec, 67 °C 30 sec, 72 °C 60 sec, 20-25 amplification cycles; 72 °C 10

min. The PCR reaction was run on a 1 % w/v agarose gel. Next the band with the correct size was excised. The DNA in the agarose fragment was purified with QIAquick Gel Extraction kit according to the manufacture instructions. The resulting eluate was then concentrated by ethanol precipitation. In summary, 0.1 volume sodium acetate (3 M, pH 5.6), 2.5 volumes 100% ethanol and 1 μ l glycogen (1 mg/ ml) were added to the eluate followed by briefly vortexing it. The solution was then incubated at -20 °C for 20 min. After the incubation, the solution was centrifuged at 4 °C, for 15 min at 20,000 x *g*. The supernatant was carefully removed and then the pellet was washed two times with 150 μ l 70% ethanol. After the second washing step, the pellet was let to air dry for 5 min, and then it was dissolved in 10 μ l ddH₂O. The concentration was measured using NanoDrop accordingly to the manufacture instructions. The eluate was then diluted with ddH₂O to a concentration of 200 ng/ μ l and stored at -20°C until section **5.2.1.1.3**.

5.2.1.1.2 Transforming the bacteria containing the fosmid FlyFos021621 with *pRed/Flp4*

The fosmid clone *FlyFos021621* (Ejsmont et al., 2009) was plated onto LB agar containing 15 μ g/ ml chloramphenicol and incubated at 37 °C overnight. A single colony was then picked and inoculated into 1 ml LB medium with 15 μ g/ ml chloramphenicol and incubated overnight at 37 °C under constant agitation. 20 μ l of overnight culture were inoculated in 1 ml LB medium with 15 μ g/ ml chloramphenicol and incubated at 37 °C to a optical density of 0.4 at a wavelength of 600 nm (OD600). The bacteria were then incubated on ice for 5 min followed by centrifugation at 10,000 x *g*, for 30 sec at 2 °C. The supernatant was discarded and the pellet resuspended in 1 ml ice-cold ddH₂O by pipetting slowly up and down three times. The washing process was repeated two more times. The pellet was resuspended in 50 μ l ddH₂O and 1 μ l *pRedFlp4* 100 ng/ μ l was added to the cell suspension, followed by 1 min incubation on ice. The cell suspension was

transferred to a chilled electroporation cuvette and electroporated at 1800 V for 5.6 ms using Eppendorf 2510 electroporator apparatus according to the manufacturer instructions. After electroporation, 1 ml LB medium without antibiotics was pipetted into the cuvette. The cell suspension was then incubated at 30 °C for 2 h under constant agitation. To note that *pRed/FLP4* is not replicated when the bacteria are incubated above 30 °C. After the incubation, 100 µl culture was transferred to 1 ml LB medium with 15 µg/ ml chloramphenicol and 20 µg/ ml hygromycin. The bacteria were incubated overnight at 30 °C until the culture was saturated.

5.2.1.1.3 Tagging by inducing the expression of the Red operon from *pRed/Flp4* with L-rhamnose

60 µl overnight culture was transferred to a new tube containing 1.5 ml LB medium with 15 µg/ ml chloramphenicol and 50 µg/ ml hygromycin. The bacteria were then incubated at 30 °C until the culture reached an OD600 of 0.2. After that 35 µl 25 % L-rhamnose solution was added to induce expression of the Red operon. The bacteria were incubated a second time at 30 °C until the culture OD600 reached 0.8. The bacteria were then placed on ice for 2 min followed by three washing steps with ice-cold ddH₂O. After washing, the pellet was resuspended in 50 µl ddH₂O, and 1 µl amplified tag 200 ng/ µl (section **5.2.1.1.1**) was added. The cell suspension was transferred to a chilled electroporation cuvette and electroporated at 1800 V for 5.6 ms using Eppendorf 2510 electroporator apparatus according to the manufacturer instructions. After electroporation, 1 ml LB medium without antibiotics was pipetted into the cuvette and incubated for 2.5 hours at 30 °C under constant agitation. 100 µl was transferred to a new tube containing 1.5 ml of LB 15 µg/ ml chloramphenicol, 50 µg/ ml hygromycin and 30 µg/ ml kanamycin and incubated at 30 °C until the culture was saturated (30 hrs).

5.2.1.1.4 Excising the *kan* resistance cassette

10 µl overnight saturated tagged culture was transferred to 1.5 ml LB 15 µg/ ml chloramphenicol, 50 µg/ ml hygromycin and 200 nM Tet, and incubated at 30 °C until the culture was saturated (16-20 hrs). Tet activates the transcription of the flippase from *pRed/Flp4*, which in turn excises the *kanamycin* gene by homologous recombination of the two *FRTs* flanking the *kan* gene.

5.2.1.1.5 Eliminating the *pRed/Flp4*

The excision of the *kan* resistance gene was followed by the elimination of the plasmid *pRed/Flp4*. 10 µl of the saturated tagged culture was transferred to 1.5 ml LB 15 µg/ ml chloramphenicol and incubated at 37 °C until the OD600 have reached 0.6. Glycerol stocks (15 %) were made for long-term storage of the clones. In summary, 150 µl of glycerol was added to 850 µl of the culture. The mixture was then vigorously vortexed until the bacteria were properly mixed with the glycerol. Next, the bacteria were frozen in liquid nitrogen and stored at -80 °C. To verify the elimination of the *kan* cassette, 4-5 colonies were analysed by colony PCR. The entire region predicted to be affected by the recombination was then sequenced.

5.2.1.1.6 Preparing fosmid DNA to generate transgenic flies

One of the correct clones was inoculated in 1ml LB 15 µg/ ml chloramphenicol and incubated at 37 °C overnight. Next, the overnight culture was diluted in 9 ml LB 15 µg/ ml chloramphenicol in presence of arabinose 0.1% to induce the amplification of the fosmid in high copy. The bacteria were incubated at 37 °C for 5 h under constant agitation. After the incubation, the bacteria were centrifuged for 10 min at 4 °C, 6,000 x *g*. The fosmid DNA was purified with PureLink HiPure Plasmid DNA Purification Kit according to the manufacturer's instructions with some modifications. In brief, the pellet was resuspended until homogeneous with 0.4 ml Resuspension Buffer (R3)

containing RNase A. Then 0.4 ml Lysis Buffer (L7) was added and the mixture was gently inverted five times. Next, the lysate was incubated at room temperature for 4 min, followed by the addition of 0.4 ml Precipitation Buffer (N3). The mixture was immediately inverted and incubated on ice for 4 min. Then the mixture was centrifuged at 15,000 x *g* at 4 °C for 10 min. In between, a HiPure Mini Column was equilibrated by applying 2 ml Equilibration Buffer (EQ1) to the column. After the buffer drained, the supernatant was applied onto the equilibrated column. The column was then washed twice with 2.5 ml Wash Buffer (W8). To elute the DNA from the column, 850 µl Elution buffer (E4), warmed to 55 °C, was added to the column and the eluate collected. Next 595 µl isopropanol was added to the eluate, followed by centrifugation at 15,000 x *g* at 4°C for 20 min. After centrifugation, the supernatant was removed and 800 µl 70% ethanol was added to the pellet. The mixture was then centrifuged at 15,000 x *g* at 4°C for 2 min. Next, the supernatant was removed and the pellet was let to air dry for 4 min. After drying, the pellet was resuspended in 20 µl Elution buffer (EB) and let it dissolve overnight at 4°C. To remove insoluble residues, the DNA was centrifuged at 15,000 x *g*, at 4°C for 30 sec. The solution was then transferred to a new microtube and the concentration was measured. Next, the fosmid DNA was diluted to a concentration of 250 ng/ µl and kept at 4°C until the injection.

5.2.1.2 Seamlessly deleting or mutating the three main protein domain types of *kon*

To pin point the contribution of each domain type to the activity of Kon during *Drosophila* myogenesis, the *kon* fosmid tagged with V5, *kon-V5* (section **5.2.1.1**), was used as a parent construct to delete the two LamGs and the 15 CSPGs, as well as to mutate the PDZ-BD (**Figure 5.3**).

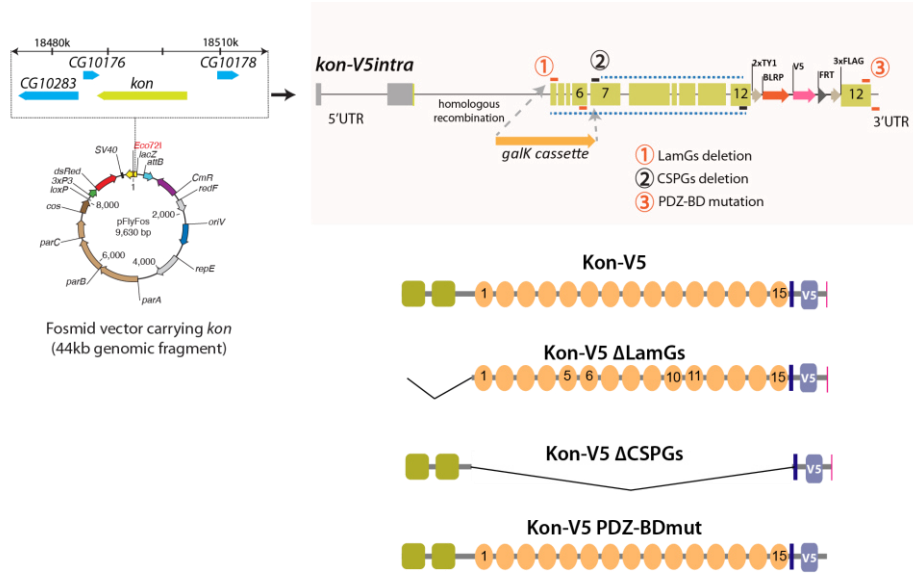


Figure 5.3. Deleting or mutating the protein domain types of *kon*
kon-V5intra is used as a parent construct either to delete or to mutate the main protein domain types of *kon*. *kon-V5intra* includes *2xTY1*, *BRLP*, *V5*, a *FRT* and *3xFLAG* after the transmembrane domain. The *Galk* system is used to engineer seamless deletions and mutations by homologous recombination in bacteria (Warming et al., 2005). A *galk* cassette is recombined with the loci flanking the region to delete or to mutate. Then the *galk* cassette is exchanged with a DNA fragment containing the sequence of the loci flanking the region deleted or mutated. Through this procedure (1) *kon-V5 ΔLamGs*, (2) *kon-V5 ΔCSPGs*, and (3) *kon-V5 PDZ-BD mutated* were generated.

kon-V5 contains one *FRT* (Figure 5.3) as the result of the excision of the *kan* cassette (section 5.2.2.1.4). Using the same protocol as before to delete or mutate the Kon domains requires a different pair of *FRTs*. A second problem of this approach is that, it does not generate seamless modification, because a *FRT* is always left behind upon excision. To overcome these two problems *Galk*-mediated selection was used (Warming et al., 2005). Warming and his colleagues developed a bacteria strain, *SW102* that is deficient for the Galactose Kinase, an enzyme from the *galactose* operon. The first step of this approach was to recombine the *galk* cassette with the loci flanking the region to modify. The ability to grow in a medium with galactose as the only carbon source indicates a successful integration of the *galk*, and thus the deletion of the region of interest. The second step was to exchange the *galk* cassette with a DNA fragment containing the sequence of the loci flanking the region modified (Figure 5.4). The

SW102 bacteria were engineered to express the recombineering enzymes upon heat shock. I used however a helping plasmid, because chemical induction was more effective than heat shock, shown by the higher number of successful integrations (data not shown).

In summary, the GalK approach was used to make seamless deletions of the two LamGs and the 15 CSPGs, as well as to mutate the PDZ-BD, by replacing the last amino acid, valine, by glycine (**Figure 5.3**)

This approach was also applied to add a N-terminal HA tag to the *kon* fosmid as well as to add a GFP tag in the intracellular part (**Figure 5.4**).

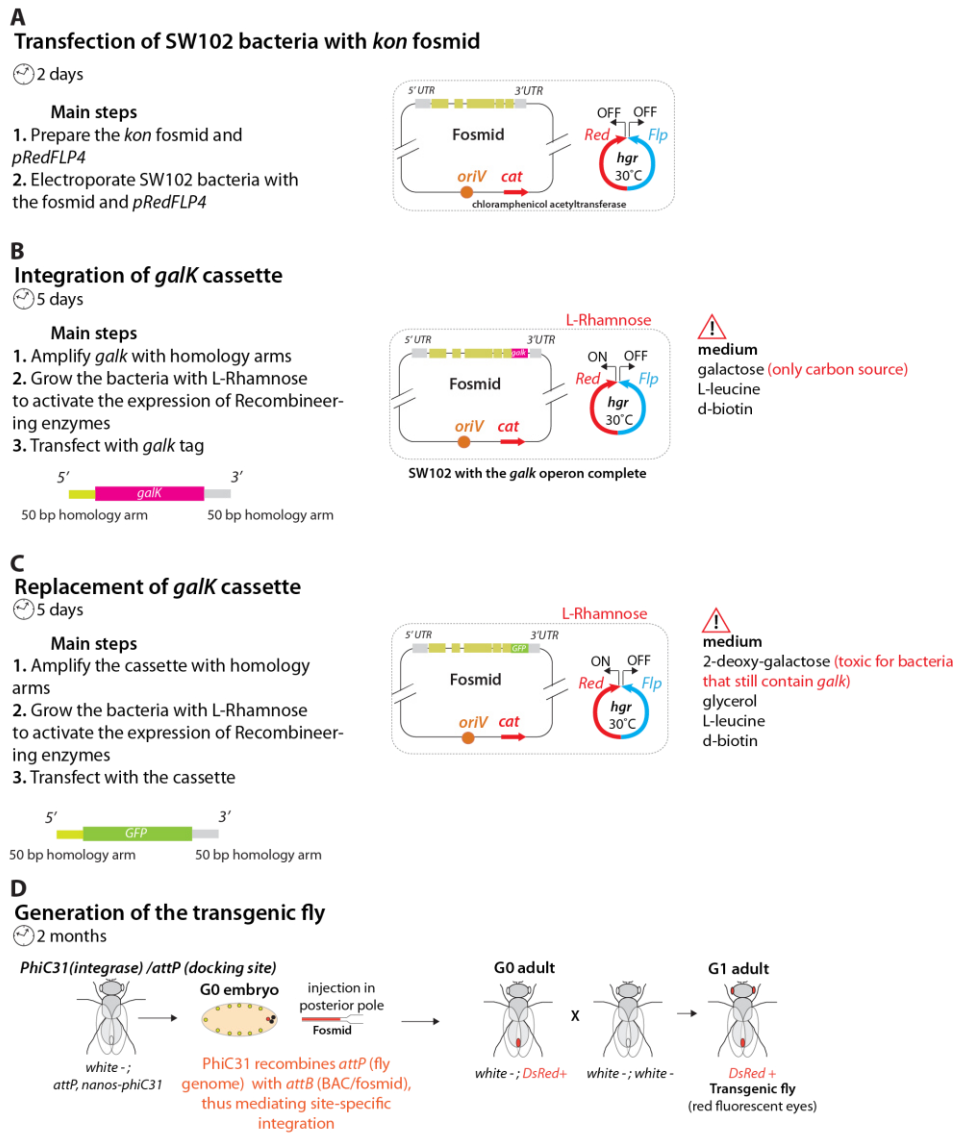


Figure 5.4. Workflow for *galk* recombineering: GFP tagging

(A) The *kon* fosmid is tagged through recombineering in bacteria. The fosmid clone *FlyFos021621* is transfected into *SW102* bacteria (Warming et al., 2005) together with the helping plasmid *pRedFLP4* (Ejsmont et al., 2009).

(B) The expression of the recombineering enzymes from *pRedFLP4* is induced with L-rhamnose. These enzymes induce the integration of the *galk* cassette with the homology arms into the *FlyFos021621*. *galk* integration renders the *SW102* bacteria able to grow in a medium with galactose as the only carbon source, which is used for selection.

(C) The second step consists in exchanging the *galk* cassette with a DNA fragment containing the sequence of interested, the *GFP* tag. This tag replaces the *galk* cassette through homologous recombination. The bacteria, which failed to mediate this step, phosphorylate 2-deoxy-galactose in the medium, producing a toxic compound.

(D) The tagged fosmid is injected into *PhiC31 (integrase) / attP (docking site)* embryos to generated a transgenic fly line.

5.2.1.2.1 Preparing the *galk* cassettes

The *galk* cassette was amplified with oligonucleotides 70-bp long and HPLC purified (**Table 5.2**). Each oligonucleotide included a region that paired with the *galk* cassette and a minimal homology arm of 50-bp to enable the cassette to recombine with the loci of interest. The *galk* cassette was amplified with Phusion polymerase. The PCR program: 95 °C 3 min; 98 °C 30 sec, 61 °C 30 sec, 72 °C 60 sec, 20-25 amplification cycles; and 72 °C 10 min. To eliminate the *galk* plasmid from the PCR mixture, and thus increasing the efficiency of selection in the subsequent steps, the PCR product was digested with *DpnI*, by adding 4 µl *DpnI* to 50 µl of reaction, followed by incubation for 2 hours at 37 °C. After digestion, the PCR reaction was run on a 1% agarose gel and then the band with the correct size was excised from the gel. The DNA was then extracted from the agarose fragment using QIAquick Gel Extraction according to the manufacture instructions. To increase the DNA concentration, the eluate of each product was concentrated by ethanol precipitation, as before described. The eluate was then diluted with ddH₂O to a concentration of 200 ng/ µl and stored at -20°C until **5.2.1.2.3**.

5.2.1.2.2 Transforming the *SW102* bacteria with *kon-V5* fosmid and *pRed/Flp4*

A *SW102* single colony was inoculated in 1 ml LB medium 10 µg/ ml tetracycline and incubated overnight at 30 °C under constant agitation. Next, 20 µl of overnight culture was inoculated in 1 ml LB 10 µg/ ml tetracycline and incubated at 30 °C until the culture reached an OD₆₀₀ of 0.4. The culture was then transferred to a microtube and incubated on ice for 5 min. After the incubation, the bacteria were centrifuged at 10,000 x *g* for 30 sec at 2 °C. The supernatant was then discarded and the pellet was resuspended in 1 ml ice-cold ddH₂O. This washing step was repeated two additional times. After the last step, the pellet was resuspended in 50 µl ddH₂O. Then 0.5 µl *pRedFlp4* 100 ng/ µl and 0.5

μl *kon-V5* fosmid $1\mu\text{g}/\mu\text{l}$ were added to the cell suspension and mixed briefly, followed by 1 min incubation on ice. The cell suspension was then transferred to a chilled electroporation cuvette and electroporated at 1800 V for 5.6 ms using an electroporator apparatus (Eppendorf 2510) according to the manufacturer instructions. After the electroporation, 1 ml LB medium without antibiotics was added to the cuvette and then the cell suspension was incubated for 2 hours at 30 °C under constant agitation. After the incubation, 100 μl of the bacteria culture was plated onto LB agar 15 $\mu\text{g}/\text{ml}$ chloramphenicol and 50 $\mu\text{g}/\text{ml}$ hygromycin. The remaining volume was centrifuged for 1 min at 4,000 x *g* and the resulting pellet resuspended in 100 μl of supernatant, which was next plated onto a LB agar 15 $\mu\text{g}/\text{ml}$ chloramphenicol and 50 $\mu\text{g}/\text{ml}$ hygromycin. The two plates were then incubated overnight at 30 °C.

5.2.1.2.3 Inserting the *galk* cassette by inducing the expression of the Red operon from *pRed/Flp4* with L-rhamnose

A single colony containing both *pRedFlp4* and *kon-V5* fosmid was inoculated in 1 ml LB medium in the presence of 15 $\mu\text{g}/\text{ml}$ chloramphenicol and 20 $\mu\text{g}/\text{ml}$ hygromycin, and incubated overnight at 30 °C under constant agitation. Two tubes containing 1.5 ml LB with 15 $\mu\text{g}/\text{ml}$ chloramphenicol and 50 $\mu\text{g}/\text{ml}$ hygromycin (one tube was used as control) were inoculated each with 60 μl of overnight culture followed by an incubation at 30 °C until the culture reached an OD600 of 0.4. The expression of the Red operon was then induced in one of the tubes by adding 35 μl of L-rhamnose 25% (the tube without L-rhamnose served as negative control). The two tubes were incubated at 30 °C until an OD600 \approx 0.7-0.8. The culture was then incubated on ice for 5 min. After the incubation, the bacteria were centrifuged for 30 sec at 2 °C, 10,000 x *g*. The supernatant was discarded and the pellet was resuspended in 1 ml ice-cold ddH₂O. This washing step was repeated two more times. After the last washing step, the pellet was

resuspended in 50 μ l ddH₂O. 1 μ l of the *galk* cassette (200-500 ng/ μ l) was added to the cell suspension (including the negative control) and mixed briefly, followed by incubation on ice for 1 minute. The cell suspension was then transferred to a chilled electroporation cuvette and electroporated at 1800 V for 5.6 ms using an electroporator apparatus (Eppendorf 2510) according to the manufacturer instructions. After the electroporation, 1 ml LB medium without antibiotics was added to the cuvette and then the cell suspension was incubated for 2.5 h at 30 °C under constant agitation. After the incubation, the bacteria were centrifuged for 30 sec at 2 °C, 10,000 x *g* and then resuspended in 1 ml ice-cold M9 buffer. This step was repeated three more times. This washing procedure aimed to eliminate all the possible carbon sources derived from LB medium. A successful integration of the *galk* cassette occurred in principle in the colonies that were able to grow on a medium that contained galactose as the only carbon source, M63 minimal plates with galactose. After the last washing step the pellet was resuspended in 1 ml M9 buffer and 100 μ l of the suspension was plated on M63 minimal plates with galactose, 15 μ g/ ml chloramphenicol and 50 μ g/ ml hygromycin. The remaining volume was centrifuged for 30 sec at 2 °C, 10,000 x *g* and the resulting pellet was resuspended in 100 μ l supernatant. The suspension was then plated on M63 minimal plates with galactose, 15 μ g/ ml chloramphenicol and 50 μ g/ ml hygromycin. The plates were incubated for 3-4 days at 30 °C. To note that, when the plate of non-induced bacteria (negative control) contained a higher number of colonies, this could mean that the *galk* cassette contained traces of the *galk* plasmid. At least 10 colonies were screened by PCR for a successful deletion/ mutation of the Kon domains through recombination with the homology arms of the *galk* cassette. The positive colonies were then streaked on MacConkey agar plates and incubated overnight at 30°C. MacConkey agar contains neutral red indicator that responds chromatically to changes of pH. A positive *galk* colony becomes purple

or rose, because the fermentation of galactose leads to a decrease of pH. A bright purple colony was selected to use on the next step.

5.2.1.2.4 Exchanging the *galk* cassette

A bright purple *galk* positive colony was inoculated in 1 ml LB 15 µg/ml chloramphenicol and 20 µg/ml hygromycin, and then incubated overnight at 30 °C under constant agitation. Two tubes containing 1.5 ml LB with 15 µg/ml chloramphenicol and 50 µg/ml hygromycin (one tube was used as control) were inoculated each with 60 µl of overnight culture followed by an incubation at 30 °C until the culture reached an OD600 of 0.2. The expression of the Red operon was then induced in one of the tubes by adding 35 µl of L-rhamnose 25% (the tube without L-rhamnose served as negative control). The two tubes were incubated at 30 °C until an OD600 ≈ 0.7-0.8. The culture was then incubated on ice for 5 min. After the incubation, the bacteria were centrifuged for 30 sec at 2 °C, 10,000 x *g*. The supernatant was discarded and the pellet was resuspended in 1 ml ice-cold ddH₂O. This washing step was repeated two more times. The supernatant was discarded and the pellet was resuspended in 1 ml ice-cold ddH₂O. This washing step was repeated two more times. After the last step, the pellet was resuspended in 50 µl ddH₂O. 1µl of the “replacing cassette” (200-500 ng/ µl) was added to the cell suspension (including the negative control) and mixed briefly, followed by incubation on ice for 1 minute. The cell suspension was then transferred to a chilled electroporation cuvette and electroporated at 1800 V for 5.6 ms using an electroporator apparatus (Eppendorf 2510) according to the manufacturer instructions. After the electroporation, 1 ml LB medium without antibiotics was added to the cuvette and then the cell suspension was incubated for 2.5 h at 30 °C under constant agitation. After the incubation, the bacteria were centrifuged for 30 sec at 2 °C, 10,000 x *g* and then resuspended in 1 ml ice-cold M9 buffer. This step was repeated three more times. After the last step the pellet was

resuspended in 1 ml M9 buffer. 100 µl of the bacteria was plated on M63 minimal plates with glycerol, DOG and 15 µg/ ml chloramphenicol. The remaining volume was centrifuged for 30 sec at 2 °C, 10,000 x *g*. The resulting pellet was resuspended in 100 µl supernatant and then plated on M63 minimal plates with glycerol, DOG and 15 µg/ ml chloramphenicol. The plates were incubated for 3-4 days at 30 °C. When the bacteria do not lose *galk*, they are able to phosphorylate DOG. When this component is phosphorylated, it becomes toxic for the bacteria. At least 10 colonies were screened by PCR for the correct integration of the replacing cassette. The positive colonies were then sent for sequencing. A glycerol stock of the correct clones was done and stored at – 80 °C.

5.2.1.2.5 Preparing fosmid DNA to generate transgenic flies

One of the correct clones was inoculated in 30 ml LB 15 µg/ ml chloramphenicol at 30 °C overnight under constant agitation. The fosmid DNA was purified with PureLink™ HiPure Plasmid DNA Purification Kit according to the manufacturer's instructions with some modifications. In brief, the overnight culture was centrifuged for 10 min at 4 °C, 6,000 x *g*. The resulting pellet was resuspended in 2 ml Resuspension Buffer (R3) containing RNase A. Next, 2 ml Lysis Buffer (L7) was added and the mixture was gently inverted five times, followed by incubation of the lysate at room temperature for 4 min. After the incubation, 2 ml Precipitation Buffer (N3) was added, and then the mixture was immediately inverted. The following steps were similar to the ones of section 5.2.1.1.6.

5.2.1.3 Generating transgenic flies

5.2.1.3.1 Injecting the constructs into *Drosophila* embryos

All the constructs generated in the sections above were injected in embryos from the fly stock $y[1], w[*], P\{nos-phiC31\int.NLS\}X; PBac\{y+-attP-3B\}VK00033$ (BL-32542). The injection procedure was

as before described (Sarov et al., 2016). In brief, embryos were collected 30 min AEL (after egg laying) and incubated in a 50 % chloride solution for 3 min to remove the chorion. The embryos were then washed abundantly with dH₂O and then aligned on a glass slide according to their A-P axis. The posterior side of the embryos was injected with the fosmid DNA using FemtoJet set-up 805. The pole cells, located in the posterior pole, give rise to the germ line. After the injection, the embryos were covered with a thin layer of oil Voltalef 10S to prevent their dehydration and incubated at 18 °C for 3 days, in a wet chamber, until their eclosion. The larvae, designated as generation F₀, were then collected into a vial with fly food and incubated at 25 °C until the adult stage.

5.2.1.3.2 Crossing and screening for the genomic integration of the constructs

The F₀ flies were single crossed with *Ly/ TM3, Sb* flies. The flies were then incubated at 25 °C for 10 days. The offspring of those single crosses, F₁ generation, was screened for the presence of red fluorescent eyes, an indicator of a successful integration of the fosmid into the fly genome. The *FlyFos* carries a selectable marker, *dsRed*, which is driven by a dominant eye-promoter (Ejsmont et al., 2009).

5.2.2 Analysing the muscular phenotype from the transgenic flies

5.2.2.1 Analysing the development of the larval somatic musculature

5.2.2.1.1 Collecting, fixing and staining embryos

Flies were transferred to a plastic cylindrical cage, containing on one of the sides a porous net to allow the ventilation of the cage, and on the other side an agar plate with 20 % apple juice and with yeast past. Flies were kept at 25 °C during embryo collection. The collection

schedule was designed to have a population of embryos enriched for the interval between stage 15 and stage 17. The embryos were then preserved for staining by either methanol or heat fixation. The step that preceded both types of fixation was the removal of the chorion. To remove the chorion, the embryos were incubated for 3 min in an aqueous solution with 50 % bleach. During the incubation, the embryos were detached from the agar surface by gently brushing it. For methanol fixation, the resuspended embryos were poured into a funnel with a mesh and abundantly washed with dH₂O. The embryos were then transferred from the mesh into a small glass flask by pipetting 5 ml heptane onto the bottom side of the mesh, which was beforehand attached to the opening of the container. Then 5 ml 3.7 % formaldehyde in 1x PBS freshly prepared was added, followed by an incubation of 20 min under strong agitation. Then the mixture was let to rest for one min, to allow (1) the embryos to sink at the bottom, and (2) heptane and the 3.7 % formaldehyde solution to separate according to their density. The 3.7 % formaldehyde solution, which is the lower phase, was removed with a Pasteur pipette glass, then 5 ml of methanol was added, and the mixture strongly agitated for 1 min to remove the vitelin membrane. The mixture was allowed to rest for 1 min to let the embryos sink, and then the embryos were collected. The embryos were then washed two times with pure methanol and stored at – 20 °C until the staining procedure.

For the heat fixation, the embryos, after the incubation with 50 % bleach, were poured into a funnel containing a mesh. After that, they were washed shortly with PBS 0.3 % Triton-X and then abundantly with dH₂O. The embryos were then transferred with a small brush into a small glass flask containing 5 ml boiling Heat fixation solution. After stirring the embryos gently for some seconds, 15 ml ice-cold Heat fixation solution was added to the flask followed by vigorous shaking. The embryos were then incubated on ice for 1 min. After the incubation, the embryos were let sink and the solution was completely

removed with a pipette. 5 ml n-heptane followed by 5 ml methanol was added. The mixture was vigorously shaken for 1 min and then the embryos were let to sink. Next, the embryos were washed two times with pure methanol and stored at $-20\text{ }^{\circ}\text{C}$ until the staining procedure.

For staining, the embryos were rehydrated with solutions with decreasing methanol content diluted in 1X PBS: first with 70 % methanol, second with 50 % methanol and finally only with 1X PBS. Then the embryos were washed three times with PBS 0.1 % Triton-X, followed by an incubation with blocking solution, 5 % goat serum in 1X PBS 0.1 % Triton-X, for 1 hour. After the blocking, the embryos were incubated with the primary antibodies (*Materials, section 5.1.5.2*) diluted in 1X PBS 0.1 % Triton-X, overnight at $4\text{ }^{\circ}\text{C}$ with slow agitation. Then they were washed three times with PBS 0.1 % Triton-X during 45 min in total, followed by incubation with the secondary antibodies (*Materials, section 5.1.5.2*) diluted in 1X PBS 0.1 % Triton-X for 2 hours in the dark. The embryos were then washed three times with 1X PBS 0.1 % Triton-X for a total time of 45 min. After the last washing step, the embryos were dispersed with Vectashield on a microscope slide between two cover slippers, which functioned as spacers. These spacers prevented that the top cover slipper smashed the embryos. To finalize, the interface between the slide and the cover slippers was sealed with transparent nail polish. The slides were stored at $4\text{ }^{\circ}\text{C}$ and protected from the light until imaging.

5.2.2.1.2 Imaging L3 larvae

L3 larvae were immersed for 1 sec in water at $65\text{ }^{\circ}\text{C}$ and then mounted on a slide with an aqueous solution of 50 % glycerol followed by immediate imaging at the confocal microscope. The ventral longitudinal muscles (VL) were imaged for phenotype quantification with LSM 780 confocal microscope. The images were then processed with Fiji (Eliceiri et al., 2012) and Adobe Illustrator CS5.

5.2.2.1.3 Measuring the VL length and attachment site size

To assess the biological activity of the diverse tagged/deleted/mutated versions of Kon, the length of the VL1 muscle of the diverse genotypes was measured. For unambiguous identification of the VL1 muscles, GFP was expressed specifically in the VL1 muscle with a *5053-GAL4* driver. The image stack of each embryo was projected with Fiji, so that the borders of the VL1 muscles were clearly visible. The length was also measured with Fiji. The resulting values were analysed statistically by Tukey's multiple comparison test in GraphPad Prism.

To measure the attachment site, the VL1 muscles were stained with Talin, which is normally present at the muscle attachment sites. The image stack of each embryo was projected with Fiji, so that the attachment sites of the VL muscles were clearly visible. The attachment site size was then measured with Fiji. The resulting values were analysed statistically by Tukey's multiple comparison test in GraphPad Prism.

5.2.2.1.4 Measuring the protein enrichment at the muscle attachment site

Stages 15-17 embryos from the following genotypes were collected: *kon-V5*, *kon-V5 ΔLamGs*, *kon-V5 ΔCSPGs*, *kon-V5 PDZ-BDmut* and as negative control, *w-* embryos. These embryos were fixed by Heat fixation and then stained with rabbit anti-β3-tubulin 1:1000 and mouse anti-V5 1:500 (section **5.2.2.1.1**). The image stack of each embryo was projected with Fiji, so that the attachment site of each VL muscle was clearly visible. The intensity of the V5 staining at the attachment site was measured with Fiji, as well as the V5 intensity from an equal area in the interior of the muscles, adjacent to the attachment site. The intensity value at the attachment site was divided by the intensity value from the adjacent area, yielding an enrichment ration value of each protein, at the different embryonic stages. The resulting values were

analysed statistically by Tukey's multiple comparison test in GraphPad Prism.

5.2.2.2 Development of the adult somatic musculature

5.2.2.2.1 Dissecting, fixing and staining 90h APF pupae

White pupae (0 h after puparium formation, APF) were collected on a glass slide and stored at 27 °C for 90 h. To dissect, pupae were glued with their ventral side to a glass slide coated with double-sided tape. The pupa case was removed with forceps, and next the membrane, by carefully rolling the pupa with a brush over the gluing surface. The wings, legs, head and abdomen were cut with a scissor and discarded while the remaining thorax was transferred to fixing solution. After a 15 min incubation under shaking, thoraces were washed with 1X PBS 0.1 % Triton-X for 10 min. Next, the thoraces were glued with their posterior side onto a slide coated with double-sided tape and cut with a blade along their sagittal plane. The resulting hemithoraces were incubated in blocking solution for 30 min and then in primary antibody (*Materials, section 5.1.5.2*) overnight. Hemithoraces were washed three times with 1X PBS 0.1 % Triton-X for a total time of 30 min, followed by the incubation with the secondary antibodies diluted in 1X PBS 0.1 % Triton-X (*Materials, section 5.1.5.2*), for 2 hours in the dark. The samples were then washed three times with 1X PBS 0.1 % Triton-X for a total of 30 min. After the last washing step, the hemithoraces were placed on a microscope slide between two spacers with Vectashield. Next, the interface between the glass slide and the cover slippers was sealed with transparent nail polish. The slides were stored at 4 °C and protected from the light until imaging with LSM 780 confocal microscope. The images were then processed with Fiji (Eliceiri et al., 2012) and Adobe Illustrator CS5.

5.2.2.2 Dissecting, fixing and staining pupal abdomen (whole mount)

White pupae (0h APF) were collected on a glass slide and incubated at 27 °C for 72 h. The pupa case was removed carefully followed by fixation overnight with 4% PFA in 1X PBS, at 4°C under agitation. The pupae were then washed three times with PBS 0.3 % Triton-X. After the washing, the pupae were attached to a glass slide coated with double-sided tape. The internal pupal membrane was carefully removed with forceps and the thorax cut from the abdomen. The abdomens were then incubated with rhodamine-phalloidin for 3 days at 4°C, under constant agitation. Next, the abdomens were incubated sequential for 30 min in each of the following aqueous solutions with increasing concentration of fructose: 20%, 40%, 60%, 80% and 100%, under constant agitation. Then the abdomens were incubated overnight at 4°C in an aqueous solution of 80.2% fructose. Next, they were mounted in 80.2% fructose solution and immediately imaged with LSM 780 confocal microscope. The images were then processed with Fiji (Eliceiri et al., 2012) and Adobe Illustrator CS5.

5.2.2.3 Live imaging pupal abdomen

White pupae (0h APF) were collected on a glass slide and incubated at 27 °C for 26 h (approximately the onset of the adult abdominal myogenesis). Half of the dorsal pupal case, overlapping the first and second abdominal segments, was removed carefully with forceps. The pupa, with the dorsal side facing up, was then placed into a 0.5 mm groove from a special imaging slide. For live imaging, the hole on the pupal case was first covered with an aqueous solution of 50% glycerol and then with a coverslip, which has fixed with tape. The development of the abdominal muscles was documented either by taking a stack image every 20 min for 24 h using a Spinning disk confocal or by taking a stack every 5 min for 24h using a multi-photon set up (La

Vision). The images were then processed with Fiji (Eliceiri et al., 2012) and Adobe Illustrator CS5.

5.2.2.2.4 Live imaging DLMs and DVMs

White pupae (0h APF) were collected on a glass slide and incubated at 27 °C either for 12 h, DLMs imaging, or for 16 h, DVMs imaging. Half of the dorsal pupal case, overlapping the mesothoracic segment, was removed carefully with forceps and scissors. The pupa, with the dorsal side facing up, was then placed into a 0.5 mm groove from a special imaging slide. The hole on the pupal case was first covered with an aqueous solution of 50% glycerol and then with a coverslip, which has fixed with tape. The development of either DLMs or DVMs was documented by taking a stack image every 20 min for 24 h using a multi-photon set up (La Vision). The images were then processed with Fiji (Eliceiri et al., 2012) and Adobe Illustrator CS5.

5.2.3 Biochemistry and mass spectrometry

5.2.3.1 Assessing the expression levels of the *kon-V5* derived constructs

5.2.3.1.1 Biological Samples

Embryos from stages 13-16 expressing the following constructs at endogenous levels: *kon-V5*, *kon-V5* Δ *LamGs*, *kon-V5* Δ *CSPGs*, *kon-V5 PDZ-BD mutated* and as negative control, *w*-embryos.

5.2.3.1.2 Workflow

100 mg of dechorionated embryos were resuspended in 1 ml pre-cooled (4° C) lysis buffer (**Materials**, section **5.1.6.2**), followed by homogenization on ice with a tissue grinder. The lysate was centrifuged at 4°C for 5 min at 20,000 x *g*. The supernatant was then transferred to a clean microtube, followed by the addition of 2 µg V5 antibody and 50 µl magnetic beads coupled with protein G

(Dynabeads), which were pre-washed with lysis buffer with the help of the a magnet (DynaMag- Spin Magnet). The lysate was then incubated for 45 min at 4 °C with gentle rotation. After the incubation, the magnetic beads were washed three times with *Washing buffer I* (**Materials**, section **5.1.6.2**), and then one time with *Washing buffer II* (**Materials**, section **5.1.6.2**). After washing, the beads suspension was transferred to a new microtube and the *Washing buffer II* was exchanged by 50 µl *Elution buffer* (**Materials**, section **5.1.6.2**). The beads suspension was gently resuspended and then incubated for 3 min at 95 °C. The eluate was then transferred to a new microtube and stored at - 20 °C until electrophoresis.

5.2.3.1.3 Western blot analysis

The samples were loaded into NuPage Tris-Acetate precast gels and run according to the manufacturer's instructions. After the electrophoresis, the proteins in the gel were transferred to a PVDF membrane, which was previously incubated in methanol for 5 min. The proteins were transferred with Towin buffer without methanol at constant voltage, 100 V, for 60 min, at 4° C. After the wet electrotransfer, the PVDF membrane was incubated with *Blocking solution* for 60 min at RT. Next, the membrane was incubated with primary antibody diluted (**Materials**, section **5.1.5.2**) in 1X PBS 0.1% Tween overnight at 4° C. After the overnight incubation, the membrane was washed three times with 1X PBS 0.1% Tween for 45 min, at RT under constant agitation. Next, the membrane was incubated with a horseradish peroxidase (HRP) conjugated antibody (**Materials**, section **5.1.6.1.2**) for 2 h at RT, under constant agitation. After the incubation, the membrane was washed three times with 1X PBS 0.1% Tween for 45 min total, at RT, under constant agitation. Then, the membrane was incubated with a chemiluminescent reagent, Immobilon HRP substrate, and immediately visualized with ImageQuant LAS 4000 according to

the manufacturer's instructions. Images were taken to document the gel.

5.2.3.2 Experimental approach to identify Kon interaction partners

5.2.3.2.1 Formation of the larval somatic musculature in the embryo: Kon-V5 and Kon-HA pull-downs

5.2.3.2.1.1 Biological Samples

Embryos from stages 13-16 expressing the following constructs at endogenous levels: *kon-V5*, *kon-HA* and as negative control, *w-*embryos.

5.2.3.2.1.2 Workflow

100 mg of dechorionated embryos were resuspended in 1 ml pre-cooled (4° C) *Lysis buffer* (**Materials**, section **5.1.6.2**), followed by homogenization on ice with a tissue grinder. The lysate was transferred to a microtube and centrifuged at 4°C for 5 min at 20,000 x *g*. The supernatant was then transferred to a clean microtube and processed as described previously (Hubner et al., 2010). In brief, each genotype was done in triplicate. The eluate was then analysed by mass spectrometry at the core facility of the MPI of Biochemistry and the data processed as described previously (Cox et al., 2014; Keilhauer et al., 2014).

5.2.3.2.2 Formation of the larval somatic musculature in the embryo: Kon PDZ-BD peptide pull-downs

5.2.3.2.2.1 Biological Samples

*w-*embryo from stages 13-16.

5.2.3.2.2.2 Workflow

This protocol was adapted from (Schulze and Mann, 2004). In brief, 40 µl streptavidin beads (Myone) was pipetted to a microtube and washed

three times with 250 μ l I-PER buffer. After the washing, 250 μ l peptide solution (**Table 5.3**) (1mM peptide in ddH₂O) was mixed with 250 μ l I-PER buffer containing 2 mM DTT. 460 μ l of this mixture was pipetted into the microtube containing the beads and then rotated for 4 h at 4°C for coating the beads with the peptide. After the incubation, the beads were washed four times with ice cold I-PER buffer followed by a second incubation with 500 μ l embryo lysate containing 1mM DTT at 4°C for 4h. The beads were then washed three times with I-PER buffer. For elution of the proteins, 60 μ l *Elution buffer* was added followed by an incubation for 7 min at 95°C. The eluate was then analysed by mass spectrometry at the core facility of the MPI of Biochemistry and the data processed as described previously (Cox et al., 2014; Keilhauer et al., 2014). Each condition was done in triplicate.

5.2.3.2.3 Development of the adult somatic musculature in the pupa: Kon-GFP and Kon-YFP pull-downs

5.2.3.2.3.1 Biological Samples

Pupae of 24-48 h APF expressing the following constructs: *kon-GFP* (endogenous level), *kon-YFP* (overexpression, *Mef2-GAL4* driver), and as a negative control, *w-* pupae.

5.2.3.2.3.2 Workflow

400 pupae were collected per genotype and snap-frozen. Next, they were grounded to a powder. The powder was resuspended, further processed and analysed as described previously (Hubner et al., 2010; Cox et al., 2014; Keilhauer et al., 2014) in collaboration with Marco Hein (Mann Department in the MPI of Biochemistry) (Hein et al., 2015).

6 References

- Adachi, M., Hamazaki, Y., Kobayashi, Y., Itoh, M., Tsukita, S., Furuse, M., and Tsukita, S. (2009). Similar and Distinct Properties of MUPP1 and Patj, Two Homologous PDZ Domain-Containing Tight-Junction Proteins. *Molecular and Cellular Biology* *29*, 2372–2389.
- Atreya, K.B., and Fernandes, J.J. (2008). Founder cells regulate fiber number but not fiber formation during adult myogenesis in *Drosophila*. *Dev Biol* *321*, 123–140.
- Barritt, D.S., Pearn, M.T., Zisch, A.H., Lee, S.S., Javier, R.T., Pasquale, E.B., and Stallcup, W.B. (2000). The multi-PDZ domain protein MUPP1 is a cytoplasmic ligand for the membrane-spanning proteoglycan NG2. *J. Cell. Biochem.* *79*, 213–224.
- Bataillé, L., Delon, I., Da Ponte, J.P., Brown, N.H., and Jagla, K. (2010). Downstream of Identity Genes: Muscle-Type-Specific Regulation of the Fusion Process. *Dev Cell* *19*, 317–328.
- Bate, M., Rushton, E., and Currie, D.A. (1991). Cells with persistent twist expression are the embryonic precursors of adult muscles in *Drosophila*. *Development* *113*, 79–89.
- Baylies, M.K., Bate, M., and Ruiz Gomez, M. (1998). Myogenesis: a view from *Drosophila*. *Cell* *93*, 921–927.
- Becker, S., Pasca, G., Strumpf, D., Min, L., and Volk, T. (1997). Reciprocal signaling between *Drosophila* epidermal muscle attachment cells and their corresponding muscles. *Development* *124*, 2615–2622.
- Beckett, K., and Baylies, M.K. (2007). 3D analysis of founder cell and fusion competent myoblast arrangements outlines a new model of myoblast fusion. *Dev Biol* *309*, 113–125.
- Beckmann, G., Hanke, J., Bork, P., and Reich, J.G. (1998). Merging extracellular domains: fold prediction for laminin G-like and amino-terminal thrombospondin-like modules based on homology to pentraxins. *J Mol Biol* *275*, 725–730.
- Behm, F., Smith, F., Raimondi, S., and Pui, C. (1996). Human Homologue of the Rat Chondroitin Sulfate Proteoglycan, NG2, Detected by Monoclonal Antibody 7.1, Identifies Childhood Acute Lymphoblastic Leukemias With t(4;11)(q21;q23) or t(11; 19)(q23; p13) and *MLL* Gene Rearrangements. *Blood* *87*, 1134–1113.
- Benassi, M.S., Pazzaglia, L., Chiechi, A., Alberghini, M., Conti, A., Cattaruzza, S., Wassermann, B., Picci, P., and Perris, R. (2009). NG2 expression predicts the metastasis formation in soft-tissue sarcoma patients. *J. Orthop. Res.* *27*, 135–140.

- Beuming, T., Skrabanek, L., Niv, M.Y., Mukherjee, P., and Weinstein, H. (2005). PDZBase: a protein-protein interaction database for PDZ-domains. *Bioinformatics* *21*, 827–828.
- Bhandari, P., Hill, J.S., Farris, S.P., Costin, B., Martin, I., Chan, C.L., Alaimo, J.T., Bettinger, J.C., Davies, A.G., Miles, M.F., et al. (2012). Chloride intracellular channels modulate acute ethanol behaviors in *Drosophila*, *Caenorhabditis elegans* and mice. *Genes, Brain and Behavior* *11*, 387–397.
- Binamé, F., Sakry, D., Dimou, L., Jolivel, V., and Trotter, J. (2013). NG2 regulates directional migration of oligodendrocyte precursor cells via Rho GTPases and polarity complex proteins. *J Neurosci* *33*, 10858–10874.
- Birey, F., Kloc, M., Chavali, M., Hussein, I., Wilson, M., Christoffel, D.J., Chen, T., Frohman, M.A., Robinson, J.K., Russo, S.J., et al. (2015). Genetic and Stress-Induced Loss of NG2 Glia Triggers Emergence of Depressive-like Behaviors through Reduced Secretion of FGF2. *Neuron* *88*, 941–956.
- Bischoff, M., Gradilla, A.-C., Seijo, I., Andrés, G., Rodríguez-Navas, C., González-Méndez, L., and Guerrero, I. (2013). Cytosomes are required for the establishment of a normal Hedgehog morphogen gradient in *Drosophila* epithelia. *Nat. Cell Biol.* *15*, 1269–1281.
- Blunk, A.D., Akbergenova, Y., Cho, R.W., Lee, J., Walldorf, U., Xu, K., Zhong, G., Zhuang, X., and Littleton, J.T. (2014). Postsynaptic actin regulates active zone spacing and glutamate receptor apposition at the *Drosophila* neuromuscular junction. *Molecular and Cellular Neuroscience* *61*, 241–254.
- Bonn, B.R., Rudolf, A., Hornbruch-Freitag, C., Daum, G., Kuckwa, J., Kastl, L., Buttgerit, D., and Renkawitz-Pohl, R. (2013). Myosin heavy chain-like localizes at cell contact sites during *Drosophila* myoblast fusion and interacts in vitro with Rolling pebbles 7. *Experimental Cell Research* *319*, 402–416.
- Borchiellini, C., Coulon, J., and Le Parco, Y. (1996). The function of type IV collagen during *Drosophila* muscle development. *Mech. Dev.* *58*, 179–191.
- Böttcher, R.T., Stremmel, C., Meves, A., Meyer, H., Widmaier, M., Tseng, H.-Y., and Fässler, R. (2012). Sorting nexin 17 prevents lysosomal degradation of beta 1 integrins by binding to the beta 1-integrin tail. *Nat. Cell Biol.* *14*, 584–592.
- Brower, D., Bunch, T., Mukai, L., and Adamson, T. (1995). Nonequivalent requirements for PS1 and PS2 integrin at cell attachments in *Drosophila*: genetic analysis of the alpha PS1 integrin subunit. *Development* *121*, 1311–1320.
- Brown, N.H. (1994). Null mutations in the α PS2 and β PS integrin subunit genes have distinct phenotypes. *Development* *120*, 1221–1231.
- Brown, N.H. (2000). Cell-cell adhesion via the ECM: integrin genetics in fly and worm. *Matrix Biol.* *19*, 191–201.
- Brown, N.H. (2011). *Extracellular Matrix in Development: Insights from*

Mechanisms Conserved between Invertebrates and Vertebrates. *Cold Spring Harb Perspect Biol* 3, a005082.

Brown, N.H., Gregory, S.L., and Martin-Bermudo, M.D. (2000). Integrins as mediators of morphogenesis in *Drosophila*. *Dev Biol* 223, 1–16.

Brown, N.H., Gregory, S.L., Rickoll, W.L., Fessler, L.I., Prout, M., White, R.A.H., and Fristrom, J.W. (2002). Talin is essential for integrin function in *Drosophila*. *Dev Cell* 3, 569–579.

Bunch, T.A., Graner, M.W., Fessler, L.I., Fessler, J.H., Schneider, K.D., Kerschen, A., Choy, L.P., Burgess, B.W., and Brower, D.L. (1998). The PS2 integrin ligand tigrin is required for proper muscle function in *Drosophila*. *Development* 125, 1679–1689.

Burg, M.A., Grako, K.A., and Stallcup, W.B. (1998). Expression of the NG2 proteoglycan enhances the growth and metastatic properties of melanoma cells. *J. Cell. Physiol.* 177, 299–312.

Busser, B.W., Shokri, L., Jaeger, S.A., Gisselbrecht, S.S., Singhanian, A., Berger, M.F., Zhou, B., Bulyk, M.L., and Michelson, A.M. (2012). Molecular mechanism underlying the regulatory specificity of a *Drosophila* homeodomain protein that specifies myoblast identity. *Development* 139, 1164–1174.

Carmena, A., Bate, M., and Jiménez, F. (1995). Lethal of scute, a proneural gene, participates in the specification of muscle progenitors during *Drosophila* embryogenesis. *Genes Dev* 9, 2373–2383.

Carmena, A., Gisselbrecht, S., Harrison, J., Jiménez, F., and Michelson, A.M. (1998). Combinatorial signaling codes for the progressive determination of cell fates in the *Drosophila* embryonic mesoderm. *Genes Dev* 12, 3910–3922.

Cattaruzza, S., Nicolosi, P.A., Braghetta, P., Pazzaglia, L., Benassi, M.S., Picci, P., Lacrima, K., Zanocco, D., Rizzo, E., Stallcup, W.B., et al. (2013). NG2/CSPG4-collagen type VI interplays putatively involved in the microenvironmental control of tumour engraftment and local expansion. *Journal of Molecular Cell Biology* 5, 176–193.

Charvet, B., Ruggiero, F., and Le Guellec, D. (2012). The development of the myotendinous junction. A review. *Muscles Ligaments Tendons J* 2, 53–63.

Chekenya, M., Hjelstuen, M., Enger, P.Ø., Thorsen, F., Jacob, A.L., Probst, B., Haraldseth, O., Pilkington, G., Butt, A., Levine, J.M., et al. (2002). NG2 proteoglycan promotes angiogenesis-dependent tumor growth in CNS by sequestering angiostatin. *Faseb J* 16, 586–588.

Chiang, A.C., and Massagué, J. (2008). Molecular basis of metastasis. *N. Engl. J. Med.* 359, 2814–2823.

Ciglar, L., Girardot, C., Wilczy ski, B., Braun, M., and Furlong, E.E.M. (2014). Coordinated repression and activation of two transcriptional programs

- stabilizes cell fate during myogenesis. *Development* *141*, 2633–2643.
- Cox, J., Hein, M.Y., Lubner, C.A., Paron, I., Nagaraj, N., and Mann, M. (2014). Accurate proteome-wide label-free quantification by delayed normalization and maximal peptide ratio extraction, termed MaxLFQ. *Mol Cell Proteomics* *13*, 2513–2526.
- Currie, D.A., and Bate, M. (1991). The development of adult abdominal muscles in *Drosophila*: myoblasts express twist and are associated with nerves. *Development* *113*, 91–102.
- Dean, C., and Dresbach, T. (2006). Neuroligins and neuexins: linking cell adhesion, synapse formation and cognitive function. *Trends in Neurosciences* *29*, 21–29.
- Devenport, D., Bunch, T.A., Bloor, J.W., Brower, D.L., and Brown, N.H. (2007). Mutations in the *Drosophila* α PS2 integrin subunit uncover new features of adhesion site assembly. *Dev Biol* *308*, 294–308.
- Dickinson, M. (2006). Insect flight. *Current Biology* *16*, R309–R314.
- Dimou, L., and Gallo, V. (2015). NG2-glia and their functions in the central nervous system. *Glia* *63*, 1429–1451.
- Dobi, K.C., Halfon, M.S., and Baylies, M.K. (2014). Whole-Genome Analysis of Muscle Founder Cells Implicates the Chromatin Regulator Sin3A in Muscle Identity. *CellReports* *8*, 858–870.
- Dobi, K.C., Schulman, V.K., and Baylies, M.K. (2015). Specification of the somatic musculature in *Drosophila*. *WIREs Dev Biol* *4*, 357–375.
- Doyle, D.A., Lee, A., Lewis, J., Kim, E., Sheng, M., and MacKinnon, R. (1996). Crystal structures of a complexed and peptide-free membrane protein-binding domain: molecular basis of peptide recognition by PDZ. *Cell* *85*, 1067–1076.
- Duan, H., Skeath, J., and Nguyen, H. (2001). *Drosophila* *Lame duck*, a novel member of the Gli superfamily, acts as a key regulator of myogenesis by controlling fusion-competent myoblast development. *Development* *128*, 4489–4500.
- Duan, H., Zhang, C., Chen, J., Sink, H., Frei, E., and Noll, M. (2007). A key role of *Pox meso* in somatic myogenesis of *Drosophila*. *Development* *134*, 3985–3997.
- Dutta, D. (2004). Founder myoblasts and fibre number during adult myogenesis in *Drosophila*. *Development* *131*, 3761–3772.
- Dworkin, I., and Gibson, G. (2006). Epidermal growth factor receptor and transforming growth factor-beta signaling contributes to variation for wing shape in *Drosophila melanogaster*. *Genetics* *173*, 1417–1431.
- Eisenmann, K., McCarthy, J., and Simpson, M. (1999). Melanoma chondroitin

- sulphate proteoglycan regulates cell spreading through Cdc42, Ack-1 and p130cas. *Nat. Cell Biol.* *1*, 507–513.
- Ejsmont, R.K., Bogdanzaliewa, M., Lipinski, K.A., and Tomancak, P. (2011). Production of fosmid genomic libraries optimized for liquid culture recombineering and cross-species transgenesis. *Methods Mol. Biol.* *772*, 423–443.
- Ejsmont, R.K., Sarov, M., Winkler, S., Lipinski, K.A., and Tomancak, P. (2009). A toolkit for high-throughput, cross-species gene engineering in *Drosophila*. *Nat Meth* *6*, 435–437.
- Eliceiri, K.W., Berthold, M.R., Goldberg, I.G., Ibáñez, L., Manjunath, B.S., Martone, M.E., Murphy, R.F., Peng, H., Plant, A.L., Roysam, B., et al. (2012). Biological imaging software tools. *Nat Meth* *9*, 697–710.
- Estrada, B., Choe, S.E., Gisselbrecht, S.S., Michaud, S., Raj, L., Busser, B.W., Halfon, M.S., Church, G.M., and Michelson, A.M. (2006). An Integrated Strategy for Analyzing the Unique Developmental Programs of Different Myoblast Subtypes. *PLoS Genet* *2*, e16.
- Farrell, E.R.E.A., Farrell, E.R., Fernandes, J., and Keshishian, H. (1996). Muscle Organizers in *Drosophila*: The Role of Persistent Larval Fibers in Adult Flight Muscle Development. *Dev Biol* *176*, 220–229.
- Fernandes, J., Bate, M., and Vijayraghavan, K. (1991). Development of the indirect flight muscles of *Drosophila*. *Development* *113*, 67–77.
- Fernandes, J.J., and Keshishian, H. (1996). Patterning the dorsal longitudinal flight muscles (DLM) of *Drosophila*: insights from the ablation of larval scaffolds. *Development* *122*, 3755–3763.
- Fernandes, J.J., Celniker, S.E., and VijayRaghavan, K. (1996). Development of the Indirect Flight Muscle Attachment Sites in *Drosophila*: Role of the PS Integrins and the stripe Gene. *Dev Biol* *176*, 116–11184.
- Feutlinske, F., Browarski, M., Ku, M.-C., Trnka, P., Waiczies, S., Niendorf, T., Stallcup, W.B., Glass, R., Krause, E., and Maritzen, T. (2015). Stonin1 mediates endocytosis of the proteoglycan NG2 and regulates focal adhesion dynamics and cell motility. *Nat Commun* *6*, 1–13.
- Figeac, N., Jagla, T., Aradhya, R., Da Ponte, J.P., and Jagla, K. (2010). *Drosophila* adult muscle precursors form a network of interconnected cells and are specified by the rhomboid-triggered EGF pathway. *Development* *137*, 1965–1973.
- Finn, R.D., Coghill, P., Eberhardt, R.Y., Eddy, S.R., Mistry, J., Mitchell, A.L., Potter, S.C., Punta, M., Qureshi, M., Sangrador-Vegas, A., et al. (2016). The Pfam protein families database: towards a more sustainable future. *Nucleic Acids Res* *44*, D279–D285.
- Fogerty, F., Fessler, L., Bunch, T., and Yaron, Y. (1994). Tiggrin, a novel *Drosophila* extracellular matrix protein that functions as a ligand for

- Drosophila* alpha PS2 beta PS integrins. *Development* 120, 1747–1758.
- Frasch, M. (1999). Controls in patterning and diversification of somatic muscles during *Drosophila* embryogenesis. *Curr Opin Genet Dev* 9, 522–529.
- Frommer, G., Vorbrüggen, G., Pasca, G., Jäckle, H., and Volk, T. (1996). Epidermal *egr*-like zinc finger protein of *Drosophila* participates in myotube guidance. *Embo J* 15, 1642–1649.
- Georgieva, S., Kirschner, D., and Jagla, T. (2000). Two novel *Drosophila* TAFIIs have homology with human TAFII30 and are differentially regulated during development. *Molecular and Cellular Biology* 20, 1639–1648.
- Giangreco, A., Goldie, S.J., Failla, V., Saintigny, G.E.L., and Watt, F.M. (2009). Human Skin Aging Is Associated with Reduced Expression of the Stem Cell Markers Beta1 Integrin and MCSP. *Journal of Investigative Dermatology* 130, 604–608.
- Grako, K.A., Ochiya, T., Barritt, D., Nishiyama, A., and Stallcup, W.B. (1999). PDGF (alpha)-receptor is unresponsive to PDGF-AA in aortic smooth muscle cells from the NG2 knockout mouse. *J Cell Sci* 112, 905–915.
- Gunage, R.D., Reichert, H., and Vijayraghavan, K. (2014). Identification of a new stem cell population that generates *Drosophila* flight muscles. *Elife* 3, e03126.
- Guruharsha, K.G., Rual, J.-F., Zhai, B., Mintseris, J., Vaidya, P., Vaidya, N., Beekman, C., Wong, C., Rhee, D.Y., Cenaj, O., et al. (2011). A protein complex network of *Drosophila melanogaster*. *Cell* 147, 690–703.
- Hakeda, S., Endo, S., and Saigo, K. (2000). Requirements of Kettin, a giant muscle protein highly conserved in overall structure in evolution, for normal muscle function, viability, and flight activity of *Drosophila*. *J Cell Biol* 148, 101–114.
- Harper, J.R., and Reisfeld, R.A. (1983). Inhibition of anchorage-independent growth of human melanoma cells by a monoclonal antibody to a chondroitin sulfate proteoglycan. *J. Natl. Cancer Inst.* 71, 259–263.
- Harris, T.J.C., and Tepass, U. (2010). Adherens junctions: from molecules to morphogenesis. *Nat Rev Mol Cell Biol* 11, 502–514.
- Hatini, V., and DiNardo, S. (2001). Distinct signals generate repeating striped pattern in the embryonic parasegment. *Mol. Cell* 7, 151–160.
- Hein, M.Y., Hubner, N.C., Poser, I., Cox, J., Nagaraj, N., Toyoda, Y., Gak, I.A., Weisswange, I., Mansfeld, J., Buchholz, F., et al. (2015). A Human Interactome in Three Quantitative Dimensions Organized by Stoichiometries and Abundances. *Cell* 163, 712–723.
- Hekmat-Safe, D.S., Safe, C.R., McKinney, A.J., and Tanouye, M.A. (2002). Genome-wide analysis of the odorant-binding protein gene family in

- Drosophila melanogaster*. *Genome Res* 12, 1357–1369.
- Herold, N., Will, C.L., Wolf, E., Kastner, B., Urlaub, H., and Luhrmann, R. (2008). Conservation of the Protein Composition and Electron Microscopy Structure of *Drosophila melanogaster* and Human Spliceosomal Complexes. *Molecular and Cellular Biology* 29, 281–301.
- Hsiung, F., Ramirez-Weber, F.-A., David Iwaki, D., and Kornberg, T.B. (2005). Dependence of *Drosophila* wing imaginal disc cytonemes on Decapentaplegic. *Nat. Cell Biol.* 437, 560–563.
- Hubner, N.C., Bird, A.W., Cox, J., Splettstoesser, B., Bandilla, P., Poser, I., Hyman, A., and Mann, M. (2010). Quantitative proteomics combined with BAC TransgeneOmics reveals in vivo protein interactions. *J Cell Biol* 189, 739–754.
- Hynes, R.O., and Zhao, Q. (2000). The evolution of cell adhesion. *J Cell Biol* 150, F89–96.
- Iida, J., Meijne, A., Oegema, T., and Yednock, T. (1998). A role of chondroitin sulfate glycosaminoglycan binding site in $\alpha 4\beta 1$ integrin-mediated melanoma cell adhesion. *J Biol Chem* 273, 5955–5962.
- Jacquemet, G., Hamidi, H., and Ivaska, J. (2015). Filopodia in cell adhesion, 3D migration and cancer cell invasion. *Curr Opin Cell Biol* 36, 23–31.
- Jagla, T., Bellard, F., Lutz, Y., Dretzen, G., Bellard, M., and Jagla, K. (1998). ladybird determines cell fate decisions during diversification of *Drosophila* somatic muscles. *Development* 125, 3699–3708.
- Ji, S., Sun, M., Zheng, X., Li, L., Sun, L., Chen, D., and Sun, Q. (2014). Cell-surface localization of Pellino antagonizes Toll-mediated innate immune signalling by controlling MyD88 turnover in *Drosophila*. *Nat Commun* 5, 1–14.
- Kalluri, R. (2003). Angiogenesis: Basement membranes: structure, assembly and role in tumour angiogenesis. *Nat Rev Cancer* 3, 422–433.
- Katanaev, V.L., Solis, G.P., Hausmann, G., Buestorf, S., Katanayeva, N., Schrock, Y., Stuermer, C.A., and Basler, K. (2008). Reggie-1/flotillin-2 promotes secretion of the long-range signalling forms of Wingless and Hedgehog in *Drosophila*. *Embo J* 27, 509–521.
- Keilhauer, E.C., Hein, M.Y., and Mann, M. (2014). Accurate Protein Complex Retrieval by Affinity Enrichment Mass Spectrometry (AE-MS) Rather than Affinity Purification Mass Spectrometry (AP-MS). *Mol Cell Proteomics* 14, 120–135.
- Keller, C.A.E.A. (1998). A Role for nautilus in the Differentiation of Muscle Precursors. *Dev Biol* 202, 157–171.
- Kim, D.I., KC, B., Zhu, W., Motamedchaboki, K., Doye, V., and Roux, K.J. (2014). Probing nuclear pore complex architecture with proximity-dependent biotinylation. *Proceedings of the National Academy of Sciences* 111, E2453–

E2461.

Klapholz, B., Herbert, S.L., Wellmann, J., Johnson, R., Parsons, M., and Brown, N.H. (2015). Alternative mechanisms for talin to mediate integrin function. *Curr Biol* 25, 847–857.

Knight, D., Xie, W., and Boulianne, G.L. (2011). Neurexins and neuroligins: recent insights from invertebrates. *Mol. Neurobiol.* 44, 426–440.

Knirr, S., Azpiazu, N., and Frasch, M. (1999). The role of the NK-homeobox gene *slouch* (S59) in somatic muscle patterning. *Development* 126, 4525–4535.

Kramer, S.G., Kidd, T., Simpson, J.H., and Goodman, C.S. (2001). Switching repulsion to attraction: changing responses to slit during transition in mesoderm migration. *Science* 292, 737–740.

Krzemien, J., Fabre, C.C.G., Casal, J., and Lawrence, P.A. (2012). The muscle pattern of the *Drosophila* abdomen depends on a subdivision of the anterior compartment of each segment. *Development* 139, 75–83.

Lasko, P. (2000). The *Drosophila melanogaster* genome: translation factors and RNA binding proteins. *Journal of Cell Biology* 150, F51–F56.

Lee, H.H., and Frasch, M. (2000). Wingless effects mesoderm patterning and ectoderm segmentation events via induction of its downstream target *sloppy paired*. *Development* 127, 5497–5508.

Leptin, M., and Grunewald, B. (1990). Cell shape changes during gastrulation in *Drosophila*. *Development* 110, 73–84.

Martin-Bermudo, M., and Brown, N. (1999). Uncoupling integrin adhesion and signaling: the β PS cytoplasmic domain is sufficient to regulate gene expression in the *Drosophila* embryo. *Genes Dev* 13, 729–739.

Martin-Bermudo, M.D., and Brown, N.H. (2000). The localized assembly of extracellular matrix integrin ligands requires cell-cell contact. *J Cell Sci* 113, 3715–3723.

Meves, A., Geiger, T., Zanivan, S., DiGiovanni, J., Mann, M., and Fässler, R. (2011). Beta1 integrin cytoplasmic tyrosines promote skin tumorigenesis independent of their phosphorylation. *Proceedings of the National Academy of Sciences* 108, 15213–15218.

Montell, D.J. (2003). Border-cell migration: the race is on. *Nat Rev Mol Cell Biol* 4, 13–24.

Moussian, B., and Roth, S. (2005). Dorsoventral Axis Formation in the *Drosophila* Embryo—Shaping and Transducing a Morphogen Gradient. *Current Biology* 15, R887–R899.

Müller, A., Homey, B., Soto, H., Ge, N., Catron, D., Buchanan, M.E., McClanahan, T., Murphy, E., Yuan, W., Wagner, S.N., et al. (2001).

Involvement of chemokine receptors in breast cancer metastasis. *Nature* 410, 50–56.

Nabel-Rosen, H., Dorevitch, N., Reuveny, A., and Volk, T. (1999). The balance between two isoforms of the *Drosophila* RNA-binding protein how controls tendon cell differentiation. *Mol. Cell* 4, 573–584.

Nabel-Rosen, H., Volohonsky, G., and Reuveny, A. (2002). Two isoforms of the *Drosophila* RNA binding protein, how, act in opposing directions to regulate tendon cell differentiation. *Dev Cell* 2, 183–193.

Nicolosi, P.A., Dallatomasina, A., and Perris, R. (2015). Theranostic Impact of NG2/CSPG4 Proteoglycan in Cancer. *Theranostics* 5, 530–544.

Nobes, C.D., and Hall, A. (1995). Rho, rac, and cdc42 GTPases regulate the assembly of multimolecular focal complexes associated with actin stress fibers, lamellipodia, and filopodia. *Cell* 81, 53–62.

Panáková, D., Sprong, H., Marois, E., Thiele, C., and Eaton, S. (2005). Lipoprotein particles are required for Hedgehog and Wingless signalling. *Nature* 435, 58–65.

Paňková, D., Jobe, N., Kratochvílová, M., Buccione, R., Brábek, J., and Rösel, D. (2012). NG2-mediated Rho activation promotes amoeboid invasiveness of cancer cells. *Eur. J. Cell Biol.* 91, 969–977.

Paňková, K., Rösel, D., Novotný, M., and Brábek, J. (2009). The molecular mechanisms of transition between mesenchymal and amoeboid invasiveness in tumor cells. *Cell. Mol. Life Sci.* 67, 63–71.

Pastor-Pareja, J.C., and Xu, T. (2011). Shaping Cells and Organs in *Drosophila* by Opposing Roles of Fat Body-Secreted Collagen IV and Perlecan. *Dev Cell* 21, 245–256.

Pawson, T., and Scott, J.D. (1997). Signaling through scaffold, anchoring, and adaptor proteins. *Science* 278, 2075–2080.

Perez-Moreno, J.J., Bischoff, M., Martin-Bermudo, M.D., and Estrada, B. (2014). The conserved transmembrane proteoglycan Perdido/Kon-tiki is essential for myofibrillogenesis and sarcomeric structure in *Drosophila*. *J Cell Sci* 127, 3162–3173.

Petrini, S., Tessa, A., Carrozzo, R., Verardo, M., Pierini, R., Rizza, T., and Bertini, E. (2003). Human melanoma/NG2 chondroitin sulfate proteoglycan is expressed in the sarcolemma of postnatal human skeletal myofibers. *Molecular and Cellular Neuroscience* 23, 219–231.

Pines, M., Das, R., Ellis, S.J., Morin, A., Czerniecki, S., Yuan, L., Klose, M., Coombs, D., and Tanentzapf, G. (2012). Mechanical force regulates integrin turnover in *Drosophila* in vivo. *Nat. Cell Biol.* 14, 935–943.

Poli, A., Wang, J., Domingues, O., Planagumà, J., Yan, T., Rygh, C.B., Skafnesmo, K.O., Thorsen, F., McCormack, E., Hentges, F., et al. (2013).

- Targeting glioblastoma with NK cells and mAb against NG2/CSPG4 prolongs animal survival. *Oncotarget* *4*, 1527–1546.
- Ramírez-Weber, F.A., and Kornberg, T.B. (1999). Cytonemes: cellular processes that project to the principal signaling center in *Drosophila* imaginal discs. *Cell* *97*, 599–607.
- Rivlin, P.K., Schneiderman, A.M., and Booker, R. (2000). Imaginal Pioneers Prefigure the Formation of Adult Thoracic Muscles in *Drosophila melanogaster*. *Dev Biol* *222*, 450–459.
- Rochlin, K., Yu, S., Roy, S., and Baylies, M.K. (2010). Myoblast fusion: when it takes more to make one. *Dev Biol* *341*, 66–83.
- Roh, M.H., and Margolis, B. (2003). Composition and function of PDZ protein complexes during cell polarization. *Am. J. Physiol. Renal Physiol.* *285*, F377–387.
- Roth, S., Stein, D., and Nüsslein-Volhard, C. (1989). A gradient of nuclear localization of the dorsal protein determines dorsoventral pattern in the *Drosophila* embryo. *Cell* *59*, 1189–1202.
- Roux, K.J., Kim, D.I., Raida, M., and Burke, B. (2012). A promiscuous biotin ligase fusion protein identifies proximal and interacting proteins in mammalian cells. *J Cell Biol* *196*, 801–810.
- Roy, S., Hsiung, F., and Kornberg, T.B. (2011). Specificity of *Drosophila* cytonemes for distinct signaling pathways. *Science* *332*, 354–358.
- Rugjee, K.N., Roy Chaudhury, S., Al-Jubran, K., Ramanathan, P., Matina, T., Wen, J., and Brogna, S. (2013). Fluorescent protein tagging confirms the presence of ribosomal proteins at *Drosophila* polytene chromosomes. *PeerJ* *1*, e15.
- Ruiz Gomez, M., Romani, S., Hartmann, C., Jäckle, H., and Bate, M. (1997). Specific muscle identities are regulated by Krüppel during *Drosophila* embryogenesis. *Development* *124*, 3407–3414.
- Rusconi, J.C., and Corbin, V. (1998). Evidence for a novel Notch pathway required for muscle precursor selection in *Drosophila*. *Mech. Dev.* *79*, 39–50.
- Rushton, E., Drysdale, R., Abmayr, S.M., Michelson, A.M., and Bate, M. (1995). Mutations in a novel gene, myoblast city, provide evidence in support of the founder cell hypothesis for *Drosophila* muscle development. *Development* *121*, 1979–1988.
- Saisawang, C., Wongsantichon, J., and Ketterman, A.J. (2012). A preliminary characterization of the cytosolic glutathione transferase proteome from *Drosophila melanogaster*. *Biochem. J.* *442*, 181–190.
- Sandmann, T., Girardot, C., Brehme, M., Tongprasit, W., Stolc, V., and Furlong, E.E.M. (2007). A core transcriptional network for early mesoderm development in *Drosophila melanogaster*. *Genes Dev* *21*, 436–449.

- Sarov, M., Barz, C., Jambor, H., Hein, M.Y., Schmied, C., Suchold, D., Stender, B., Janosch, S., KJ, V.V., Krishnan, R.T., et al. (2016). A genome-wide resource for the analysis of protein localisation in *Drosophila*. *Elife* 5, e12068.
- Schnorrer, F., and Dickson, B.J. (2004). Muscle building; mechanisms of myotube guidance and attachment site selection. *Dev Cell* 7, 9–20.
- Schnorrer, F., Kalchauer, I., and Dickson, B.J. (2007). The transmembrane protein Kon-tiki couples to Dgrip to mediate myotube targeting in *Drosophila*. *Dev Cell* 12, 751–766.
- Schrapppe, M., Klier, F., Spiro, R., Waltz, T., and Reifeld, R. (1991). Correlation of chondroitin sulfate proteoglycan expression on proliferating brain capillary endothelial cells with the malignant phenotype of astroglial cells. *Cancer Research* 51, 4986–4993.
- Schulman, V.K., Dobi, K.C., and Baylies, M.K. (2015). Morphogenesis of the somatic musculature in *Drosophila melanogaster*. *WIREs Dev Biol* 4, 313–334.
- Schulze, W.X., and Mann, M. (2004). A Novel Proteomic Screen for Peptide-Protein Interactions. *J Biol Chem* 279, 10756–10764.
- Schweitzer, R., Zelzer, E., and Volk, T. (2010). Connecting muscles to tendons: tendons and musculoskeletal development in flies and vertebrates. *Development* 137, 2807–2817.
- Shoshan, Y., Nishiyama, A., Chang, A., Mörk, S., Barnett, G.H., Cowell, J.K., Trapp, B.D., and Staugaitis, S.M. (1999). Expression of oligodendrocyte progenitor cell antigens by gliomas: implications for the histogenesis of brain tumors. *Proc Natl Acad Sci USA* 96, 10361–10366.
- Spletter, M.L., Barz, C., Yeroslaviz, A., Schonbauer, C., Ferreira, I.R.S., Sarov, M., Gerlach, D., Stark, A., Habermann, B.H., and Schnorrer, F. (2015). The RNA-binding protein Arrest (Bruno) regulates alternative splicing to enable myofibril maturation in *Drosophila* flight muscle. *EMBO Rep* 16, 178–191.
- Stathopoulos, A., and Levine, M. (2002). Dorsal Gradient Networks in the *Drosophila* Embryo. *Dev Biol* 246, 57–67.
- Stathopoulos, A., and Levine, M. (2004). Whole-genome analysis of *Drosophila* gastrulation. *Curr Opin Genet Dev* 14, 477–484.
- Staub, E., Hinzmann, B., and Rosenthal, A. (2002). A novel repeat in the melanoma-associated chondroitin sulfate proteoglycan defines a new protein family. *FEBS Lett.* 527, 114–118.
- Stein, D.S., and Stevens, L.M. (2014). Maternal control of the *Drosophila* dorsal-ventral body axis. *WIREs Dev Biol* 3, 301–330.
- Strumpf, D., and Volk, T. (1998). Kakapo, a novel cytoskeletal-associated

protein is essential for the restricted localization of the neuregulin-like factor, vein, at the muscle-tendon junction site. *J Cell Biol* *143*, 1259–1270.

Subramanian, A., Prokop, A., Yamamoto, M., Sugimura, K., Uemura, T., Betschinger, J., Knoblich, J.A., and Volk, T. (2003). Shortstop Recruits EB1/APC1 and Promotes Microtubule Assembly at the Muscle-Tendon Junction. *Current Biology* *13*, 1086–1095.

Subramanian, A., Wayburn, B., Bunch, T., and Volk, T. (2007). Thrombospondin-mediated adhesion is essential for the formation of the myotendinous junction in *Drosophila*. *Development* *134*, 1269–1278.

Südhof, T.C. (2008). Neuroligins and neuexins link synaptic function to cognitive disease. *Nature* *455*, 903–911.

Swan, L.E., Schmidt, M., Schwarz, T., Ponimaskin, E., Prange, U., Boeckers, T., Thomas, U., and Sigrist, S.J. (2006). Complex interaction of *Drosophila* GRIP PDZ domains and Echinoid during muscle morphogenesis. *Embo J* *25*, 3640–3651.

Swan, L.E., Wichmann, C., Prange, U., Schmid, A., Schmidt, M., Schwarz, T., Ponimaskin, E., Madeo, F., Vorbrüggen, G., and Sigrist, S.J. (2004). A glutamate receptor-interacting protein homolog organizes muscle guidance in *Drosophila*. *Genes Dev* *18*, 223–237.

Tepass, U. (2012). The apical polarity protein network in *Drosophila* epithelial cells: regulation of polarity, junctions, morphogenesis, cell growth, and survival. *Annu. Rev. Cell Dev. Biol.* *28*, 655–685.

Tillet, E., Ruggiero, F., Nishiyama, A., and Stallcup, W.B. (1997). The membrane-spanning proteoglycan NG2 binds to collagens V and VI through the central nonglobular domain of its core protein. *J Biol Chem* *272*, 10769–10776.

Tiwari, P., Kumar, A., Das, R.N., Malhotra, V., and Vijayraghavan, K. (2015). A Tendon Cell Specific RNAi Screen Reveals Novel Candidates Essential for Muscle Tendon Interaction. *PLoS ONE* *10*, e0140976.

Tonikian, R., Zhang, Y., Sazinsky, S.L., Currell, B., Yeh, J.-H., Reva, B., Held, H.A., Appleton, B.A., Evangelista, M., Wu, Y., et al. (2008). A specificity map for the PDZ domain family. *PLoS Biol.* *6*, e239.

Urbano, J.M., Torgler, C.N., Molnar, C., Tepass, U., López-Varea, A., Brown, N.H., de Celis, J.F., and Martín-Bermudo, M.D. (2009). *Drosophila* laminins act as key regulators of basement membrane assembly and morphogenesis. *Development* *136*, 4165–4176.

Venken, K., He, Y., Hoskins, R., and Bellen, H. (2006). P [acman]: a BAC transgenic platform for targeted insertion of large DNA fragments in *D. melanogaster*. *Science* *314*, 1747–1751.

Voelker, R., Huang, S., Wisely, G., and Sterling, J. (1989). Molecular and genetic organization of the suppressor of sable and minute (1) 1B region in

- Drosophila melanogaster*. *Genetics* 122, 625–642.
- Volohonsky, G., Edenfeld, G., Klambt, C., and Volk, T. (2007). Muscle-dependent maturation of tendon cells is induced by post-transcriptional regulation of stripeA. *Development* 134, 347–356.
- Wan, P., Wang, D., Luo, J., Chu, D., Wang, H., Zhang, L., and Chen, J. (2013). Guidance receptor promotes the asymmetric distribution of exocyst and recycling endosome during collective cell migration. *Development* 140, 4797–4806.
- Wang, J., Svendsen, A., Kmiecik, J., Immervol, H., Skaftnesmo, K.O., Planagumà, J., Reed, R.K., Bjerkgvig, R., Miletic, H., Enger, P.Ø., et al. (2011a). Targeting the NG2/CSPG4 Proteoglycan Retards Tumour Growth and Angiogenesis in Preclinical Models of GBM and Melanoma. *PLoS ONE* 6, e23062.
- Wang, Q., Zhao, C., and Swank, D.M. (2011b). Calcium and stretch activation modulate power generation in *Drosophila* flight muscle. *Biophys J* 101, 2207–2213.
- Warming, S., Costantino, N., Court, D.L., Jenkins, N.A., and Copeland, N.G. (2005). Simple and highly efficient BAC recombineering using galK selection. *Nucleic Acids Res* 33, e36.
- Weitkunat, M., Kaya-Çopur, A., Grill, S.W., and Schnorrer, F. (2014). Tension and Force-Resistant Attachment Are Essential for Myofibrillogenesis in *Drosophila* Flight Muscle. *Current Biology* 24, 705–716.
- Wittkopp, P.J., True, J.R., and Carroll, S.B. (2002). Reciprocal functions of the *Drosophila* yellow and ebony proteins in the development and evolution of pigment patterns. *Development* 129, 1849–1858.
- Yamamoto-Hino, M., Yoshida, H., Ichimiya, T., Sakamura, S., Maeda, M., Kimura, Y., Sasaki, N., Aoki-Kinoshita, K.F., Kinoshita-Toyoda, A., Toyoda, H., et al. (2015). Phenotype-based clustering of glycosylation-related genes by RNAi-mediated gene silencing. *Genes Cells* 20, 521–542.
- Yarnitzky, T., Min, L., and Volk, T. (1997). The *Drosophila* neuregulin homolog Vein mediates inductive interactions between myotubes and their epidermal attachment cells. *Genes Dev* 11, 2691–2700.
- Ypsilanti, A.R., Zagar, Y., and Chédotal, A. (2010). Moving away from the midline: new developments for Slit and Robo. *Development* 137, 1939–1952.
- Yuan, L., Fairchild, M.J., Perkins, A.D., and Tanentzapf, G. (2010). Analysis of integrin turnover in fly myotendinous junctions. *J Cell Sci* 123, 939–946.
- Zhang, F., Zhao, Y., and Han, Z. (2013). An In Vivo Functional Analysis System for Renal Gene Discovery in *Drosophila* Pericardial Nephrocytes. *Journal of the American Society of Nephrology* 24, 191–197.
- Zirin, J., Cheng, D., Dhanyasi, N., Cho, J., Dura, J.-M., VijayRaghavan, K.,

6. References

and Perrimon, N. (2013). Ecdysone signaling at metamorphosis triggers apoptosis of *Drosophila* abdominal muscles. *Dev Biol* 383, 275–284.

Acknowledgements

I would like to express my deepest gratitude to Dr Frank Schnorrer for the opportunity to develop my PhD work in his lab. Frank, with his sharp and inquisitive mind, was constantly a great source of input for my project. However, what makes Frank especially unique is that all these great scientific qualities are seasoned with care and interest for all the group members. I would like also to acknowledge my *Doktormutter*, Prof. Dr. Barbara Conradt, for her great help and support. In addition, I would like to thank the Muscle Dynamics group for scientific input and support. Furthermore, I would like to acknowledge Prof. Dr. Faessler and his department members for providing an enriching scientific environment, besides of great infrastructures, which enabled me to conduct efficiently my research.

I would like to thank the Graduate Program of the MPI of Biochemistry for the opportunity to organize the seminar series “Career for PhDs”, as well as for providing numerous soft skills workshops, which were immensely valuable for my professional development. I would also like to thank the InPharma team, especially Sneha Kumar and Marija Pesic, for friendship and support.

I would also like to thank my mother, Alice Pinheiro, and my sister and brother, Amelia and Arlindo Ferreira, for constant support and love. Finally, I would like to thank Marc Bettscheider for his love, and his adorable smile, as well as his optimistic view of the world.

Curriculum Vitae

Name Irene Rebelo da Silva Ferreira

Address Georgenstr. 128, Munich

Higher Education in Life sciences

01/2011 to date

Doctoral study, Max Planck Institute of Biochemistry (Germany)

Published work

Sarov, M., Barz, C., Jambor, H., Hein, M.Y., Schmied, C., Suchold, D., Stender, B., Janosch, S., KJ, V.V., Krishnan, R.T., Aishwarya K., **Ferreira IR.**, Ejsmont R., Finkl K., Hasse S., Kämpfer P., Plewka N., Vinis E., Schloissnig S., Knust E., Hartenstein V., Mann M., Ramaswami M., VijayRaghavan K., Tomancak P., and Schnorrer, F. (2016). A genome-wide resource for the analysis of protein localisation in *Drosophila*. *Elife* 5, e12068

Spletter ML., Barz C., Yeroslaviz A., Schönbauer C., **Ferreira IR.**, Sarov M., Gerlach D., Stark A., Habermann BH., and Schnorrer F. (2014). The RNA-binding protein Arrest (Bruno) regulates alternative splicing to enable myofibril maturation in *Drosophila* flight muscle. *EMBO Rep* 16, 178–191

Zhang, X., **Ferreira, I.R.**, and Schnorrer, F. (2014) A simple protocol to efficiently engineer the *Drosophila* genome by TALENs. *Methods* 1, 111-118

2008 to 2010

Advanced Training in Neurosciences, University of Regensburg and Max Planck of Neurobiology (Germany)

Published work

Mueler R., **Ferreira I.**, et al., (2009). Application of hydrogels to rewire the injured spinal cord. In D. B. Stein, *Handbook of hydrogels: properties, preparation and applications* (pp. 397-426). Hauppauge NY: Nova Science.

2002 to 2007

Diploma in Biology, University of Minho (Portugal) and University of Amsterdam (the Netherlands)

Published work

M. van Wingerden, M. Vinck, V. Tijms, **I.R.S. Ferreira**, A.J. Jonker, C.M.A. Pennartz (2012). NMDA receptors control cue-outcome selectivity and plasticity of orbitofrontal firing patterns during associative stimulus-reward learning. *Neuron* 21, 813-25

Grant and fellowship

2010 to 2013 Doctoral fellowship, FCT (Portuguese Foundation of Science and Technology)

2006 to 2007 Erasmus Grant (the Netherlands)

Presentations

Talks

Ferreira, I.R.S and Schnorrer, F. (2016): Molecular role of Kon-tiki during myotube migration and attachment. FOR 1756, Ringberg, Germany

Ferreira, I.R.S and Schnorrer, F. (2012): In a journey to find “home”: myotube-tendon targeting through Kon-tiki. EMBO Young Investigator course, EMBL, Heidelberg, Germany

Posters

23rd European *Drosophila* Research Conference (2013), Barcelona, Spain

22nd European *Drosophila* Research Conference (2011), Lisbon, Portugal

International Conference on Neural Transplantation and Repair (2008), Freiburg, Germany